

# **'SPIN PROBE STUDIES ON THE EFFECT OF SOLUTES ON THE STRUCTURE OF WATER**

A Thesis Submitted  
In partial Fulfilment of the Requirements  
for the Degree of  
DOCTOR OF PHILOSOPHY

By  
RAMACHANDRAN CHANDRASEKHARAN

TH  
CHM/1976/D  
C 3615

to the  
DEPARTMENT OF CHEMISTRY  
INDIAN INSTITUTE OF TECHNOLOGY KANPUR  
JANUARY, 1976

TO  
MY PARENTS

✓CHM-1876-D-CHA-SPI

UNIVERSITY OF  
CENTRAL LIBRARY

Acc. No. **A 52174**

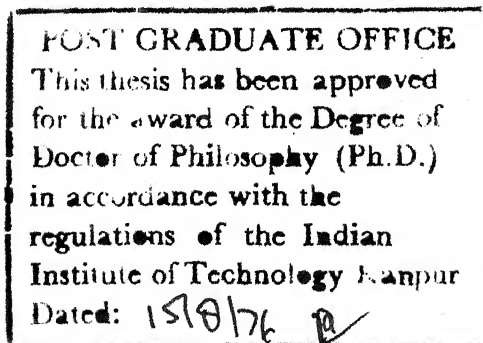
19 DEC 1977

CERTIFICATE I

Certified that the work contained in this thesis entitled "SPIN PROBE STUDIES ON THE EFFECT OF SOLUTES ON THE STRUCTURE OF WATER" has been carried out by Mr. Ramachandran Chandrasekharan under my supervision and the same has not been submitted elsewhere for a degree.

D. Balasubramanian  
Thesis Supervisor

Kanpur:  
January 22, 1976





STATEMENT

I hereby declare that the matter embodied in this thesis entitled, "SPIN PROBE STUDIES ON THE EFFECT OF SOLUTES ON THE STRUCTURE OF WATER" is the result of investigations carried out by me in the Department of Chemistry, Indian Institute of Technology, Kanpur, India under the supervision of Professor D. Balasubramanian.

In keeping with the general practice of reporting scientific observations, due acknowledgement has been made wherever the work described is based on the findings of other investigators.

Ramachandran Chandrasekharan

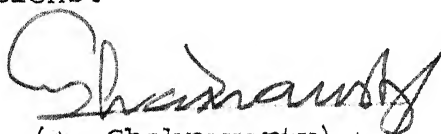
DEPARTMENT OF CHEMISTRY  
INDIAN INSTITUTE OF TECHNOLOGY KANPUR, INDIA

CERTIFICATE OF COURSE WORK

This is to certify that Mr. C. Ramachandran has satisfactorily completed all the course requirements for the Ph. programme in Chemistry. The courses include:

Chm 500 Basic Course in Mathematics I  
Chm 501 Advanced Organic Chemistry I  
Chm 502 Advanced Organic Chemistry II  
Chm 521 Chemical Binding  
Chm 523 Chemical Thermodynamics  
Chm 524 Modern Physical Methods in Chemistry  
Chm 541 Advanced Inorganic Chemistry I  
Chm 622 Chemical Kinetics  
Chm 624 Valence Bond & Molecular Orbital Theories  
Chm 800 General Seminar  
Chm 821 Special Graduate Seminar  
Chm 900 Graduate Research.

Mr. Ramachandran Chandrasekharan was admitted to the candidacy of Ph.D. degree in August 1971, after he successfully completed the written and oral qualifying examinations.



(A. Chakravorty)  
Head,  
Department of Chemistry



(P.S. Goel)  
Convener  
Post-Graduate Studies Committee  
Department of Chemistry

ACKNOWLEDGEMENTS

It is with pleasure that I place on record my gratitude and regard for Dr. D. Balasubramanian for suggesting the problem and giving me the opportunity to venture into new techniques. His painstaking efforts and able guidance combined with a thoroughly pleasant outlook made this work all the more fruitful and enjoyable.

I am indebted to Professor P.T. Narasimhan for his invaluable suggestions regarding the ESR spectral analysis and for the great amount of time he so graciously agreed to devote on this. My sincere thanks to Professor J.C.Ahluwalia for many stimulating discussions and for his kind encouragement.

I thank Professor P.T. Manoharan of IIT-Madras for the generous help and excellent facilities extended at IIT-Madras in the recording of ESR spectra and for the computer time made available on the IBM 370 system.

Dr. S. Aravamudhan rendered expert advice in the initial stages of the ESR spectral analysis and in the programming for the simulation of the spectra. Mr. V.H. Subramanian was a great help in the understanding of the theoretical aspects of the problem. My thanks to Dr. V.P. Chacko without whose help it would have been impossible to record the spectra at IIT-Madras.

The programming expertise of Mr. K.C. Rao rescued me from several computational tangles at various stages.

The co-operation and comradeship extended by my colleagues Mr. B.C. Misra, Mr. C. Kumar and Miss P. Chopra was of special importance. Birbal Chawla was generous with the gifts of chemicals and his friendship. The help rendered in myriads of ways by my research scholar friends is deeply appreciated. A word for Mr. S. Ramasesha, Mr. S.K.R. Sahasrabudhey and my friends at Hall 5 for making life a most meaningful and pleasant experience.

The assistance and co-operation of messrs R.D. Singh, H.N. Singh, K.K. Bajpai, B.N. Shukla and A.L. Gupta of the Chemistry Department and the prompt help of Mr. D.S. Panesar of the Chemical Engineering Department, in the drawings is gratefully acknowledged.

I am grateful to the CSIR and IIT-Kanpur for the financial assistance rendered.

Finally, my heartfelt gratitude to the mess workers of Hall 5 for their pleasant and boundless love they have bestowed upon me throughout my stay at IIT-Kanpur.

Ramachandran Chandrasekharan

## SYNOPSIS

This thesis entitled "Spin Probe Studies on the Effect of Solutes on the Structure of Water" reports studies using a paramagnetic, stable free radical, 2,2,6,6-tetramethyl-piperid-4-one-N-oxide (abbreviated as TEMPO), as a probe to investigate changes that happen in the structural equilibrium of liquid water upon the addition of certain solutes. The solutes chosen are of two categories: (i) solutes that denature proteins, i.e., denaturants of the urea-guanidinium family, and (ii) amphiphilic salts such as tetra-n-amylammonium bromide and sodium butyrate. In addition to this an attempt has also been made to study the conformational dynamics of a globular protein in aqueous solutions by using TEMPO as a spin-probe rather than a spin-label.

Chapter I describes the background of the problem, a brief survey of literature, and the argument in favour of the e.s.r. spin-probe method to study water structure.

Chapter II describes the relevant e.s.r. theory and treats the different interactions and perturbations in some detail. A brief summary of previous spin-probe studies and the parameters of importance obtainable are given. The experimental technique and the computational method are also discussed.

Chapter III describes the results and the interpretation of the e.s.r. parameters obtained for TEMPO in the aqueous solutions of the urea-guanidinium class of denaturants. Evidence is presented to show that urea, thiourea and guanidinium chloride disrupt water structure at all concentrations. The changes that occur in the tumbling correlation time,  $\tau_{\theta}$ , of the probe in increasing molarities of the denaturants are ascribed to decrease in the local microviscosity arising due to structure breaking, alteration in the solvation profile of the probe and water-solute interactions and medium viscosity effects. The contribution to the proton hyperfine linewidth from the spin-rotational  $a_{\text{O}}$  (SR) term is assessed from variable temperature studies. At high concentrations of urea, it is possible that a Debye-sphere model for the motion of the probe may not be strictly applicable and a two-state model may be meaningful. Dimethyl urea, on the other hand, may have a slight structure making propensity towards water. The spin-probe studies reported in this chapter agree in their interpretation with the nitrogen magnetic resonance studies on aqueous urea systems.

Chapter IV describes spin-probe studies of TEMPO in aqueous solutions of amphiphilic hydrophobic salts such as tetra-n-amyllumonium bromide and sodium butyrate. The results on sodium butyrate point out to the structure making ability of the butyrate ion and its hydrophobic hydration. This salt

behaves very similar to n-hexyl ammonium bromide and tetra-n-butyl ammonium bromide in its effect on water structure. A two-state model for the probe in this solution appears likely.

The case of aqueous solutions of tetra-n-amyl ammonium bromide is more complex. Our results indicate the possibility of an independent effect on water structure by the anion and the cation, discernible at low concentrations of the salt ( $\sim 0.025$  M). At higher concentrations, besides the structure making effects seen, a two-site model, one a structured cage-like clathrate and the other free monomer water seems to be present, if we assume a rapid exchange of the probe between these two environments.

Chapter V is an attempt to study whether a spin-probe molecule would bind to appropriate sites in a globular protein, and whether the e.s.r. spectrum of the bound probe would monitor conformational changes in the protein. Spectral analysis of TEMPO in aqueous solutions of Bovine Serum Albumin at various pH looked encouraging but not sufficiently rewarding. The shortcomings of the present approach and suggestions for more fruitful studies are discussed.

TABLE OF CONTENTS

	Page
CHAPTER I - THE PROBLEM AND ITS BACKGROUND	... 1
EFFECT OF SOLUTES	... 4
REFERENCES	... 18
CHAPTER II - THEORETICAL AND EXPERIMENTAL ASPECTS	... 20
EXPERIMENTAL	... 37
REFERENCES	... 43
CHAPTER III - SPIN PROBE STUDIES ON THE EFFECT OF UREA CLASS DENATURANTS ON WATER STRUCTURE	... 44
EXPERIMENTAL	... 50
RESULTS AND DISCUSSION	... 51
(1) Urea Solutions	... 51
(2) Urea Derivatives	... 86
(A) Thiourea	... 86
(B) Dimethyl Urea	... 90
(3) Guanidinium Chloride	... 94
A NOTE ON THE LIMITATIONS OF THE METHOD	... 103
REFERENCES	... 112
CHAPTER IV - EFFECT OF TWO AMPHIPHILIC SOLUTES ON WATER STRUCTURE-SPIN PROBE STUDY	... 114
EXPERIMENTAL	... 119
RESULTS AND DISCUSSION	... 120
REFERENCES	... 139
CHAPTER V - AN ATTEMPT TO USE A SPIN PROBE TO MONITOR CONFORMATIONAL CHANGES IN A GLOBULAR PROTEIN	... 141
EXPERIMENTAL	... 144
RESULTS AND DISCUSSION	... 145
REFERENCES	... 151
VITAE	... 152



## CHAPTER I

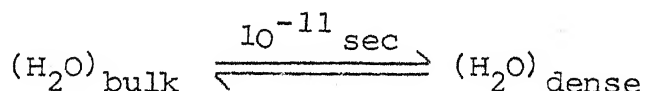
### THE PROBLEM AND ITS BACKGROUND

The structure of liquid water still is an enigma despite four decades of intensive investigations. In recent past the importance of the study of the structure of water has gained greater focus since it has been recognized to be a governing factor in deciding the conformations of proteins and biopolymers in their aqueous solutions.

Current ideas about the structure of liquid water are broadly classifiable<sup>1</sup> as based on the (i) continuum model and (ii) mixture model. In the former, the liquid is treated as a uniform dielectric medium with the average environment around a given water molecule being the same as that around any other. Hydrogen bonding that exists among various water molecules is considered to be both of uniform average energy and uniform characteristics. The former gives rise to the concept of 'bent' hydrogen bonds among monomers as well.

The mixture model envisages the presence of several distinguishable environments around water molecules, so that liquid water will contain several distinguishable molecular species. In the Nemethy-Scheraga treatment,<sup>2</sup> one considers several stages of hydrogen bonding involving mono-, di-, tri-, and tetra-hydrogen bonded water molecules in statistical equilibrium with free or unbonded monomers. This statistical-mechanical picture is a further development of the ideas of Frank and Wen,<sup>3</sup> who suggested that liquid water is an equilibrium mixture of clusters of hydrogen bonded water and free unbonded water monomers. The clusters are thus in a sense 'ice-like' and thus 'bulky' or 'light' (recall ice is less dense than liquid water), while the unbonded free monomers are 'steam-like' or 'dense'. At any given temperature there is considerable flickering or a flux where monomers can enter a cluster and a water molecule in the cluster may depart to become free. Thus the picture is one of a "flickering cluster" with statistical fluctuations in the status of individual water molecules. On the average, it is suggested that about 30-35% of the molecules are in the cluster form at room temperature and the half-life of the flickering clusters is suggested to be  $10^{-11}$  sec. This is a time short enough to produce a single relaxation time for water but sufficiently long to ascribe a meaningful existence to the clusters, as the half-life is  $10^2$ - $10^3$  times the molecular vibration time.

While this is the general idea behind the mixture models, details about the number of distinguishable species, number of hydrogen bonds, and such are somewhat controversial. While attempts have been made to distinguish spectroscopically the number of mono-, di-, tri- and tetra-hydrogen bonded water molecules and to ascribe statistical weights and energy levels for these, such attempts and estimates have been criticised with some justification. In any event, the presence of the tetra co-ordinated water has been accepted as also the free 'dense' water and in our opinion, it is meaningless to make finer distinctions from among the 'bulk' water clusters especially since the time scale involved for molecules to flicker, i.e. enter or leave a cluster is  $10^{-11}$  sec. i.e. a time so short as to be essentially a diffusion controlled process. Walrafen's Raman experiments on liquid water essentially justify the presence of bulk water and the flickering cluster model. It is thus possible to write an equilibrium for liquid water as



It has also been possible<sup>4</sup> to view the above equilibrium as one where water exists in two 'microphases', one microphase that is clustered bulk water and the other being the dense, free monomeric water. Even though the Frank-Wen-

Franks model is not entirely adequate, it has been able to account for the properties of aqueous solutions more satisfactorily than any other model, and for this reason, the flickering cluster model of liquid water is most commonly accepted at present, and it is to this that we shall turn our attention primarily in this thesis.

### EFFECTS OF SOLUTES

With the description of the structure of water as an equilibrating mixture of bonded clusters and free monomers, it is to be expected that addition of solutes will alter this equilibrium one way or the other. A solute may behave either as a structure maker, i.e., one that shifts the liquid water equilibrium more towards the bonded microphase, or as a structure breaker i.e., causes depolymerization or 'melting' of the clusters. A structure maker such as LiF, causes a net increase in the structure of water more towards the bonded clusters, and consequently will affect the thermodynamic, spectroscopic and hydrodynamic properties of the solvent in a fashion opposite to that of a structure-breaking solute such as CsI. Structure making solutes have been shown to increase the viscosity and reorientation time of water and also cause an increase in the excess partial molal heat capacity in water, while structure-breakers behave in

the opposite fashion.<sup>1</sup> Many papers have appeared in the literature that monitor the structure-altering ability of solutes on water, by using a variety of methods the most notable of which have been vibrational<sup>5</sup> and nmr spectroscopy,<sup>6</sup> self-diffusion measurements,<sup>7</sup> heat capacity studies,<sup>8</sup> ultrasonic attenuation methods,<sup>9,10</sup> and other relaxation methods.<sup>11</sup>

An important consequence of the unique structure of liquid water and the structural alteration by solutes occurs in biochemistry, namely in the maintenance of the native structure of globular proteins in aqueous solutions. The forces governing the spatial fold of a protein in aqueous solution are thought to be (i) hydrogen bonding among peptide groups, and between backbone and side-chain groups wherever possible, (ii) ionic interactions such as may happen between e.g., ionised carboxyls and  $\text{NH}_3^+$ , (iii) non-bonded contact interactions between residues, and (iv) what has been termed as hydrophobic interaction between side-chains.<sup>12</sup> The last mentioned factor has been shown to be of considerable importance in the maintenance of the native structure of many globular proteins. The rationale behind hydrophobic interactions is the same as behind micellar aggregation of surfactants in water, and of the immiscibility of hydrocarbons with water.

Introduction of a non-polar hydrocarbon into aqueous medium would result in a solute-solvent interaction of the induced dipolar-dipolar type, and the corresponding enthalpy of solution is expected to be small and negative ( $-2$  kcal/mol). This attractive interaction results in a net ordering and orientation of solvent water molecules around the dissolved hydrocarbon. Such an ordering would clearly mean a decrease in entropy in the system. Consequently we have a compensatory situation operating at any given temperature between the enthalpy and entropy of dissolution. In the vicinity of room temperature, the entropy term predominates the free energy of the process and consequently the tendency would be towards non-dissolution and phase separation. To illustrate this we may point out that at  $298^{\circ}\text{K}$  the enthalpy of dissolution of liquid propane in water is  $-1800$  cal/mol while the unitary entropy change for the process is  $-23$  e.u., resulting in a free energy change for the dissolution process of  $+5050$  cal/mol, thereby making a solution of propane in water unfavourable. The reversal of solution, i.e., phase separation of propane in water results in an entropy gain for the system. Somewhat of a similar situation operates when a protein chain is immersed in water. Due to the unfavourable free energy of interaction between the non-polar side-chains (ala, leu, val, phe, etc) and water, there is a tendency towards a partial reversal of solution of the protein.

In effect the protein chain then adopts a conformation where as much of the non-polar side-chains as possible (within the constraints of the primary structure) tend to aggregate much like an internal micelle and avoid contact with the solvent water. There is then a tendency for maximising polar side-chain contacts with water, and the non-polar side-chains to get away from the water surface and fold to form an interior non-polar core within the macromolecule, generating thereby an overall globular conformation of the protein chain. This rule of the thumb, 'polar out, non-polar in', seems to be one of the governing principles in native structure of globular proteins.<sup>13</sup>

It is important to realize that entropic changes are primarily responsible for this kind of hydrophobic interactions in proteins, and such a situation arises primarily because of the unique macromolecular structure of solvent water itself. As a corollary it is to be expected that any change caused to the structure of solvent water should alter the conformational equilibrium and thus the folding pattern of the protein. Efforts have been made in literature<sup>14</sup> to correlate the structure-altering ability of a given solute with its potency to denature (significantly alter the native globular structure) proteins in aqueous solutions. For example, while a structure maker such as  $(\text{NH}_4)_2\text{SO}_4$  is known not to denature proteins significantly

in water, a structure breaker such as  $\text{LiClO}_4$  or  $\text{KCNS}$  is known to be an effective denaturant. Clearly, factors such as direct binding and other interactions may play a part in the denaturation process but it appears likely that an agent that disrupts water structure will thereby alter the stability of hydrophobic interactions and thus indirectly cause an unfolding of globular proteins in aqueous solutions.

One of the most effective set of denaturing agents are the ones that belong to the urea-guanidinium class of compounds, particularly urea, guanidinium chloride and guanidinium thiocyanate. Indeed the chain statistical configurations of most proteins have been determined to be of the true random coil state in 6 M  $\text{GuHCl}$ , and often in 7-8 M urea.<sup>15</sup> It is often sufficient to use 4 M concentrations of these denaturants to achieve protein chain disorder. While lot of work has been done on the mechanism of urea denaturation, it appears to us that the factors involved are (i) Direct 'binding' of the denaturant molecules to the proteins, (ii) possible weakening of interpeptide hydrogen bonding that offer stability to the secondary structure of the protein and (iii) urea induced structural damage of solvent water. The latter is believed to be responsible for weakening of hydrophobic interactions involved in the native structure of proteins. Equilibrium dialysis measurements

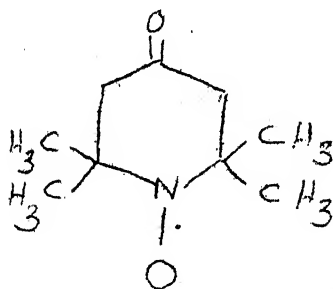


have shown that urea<sup>16</sup> and guanidinium chloride<sup>17</sup> bind to a few proteins although it may be too early to generalize this to all proteins. Model experiments by Klotz,<sup>18</sup> Levy,<sup>19</sup> Schellman,<sup>20</sup> and others do not seem to support the idea of urea as an agent that disrupts peptide hydrogen bonds. It would thus be of interest to study the effect of urea on water structure and assess the importance of this in the denaturation mechanism. Compounds belonging to the urea family have also been tried as agents that perturb protein structures in aqueous solution. Thiourea, which is unfortunately not very soluble in water ( $\sim 3\text{ M}$ ), seems effective as a denaturant while dimethyl urea is a weak denaturant and tetramethyl urea is not a denaturant at all.<sup>16</sup> The progressive methylation of urea seems to play a role in this process. Swenson<sup>21</sup> has studied the effect of several of these urea derivatives on water structure in an attempt to assess the importance of this factor in their denaturing ability. Guanidinium chloride ( $(\text{NH}_2)_2\text{C}=\text{NH}_2^+ \text{Cl}^-$ ), isoelectronic with urea, behaves as efficiently or better than urea in denaturing globular proteins. In all these cases, it has been variously suggested that the denaturant causes protein conformational transition either by direct interaction with ligands in the peptide chain or by altering the water structure in a fashion as to weaken the hydrophobic associations between side-chain groups in the macromolecule. We thought

that it would be of interest if an investigation into the effects of these compounds on the structure of water be undertaken.

Amphiphilic compounds that possess both nonpolar and polar moieties display interesting effects on the structure of water, as evidenced by thermochemical studies. Examples of such substances are the tetra-alkyl ammonium salts, e.g.,  $(C_5H_{11})_4N^+ Br^-$ , fatty acid salts, e.g.,  $C_3H_7COONa$ , and also detergents such as sodium dodecyl sulphate,  $CH_3(CH_2)_{11}SO_3^- Na^+$ . Hydration of the second kind, i.e, the so called hydrophobic hydration, has been observed in these systems, and the detergent dodecyl sulphate is known to aggregate in water to produce micellar aggregates beyond 10 mM.<sup>22</sup> Here again a detailed study of the effect of these amphiphiles on water structure was thought to be of interest and we have undertaken such a study. Yet another system that we considered of interest to study is the binding of hydrophobic solutes by the globular protein, bovine serum albumin (BSA). This protein is known to bind hydrophobic compounds efficiently. We argued that if the spin probe TEMPO were allowed to bind to BSA, at different pH (as a function of the conformational status of BSA), then it should be possible to monitor the conformation of the protein by studying the esr signal of the bound probe. This is attempted in Chapter V, and is a variation from the usual procedure of directly spin-labelling BSA.

It is in this light that spin probe studies by using a stable free radical are attractive. Such a study was undertaken earlier by Jolicoeur and Friedman,<sup>23</sup> and Jolicoeur.<sup>24</sup> The inherent advantage in using the EPR spin probe method is that the relaxation processes involved are of the order of  $10^{-11}$  sec for a properly chosen molecule, a time scale that is comparable to that of the molecular events occurring in solution. The tumbling correlation time of a stable, water-soluble, hydrophobic, paramagnetic probe molecule such as 2,2,6,6-tetramethyl-piperid-4-one-N-1-oxyl (TEMPO),



is of the order of  $10^{-11}$  sec. This tumbling correlation time,  $\tau_0$ , can be easily determined from an analysis of the e.s.r. spectra of TEMPO in several media by using the treatment well known in literature. One can imagine a situation in which the spectrum of a solution of TEMPO is a composite one, containing information about the different microphases that exist in aqueous solutions, or the local viscosity changes that arise in the environment around TEMPO as a solute is added to water in which TEMPO is dissolved as a spin probe. In a sense then, the role of TEMPO, the spin probe molecule,

is that of a Maxwell's demon which is able to monitor changes that occur in the medium and report it by means of linewidth and  $\tau_0$  value alterations. TEMPO is particularly suitable as a spin probe in aqueous solutions since its  $\tau_0$  value is about the same as a cluster flickering time. Although the spin probe cannot distinguish between the two species or microphases in solution, the time of exchange of the probe between the two environments is comparable to the characteristic time of measurement. Changes in the spectra thus reflect the changes that occur in the microphases and hence could lead to a more meaningful interpretation of the structure of water and its role in the stability of protein configuration.

The essential parameters that we can obtain from an esr spectrum of the spin probe TEMPO in aqueous solutions are the linewidth of a given line and the correlation time for reorientation of tumbling molecule in solution. For a free radical in sufficiently dilute solutions, the linewidth almost entirely results from rotational effects. From the theory due to Kivelson<sup>25</sup> described in some detail in Chapter II, the following equation results;

$$\pi \sqrt{3} T_2^{-1} = a_0 + a_1 m + a_2 m^2 + a_1' m_H + a_2' m_H^2 + a_2'' m m_H \dots (1)$$

The coefficients have been enumerated in Chapter II and

it is sufficient for our purpose to write Eq (1) as:

$$\pi \sqrt{3} T_2^{-1} = a_0 + a_1 m + a_2 m^2 \quad \dots (2)$$

where  $m$  is the quantum number defining the manifold. Eq (2) has been used in two ways, namely to obtain the correlation time and the linewidth of the hydrogen hyperfine line of TEMPO in solution.

The correlation time for reorientation of the tumbling probe,  $\tau_\theta$ , or roughly the time taken for a single revolution of the probe, is clearly a function of the local viscosity around the probe. We can expect  $\tau_\theta$  to increase if the local viscosity decreases and vice-versa. The theory of linewidths used here applies only to a situation where the product  $\omega_0 \tau_\theta$  (where  $\omega_0$  the microwave frequency used is  $10^9$  Hz) is much less than unity. Thus,  $\tau_\theta$  should be of the order of  $10^{-10}$  sec or less. Motional narrowing of lines occur only where the tumbling is fast and consequently the relationship between linewidth and  $\tau_\theta$  is roughly proportional. TEMPO in aqueous solutions satisfies these conditions and thus Kivelson's theory can be used to analyse linewidth and  $\tau_\theta$  values.

Coming back to Eq (2), the correlation time can be obtained from the intensities of the lines having different  $m$  values. In our case of TEMPO,  $m=0$  or  $\pm 1$ , since we have a

$N^{14}$  nucleus of spin  $I = 1$ . The differences in intensities are essentially due to  $m$ -dependent processes related to the tumbling motion of the probe. Thus the more the rigidity or friction to tumbling the more anisotropic the lineshapes and intensities. As evidence we can compare the spectra of two solutions, one at room temperature and the other at liquid nitrogen temperature.<sup>26</sup> The  $\tau_c$  value is thus a very good parameter by which we can judge whether the given aqueous solution is less rigid or less accommodating to the motion of the probe than in pure water. It is to be borne in mind that  $\tau_c$  gives us information which is microscopic in nature (due to the time scale), which would not be revealed by measurements of the viscosity or heat capacity changes. The case for the esr method being more effective than other methods has also been effectively argued out by Jolicoeur and Friedman.<sup>23</sup> Thus an estimation of  $\tau_c$  is an effective pathway to understand microscopic changes that occur in aqueous solutions.

The linewidth parameter on the other hand is equally important. In addition to motional effects other mechanisms also operate which determine the linewidth of the hydrogen hyperfine line of TEMPO in solution. The most important of these is the spin-rotational effect discussed in Chapter II. The presence or absence of this term could lead to considerable variations in linewidth. The least accuracy in the

simulation of linewidths is around  $\pm 5\%$ , which is acceptable.

In their treatment based on the above considerations, Jolicoeur and Friedman have studied hydrophobic solutes of the tetra-alkyl ammonium class and the tetra-aryl substituents in order to assess their effect on the structure of water, as well as the possible mechanisms through which the hydrophobic effect manifests itself. Considering only the  $m_N = 0$  manifold, whereby  $m$ -dependent terms vanish, Jolicoeur and Friedman obtained the linewidths and by the method of Stone et al. obtained  $\tau_\theta$  values. In order to eliminate the medium effect, i.e., the viscosity changes that occur when a solute is added to water, they used plots of plots of  $T/\eta$  and  $\tau_\theta/\eta$  instead of  $T$  or  $\tau_\theta$ . One could plot  $\eta/T$  instead of  $T/\eta$  but the essential characteristics remain unchanged although the variation is different. Kivelson's equation including the spin-rotational term has been written as

$$W_H = K_1 (T/\eta) + K_2 (\eta/T) + K_3 \quad \dots (3)$$

and thus if  $W_H$  is plotted either as  $T/\eta$  or  $\eta/T$  we would obtain an optimum (a maximum or a minimum). Jolicoeur and Friedman used aqueous glycerol solutions as a standard with the assumption that glycerol behaves as an inert diluent, not altering water structure significantly. Deviations from this standard behaviour were recognized as changes that had

to occur due to the effect of the solute on water structure.  $\tau_{\theta}$  studies on the other hand indicated changes which could be explained either on the basis of viscosity changes (as in glycerol) or other physical factors like micelle formation as with octyl-ammonium bromide. Any explanation for the deviation from the  $W_H$  vs  $T/\eta$  plot of glycerol solutions had to be consistent with the behaviour of  $\tau_{\theta}$  of the probe in aqueous solutions of the added solute. In other words, it is possible to deduce structural information from such spin probe studies.

In summary of the Jolicoeur and Friedman treatment, the first of its kind to use esr as a technique in studying the effect of added solutes on the structure of water, it is clear that the linewidth  $W_H$  of the hydrogen hyperfine line of TEMPO as well as  $\tau_{\theta}$  are important clues to the microscopic situation. In addition  $\tau_J$  and the plots of the Kivelson-type reveal much more information otherwise buried in the spectral changes observable.

Although Jolicoeur and Friedman have not specifically attributed structure changes that might occur upon addition of hydrophobic solutes it is evident that such effects can be inferred using esr. Keeping in mind the important role of the hydrophobic interaction in maintaining the native structure of proteins in aqueous solutions, any qualitative picture of the molecular events that occur, say, upon



addition of a solute which denatures protein would help in understanding the effect of the denaturant on the hydrophobic interaction and, more importantly, would tell us about the structural changes that occur in solvent water. A knowledge of the effect of the added solute in water structure could lead to a fuller understanding of the mechanism of denaturation and perhaps to a detailed estimation of the extent of its action on proteins.

With this in view we undertook the study of the urea-class compounds in aqueous solutions, especially urea and GuHCl as they are effective denaturants. The effect of hydrophobic solutes, though central to Jolicoeur and Friedman's work, was studied and we chose tetraamyl ammonium bromide (TAAB) as a representative amphiphilic salt; besides sodium butyrate. In addition, we have also tried to investigate whether TEMPO would bind to hydrophobic residues in a globular protein such as bovine serum albumin (BSA) as a function of the conformation of the protein and whether such binding would be useful as an extrinsic probe of the denaturation process of BSA.

# REFERENCES

1. Sarma, T.S. and Ahluwalia, J.C. (1973) in Chemical Society Reviews, Vol. 2, No. 2, is an excellent reference source for papers connected with aspects of water structure.
2. Nemethy, G. and Scheraga, H.A. (1962) J. Chem. Phys., 36, 3382.
3. Frank, H.S. and Wen, W.Y. (1957) Disc. Faraday Soc., 24, 133.
4. Frank, H.S. and Franks, F. (1968) J. Phys. Chem., 48, 4746.
5. (a) Hartman, K.A. Jr. (1966) J. Phys. Chem., 70, 270.  
(b) Walrafen, G.E. (1971), J. Chem. Phys., 55, 768.
6. Vold, R.L., Daniel, E.S. and Chan, S.O. (1970) J. Amer. Chem. Soc., 92, 6771.
7. Matyash, I.V., Toryanik, A.I. and Kiselnik, V.V. (1967) J. Struct. Chem., (Eng. Transl.), 8, 371.
8. Chawla, B. and Ahluwalia, J.C. (1973) J.C.S. Faraday I, 69, 434.
9. Hammes, G.G. and Schimmel, P.R. (1967) J. Amer. Chem. Soc., 89, 442.
10. Arakawa, K., Takenaka, N. and Sasaki, K. (1970) Bull. Chem. Soc. Jap., 43, 636.
11. Haggis, G.H., Hasted, J.B. and Buchanan, T.J. (1952) J. Chem. Phys., 20, 1452.
12. Kauzmann, W.A. (1959) Adv. Protein Chem., 14, 1.
13. Dickerson, R.E. and Geis, I. (1969) 'The structure and action of Proteins', Harper and Row, New York.
14. von Hippel, P.H. and Schleich, T. in "Structure and Stability of Biological Macromolecules", Eds: Timasheff, S.M. and Fasman, G.D. Marcell Dekker, Inc. New York.
15. Tanford, C. (1968) Adv. Protein Chem., 23, 122; also (1970) 24, 1.
16. Gordon, J.A. and Warren, J.R. (1968) J. Biol. Chem., 243, 5663.

17. Nakagaki, M. and Sano, Y. (1972) Bull. Chem. Soc. Jap., 45, 2100.
18. Klotz, I.M. and Franzen, J.S. (1962) J. Amer. Chem. Soc., 84, 3461.
19. Levy, M. and Magoulas, J.P. (1962) J. Amer. Chem. Soc., 84, 1345.
20. Schellman, J.A. (1955) Compt. rend. trav. lab. Carlsberg, Ser. Chim., 29, 223
21. Swenson, C.A. (1966) Arch. Biochem. Biophys., 117, 494.
22. Adamson, A.W. (1963) 'Physical Chemistry of Surfaces', Interscience, New York.
23. Jolicoeur, C. and Friedman, H.L. (1971) Ber. Bunsenges. physik. Chem. 75, 248.
24. Jolicoeur, C. and Friedman, H.L. (1971) J. Phys. Chem., 75, 165.
25. Kivelson, D. (1960) J. Chem. Phys., 33, 1094.
26. Stone, T.J., Buckman, T., Nordio, P.L. and McConnell, H.M. (1965) Proc. Nat. Acad. Sci. USA, 54, 1010.

## CHAPTER II

### THEORETICAL AND EXPERIMENTAL ASPECTS

A brief survey of the theory of e.s.r. would be appropriate here.<sup>1</sup> The basic resonance condition for the electron magnetic moments is given by the equation,

$$h\nu = g\beta H \quad \dots(1)$$

where  $h$  is the Planck's constant,  $\nu$  is the resonance frequency,  $g$  is the gyromagnetic ratio of the electron (2.0023),  $\beta$  is the Bohr magneton,  $eh/4\pi mc$ , and  $H$  is the magnetic field sensed by the electron. This field can be further classified as

$$\vec{H} = \vec{H}_0 + \vec{H}_{\text{local}} \quad \dots(2)$$

where  $\vec{H}_0$  is the experimental magnetic field and  $\vec{H}_{\text{local}}$  is the magnetic field that arises due to local dipole moments of other paramagnetic species and of the nuclei. In most

cases, as in ours, the radical being studied is at a low concentration so that magnetic and exchange interactions between radicals can be neglected. Therefore the local field acting on the electron originates solely from the nuclei. The magnetic field produced by a nucleus having magnetic moment  $\vec{\mu}_N$  on an electron having magnetic moment,  $\vec{\mu}_e$  may be designated as  $B(\vec{r})$ , where  $\vec{r}$  is the vector from the origin, the nucleus to the point (x,y,z), the electron.  $B(\vec{r})$  then is given by,

$$B(\vec{r}) = \vec{\mu}_N / r^3 + 3 (\vec{r} \cdot \vec{\mu}_N) / r^5 \quad \dots(3)$$

where r is the distance between the two centres. The interaction energy E between  $B(\vec{r})$  and the electronic magnetic moment at r is

$$E = -\vec{\mu}_e \cdot B(\vec{r})$$

$$E = -\vec{\mu}_e \cdot \vec{\mu}_N / r^3 - 3 (\vec{\mu}_e \cdot \vec{r}) (\vec{\mu}_N \cdot \vec{r}) / r^5 \quad \dots(4)$$

where  $r \neq 0$ . Excluding the spatial co-ordinates and substituting the appropriate operators we have the spin Hamiltonian as

$$\vec{\mu}_e \cdot \vec{\mu}_N \int \frac{|\psi|^2}{r^3} dx dy dz - 3 \int \frac{|\psi|^2 \cdot (\vec{\mu}_e \cdot \vec{r}) (\vec{\mu}_N \cdot \vec{r})}{r^5} dx dy dz$$

$$\dots(5)$$

where the Hamiltonian corresponding to Eq(4) has been averaged over the electronic spatial wave function  $\Psi(x, y, z)$ . This does not represent the complete interaction between the nuclear and the electronic moments as the equation breaks down for  $r=0$ . To account for the interaction at  $r=0$ , we have to assume that the nucleus is a rotating sphere of radius  $\xi$ , with the charge uniformly distributed over the surface. Outside the nucleus this distribution gives rise to the moment  $\vec{\mu}_N$ . The magnetic field within this sphere is given by

$$B = (2/\xi^3) \mu_N \quad \dots (6)$$

and hence the interaction energy between the electron probability density within this sphere and the field within is

$$E = - \int_{\text{nucleus}} B \cdot \vec{\mu}_e |\Psi|^2 dx dy dz \quad \dots (7)$$

Since the electron probability density is almost constant in this sphere we can write

$$E = - |\Psi(0)|^2 \int_{\text{nucleus}} B \cdot \vec{\mu}_e dx dy dz \quad \dots (8)$$

where  $|\Psi(0)|$  is the value of the electronic wave function at  $r=0$ . Substituting for  $B$  we have

$$E = -2/\xi^3 \cdot \vec{\mu}_N \cdot \vec{\mu}_e |\Psi(0)|^2 \int_{\text{nucleus}} dx dy dz \quad \dots (9)$$

which turns out to be

$$E = - 8\pi/3 \cdot |\psi(0)|^2 \cdot \vec{r}_e \cdot \vec{r}_N \quad \dots (10)$$

The corresponding spin Hamiltonian of Eq (10) is

$$\hat{H}_C = -8\pi/3 \cdot |\psi(0)|^2 \cdot \vec{r}_e \cdot \vec{r}_N \quad \dots (11)$$

This term is called the Fermi contact term or interaction. The interaction represented by Eq (4) is dependent on the angular co-ordinates of the electron and is thus anisotropic.

Hence the local magnetic field on the electron can be expressed as

$$\vec{H}_{\text{local}} = \vec{H}_{\text{dipolar}} + \vec{H}_{\text{contact}}$$

In solutions the dipolar term vanishes due to angular averaging, but the contact term remains and can be expressed as

$$H_C = g_e g_N \beta_e \beta_p 8\pi/3\hbar^2 \cdot |\psi(0)|^2 \cdot \hat{S} \cdot \hat{I} \quad \dots (12)$$

for a single unpaired electron where  $\hat{S}$  and  $\hat{I}$  are spin operators. This can be condensed to

$$H_C = h A / \hbar \cdot \hat{S} \cdot \hat{I}$$

where A is the hyperfine splitting constant in units of hertz

given by

$$A = 8\pi/3h \ g_e \ g_N \ \beta_e \ \beta_p / |\chi(0)|^2$$

as the contact term gives rise to hyperfine lines.

Although the dipolar term has no effect on the line positions in dilute solutions in a situation where there is rapid tumbling of the free radical, the mean-square fluctuations in line positions resulting from the tumbling motion contributes to the linewidths. Since the linewidths are fluctuations of the mean square fluctuations in frequency, and the anisotropic dipolar and g-tensor interactions, the expression for linewidth has quadratic terms of both interactions separately, with cross terms related to their product. There is yet another process which contributes to the linewidth and this has been termed as spin-rotational effect and treated by Kivelson and co-workers.<sup>2</sup> Each of these contributions will be taken up separately and the contribution from each added to get the overall expression.

The contributions to the instantaneous spin Hamiltonian of the g-tensor (G) and anisotropic intramolecular electron-nuclear dipolar (D) interactions can be written as

$$\mathcal{H}^{(G+D)}(t) = \mathcal{H}^{(G)}(t) + \mathcal{H}^{(D)}(t) \quad \dots (13)$$

Both the terms on the R.H.S. of the above equation are



functions of the orientation of the free radical and also of the electron and nuclear spin operators.

The g-tensor is a symmetric second rank tensor and can be diagonalized along the molecule fixed axis  $x'$ ,  $y'$ ,  $z'$  as  $g_1$ ,  $g_2$ , and  $g_3$ . Therefore,

$$\begin{aligned}\mathcal{H}^{(G)}(t) &= \beta_e \cdot g \cdot S \cdot B \\ &= |\beta_e| [i' \cdot g_1 S_{x'} + j' \cdot g_2 S_{y'} + k' \cdot g_3 S_{z'}] \cdot B \\ &= |\beta_e| [g_1 \cdot B_{x'} S_{x'} + g_2 \cdot B_{y'} S_{y'} + g_3 \cdot B_{z'} S_{z'}] \\ &\dots (14)\end{aligned}$$

where  $i'$ ,  $j'$ ,  $k'$  are unit vectors in the  $x'$ ,  $y'$ ,  $z'$  directions and  $B$  is the external field. The time dependence of Eq (14) arises out of the fluctuating orientations of the  $x'$ ,  $y'$ ,  $z'$  axes with respect to the laboratory fixed axes  $x$ ,  $y$ ,  $z$ . We have now to transform the spin operators and the magnetic field from the molecular frame to the laboratory frame. This is achieved using Wigner rotation matrices.

We illustrate this for a radical having axial symmetry, as is the case for the radical used in this study. We then have  $g_1 = g_2 = g_{\perp}$  and  $g_3 = g_{\parallel}$ , where the direction of the field is taken to be along the  $z$  direction. We have

$$\begin{aligned}\mathcal{H}^{(G)}(t) &= |\beta_e| \left[ \underline{g} \cdot \underline{S} \cdot \underline{B} + (g_{\parallel} - g_{\perp}) S_{z'} B_{z'} \right] \\ S_{z'}, B_{z'} &= [S_{x'} \sin \theta(t) \cos \phi(t) + S_{y'} \sin \theta(t) \sin \phi(t) \\ &\quad + S_{z'} \cos \theta(t)] \cdot B \cos \theta(t) \dots (15)\end{aligned}$$

where  $\theta(t)$  and  $\phi(t)$  are the angles that specify the instantaneous orientation of  $z'$  w.r.t. the  $x, y, z$ , axes. The average overall angles gives  $\langle \cos \phi(t) \rangle = \langle \sin \phi(t) \rangle = 0$  and  $\langle \cos^2(\theta)(t) \rangle = 1/3$ . Substituting we get

$$\mathcal{H}^{(G)}(t) = |\beta_e| \left[ g_{\perp} \cdot S_z \cdot B_0 + (g_{\parallel} - g_{\perp}) 1/3 \cdot S_z \cdot B_0 \right] \dots (16)$$

or

$$g_s |\beta_e| \cdot S_z \cdot B_0 \dots (17)$$

where  $g_s = 1/3 [2g_{\perp} + g_{\parallel}]$ .

The linewidth contribution from fluctuations in  $\mathcal{H}^{(G)}(t)$  depend on the correlation function of matrix elements

$$\mathcal{H}^{(G)}(t) = \langle \alpha | \mathcal{H}^{(G)}(t) | \beta \rangle$$

between spin states  $|\alpha\rangle$  and  $|\beta\rangle$

$$\langle [\mathcal{H}^{(G)}(t)_{\alpha\beta} - \langle \mathcal{H}^{(G)}(t)_{\alpha\beta} \rangle] [\mathcal{H}^{(G)*}(t+t')_{\alpha'\beta'} - \langle \mathcal{H}^{(G)*}(t)_{\alpha'\beta'} \rangle] \rangle \dots (18)$$

The correlation function evaluated in detail would contain the Wigner matrix which in turn has the time dependence. The elements of the relaxation matrix contain terms proportional to the spectral densities  $J_0$ ,  $J_1$ , and  $J_2$  expressed as

$$J_n = \tau_c / (1 + n^2 \omega_0^2 \tau_c^2) \dots (19)$$

where  $\omega_0$  is the Larmor frequency of the electronic spin and  $\tau_c$  is the characteristic correlation time for the perturbation

or fluctuation.

It is to be noted that the only time-dependent part in Eq (15) enters through the  $S_z B_z$  terms which can be expressed as

$$S_z B_z = \left[ (1/2) \left[ S_- \exp(i\phi) + S_+ \exp(-i\phi) \right] \sin \theta + S_z \cos \theta \right] B_0 \cos \theta \quad \dots (20)$$

where  $S_{\pm} = S_x \pm i S_y$  and  $B_0$  ( $B = k B_0$  and since  $S \cdot B$  is invariant to rotation,  $S \cdot B = S_z B_z = S_z B_0$ ) is the external magnetic (applied) field parallel to the  $z$  axis.

The  $S_z B_0$  term is secular since it does not induce transitions but does affect linewidth as resonance frequency varies, as  $\cos^2 \theta(t)$  changes with time. The non-secular terms are those that cause transitions and hence are not important in line broadening mechanisms. The contribution from  $g$ -tensor (fluctuations) anisotropy has been estimated to be

$$\left[ T_2^{-1} \right]^{(G)} = (8/3) j^{(G)}(0) B_0^2 \quad \dots (21)$$

where

$$j^{(G)}(0) = \left[ \tau_c / (1 + \omega_0^2 \tau_c^2) \right] * (\beta_e^2 / 20 \hbar^2) * (g_1^2 + g_2^2 + g_3^2 - 3g_s^2)$$

where  $g_s = 1/3(2g_{\perp} + g_{\parallel})$ . Eq (21) shows that the linewidths vary as the square of the magnetic field. It is to be noted that the last term in the expression for  $j^{(G)}(0)$  is equal to  $2/3(g_{\perp} - g_{\parallel})^2$  for a radical with axial symmetry, so that

$T_2^{-1}(G)$  is proportional to  $2/3 (g_{\perp} - g_{\parallel})^2$  as would be obtained qualitatively by comparing the coefficients of Eq (17) (of the time dependent terms,  $S_z' B_z'$ ) and Eq (20).

The anisotropic dipolar interaction is treated similarly but is not elaborated here.

The spin-rotational interaction<sup>2,3</sup> can be represented as

$$E_{SR} = J.C.S. \quad \dots (22)$$

where  $J$  is the rotational angular momentum in units of  $\hbar$ ,  $C$  is the spin-rotational interaction tensor and  $S$  the spin in units of  $\hbar$ . There are two correlation times connected with this interaction,  $\tau_J$  which is characteristic of  $J$  and  $\tau_C$  which is characteristic of  $C$ . The physical significance of  $\tau_J$  and  $\tau_C$  is that  $\tau_C$ , the correlation time for the reorientation of the tumbling molecule is directly proportional to  $\eta$ , the viscosity coefficient, since reorientation is plainly more difficult in viscous media.  $\tau_J$  on the other hand is inversely proportional to  $\eta$ , since the deceleration of angular momentum is more rapidly achieved in viscous media. The equations obtained using the Debye model to spherical top molecules for  $\tau_J$  and  $\tau_C$  are

$$\tau_J = I/e \pi r^3 \eta \quad \text{and} \quad \tau_C = 4\pi \eta r^3 / 3kT \quad \dots (23)$$

For a magnetic field of cylindrical symmetry

$$T_1^{-1} = T_2^{-1} = 2 kT \tau_J / 3\hbar^2 * (2C_{\perp}^2 + C_{\parallel}^2) \quad \dots (24)$$

Since  $\tau_J \ll \tau_C$  we can neglect  $\tau_C$  dependence and obtain an expression

$$T_2^{-1} = (4\pi)^{-1} (I^2/r^3 \hbar^2) * 1/3(2 C_{\perp}^2 + C_{\parallel}^2) * kT/\eta \dots (25)$$

Thus this contribution is directly proportional to  $T/\eta$ . The estimation of  $C_{\perp}$  and  $C_{\parallel}$  are experimentally difficult and hence they have been approximated by using the elements of the G tensor. Atkins and Kivelson<sup>3</sup> have shown that the agreement between theoretical estimates and experimental results are fairly satisfactory and in the absence of accurate values of  $C_{\perp}$  and  $C_{\parallel}$  the approximation using elements of the G tensor is justified. Using these values they have estimated the contribution from the spin-rotational mechanism to the linewidth and find that for the Vanadyl complexes and Chlorine dioxide in solution this is significant. An important feature to be noted here is that this contribution is independent of the applied magnetic field. The theoretical formulation has been experimentally verified by Wilson and Kivelson.<sup>2</sup>

The variations in the linewidths observed for radicals are due to relaxation mechanisms which depend on the nuclear quantum numbers and which vary as  $M$  and  $M^2$ . A theory due to Kivelson gives the linewidth of a hyperfine line as

$$T_2^{-1} = a + b M_I + c M_I^2 \dots (26)$$

for a single nucleus and for the example in question, namely

TEMPO,

$$T_2^{-1} = a_0 + a_1 m + a_1 m^2 + a_1' m_H + a_2' m_H^2 + a_2'' m m_H \dots (27)$$

where the coefficients are expressed in terms of the elements of the A and G tensors. Since only the isotropic part of the A tensor is known, we see that

$$A_H/A_N \approx a_H/a_N = 10^{-2} \dots (28)$$

and thus the  $m_H$  dependence is negligible. We thus neglect any  $m_H$  term. We then have

$$T_2^{-1} = a_0 + a_1 m + a_2 m^2 \dots (29)$$

$a_0$ ,  $a_1$  and  $a_2$  are given by<sup>4</sup>

$$a_0 = 1/45 (\beta \Delta g H_0 / \hbar)^2 * (4J_0 + 3J_1) + (1/20) b^2 (3J_0 + 7J_1) + a_0(SR) + K \dots (30)$$

$$a_1 = -(1/15) b (\beta \Delta g H_0 / \hbar) (4J_0 + 3J_1) \dots (31)$$

$$a_2 = (1/40) b^2 (5J_0 - J_1) \dots (32)$$

where  $H_0$  is the applied magnetic field,  $J_0 = \tau_c$  or  $\tau_e$ ,  $J_1 = \tau_e / (1 + \omega^2 \tau_e^2)$ , where  $\omega$  is the microwave frequency,

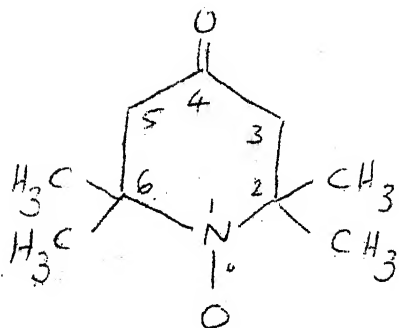
$$g = g_{\parallel} - g_{\perp} \quad \text{where } G = \begin{pmatrix} g_{\perp} & g_{\perp} & g_{\parallel} \end{pmatrix}$$

and  $b = 2/3 (A_{\parallel} - A_{\perp})$ , where  $A = \begin{pmatrix} A_{\perp} & A_{\perp} & A_{\parallel} \end{pmatrix}$ , in radians/sec.  $a_0(\text{SR})$  is a spin-rotational contribution discussed above.  $K$  accounts for still other sources of broadening such as still unresolved hyperfine splitting.

In the expression for linewidth Eq (30), it is seen that the  $m_H$  dependence is negligible and hence any linewidth contribution is directly related to the quantum number  $m_N$ . The assumptions that are further adopted in the study are: (1) the hyperfine splitting constant  $a_H$  is the same for all lines in a single manifold, i.e. the spacing between two hyperfine lines in a given manifold is the same. Although this is not correct according to the theory, the variations have so far been not calculated. (2) The second assumption is that each hyperfine line of a given manifold has the same width  $W_H$ . This of course follows from the theory of anisotropic g-tensor and dipolar interactions perturbation on linewidth. It is further assumed that the lines are Lorentzian although the overall lineshape need not be Lorentzian.

Eq (30) contains two important parameters that would tell us about the structural and dynamic factors in solution wherein the probe is tumbling rapidly such that  $\omega_0 \tau_c^2 \ll 1$ .

First of all we can find out the correlation time for reorientation of the tumbling molecule. Before we go further it would be relevant to dwell on the ESR aspect of the probe used, the free radical:



(2,2,6,6-Tetramethyl-piperid-4-one-1-N-oxide, TEMPO)

As we have noted earlier, the unpaired electron resides mostly on the nitrogen atom. Interaction with the nuclear spin of  $I=1$  of the  $N^{14}$  nucleus gives rise to  $(2I+1) = 3$ , lines, of manifold  $m_N = 0$  and  $\pm 1$ . From the studies of g-tensor anisotropy<sup>5</sup> it has been established that the high field line is generally the  $m_N = -1$  line and is less intense than the  $m_N = +1$  line, which in turn is less intense than the  $m_N = 0$  line. Theoretically we expect each of these nitrogen lines to be split further by the 12 equivalent methyl protons as also the methylene protons but in practice or experimentally is not observed because the ratio  $W_H/a_H$  is much less than 5, such that mutual overlap of the hydrogen hyperfine lines obscure and defy resolution. All we record is a single line which contains all these hyperfine lines buried in the overall single line.

It is seen that we observe the three nitrogen lines and it is from the intensities of these three lines that  $\tau_C$  can be calculated. Considering Eq (30) we have

$$T_2^{-1}(m) = a_0 + a_1 m + a_2 m^2$$

Dividing by  $a_0$  and rearranging we have



$$T_2(0)/T_2(m) = 1 - a_1 m/a_0 - a_2 m^2/a_0 \quad \dots (33)$$

Effectively the ratio of widths or the inverse of ratio of square root of height of peaks gives us an equation, i.e.,

$$\begin{aligned} T_2(0)/T_2(m = \pm 1) &= 1 - a_1 m/a_0 - a_2 m^2/a_0 = \\ &= (\text{peak ht. for } m=0/\text{peak ht. for } m=\pm 1)^{1/2} \quad \dots (34) \end{aligned}$$

From Eq (34) we can evaluate  $a_1$  and  $a_2$  if we know  $a_0$  and the peak heights for the three nitrogen lines.  $a_0$  is obtained straightaway from the central line since  $a_0 = \sqrt{3} \Delta H$ , the width of the central line. Measuring the peak intensities for the  $m_N = +1$  and  $-1$  lines we get two equations in  $a_1$  and  $a_2$ . From  $a_1$  or  $a_2$  and equations (31) and (32)  $\tau_C$  can be calculated. The values reported here are from  $a_1$  only and follow the method given by Stone, et al.<sup>6</sup>, where  $\tau_C$  is given by

$$(a_1 - a_{-1}) * (-8 b \Delta \gamma B_0 / 15 \sqrt{3} W_0)^{-1} \quad \dots (35)$$

where  $a_1$  and  $a_{-1}$  are the square root of ratios of peak heights for  $m_N = 1$ :  $m_N = 0$  line and  $m_N = -1$ :  $m_N = 0$  lines respectively,  $b$  here is given by  $4\pi(A-B)/3$ , where  $A = A_{||}$  and  $B = A_{\perp}$  in previous notation,  $\Delta \gamma = -[g_Z - 1/2(g_X + g_Y)] \beta e/h$ ,  $B_0$  = applied magnetic field and  $W_0$  is the width of the central line.

Eq (30) can also give us the hyperfine hydrogen line-width since we know the linewidth expression. As noted

earlier there are 13 hydrogen lines and the 4 methylene protons have to be considered. It has been assumed that each line is Lorentzian and with a width  $W_H$  given by Eq (30). To avoid complicated computerization and to exclude all m-dependent broadening terms, the simulation was restricted to the  $m_N = 0$  manifold and the width was straightaway used. A standard program of non-linear least-squares method was used with modifications and the overall fit was taken for the central part of the envelope as broadening mechanisms too complicated to assess theoretically enter as the spectra tapers off at the two ends. Reproducibility was excellent and the fitting unique provided reasonable parameters were used as initial values. The  $a_H$  was taken to be 0.065 gauss but simulation of widths were tried using the value of 0.10 gauss reported in literature for TEMPO. They are both qualitatively similar except for a magnitude difference in linewidth values and we prefer to choose the former set because of consistent linewidth.

We thus obtain the linewidth  $W_H$  of the hydrogen hyperfine line, which is more sensitive to viscosity changes than  $\Delta H_{pp}$  and also  $\tau_C$  which reflects the time taken for one rotation. There is in addition another correlation time  $\tau_J$  which though not experimentally obtained can be calculated using appropriate models. Before we give a brief summary of Jolicouer & Friedman's work it is necessary to keep in mind

that the  $g$ -tensor and dipolar perturbations vary as  $(\eta/T)^1$ , whereas the spin-rotational effect  $a_0(\text{SR})$  varies as  $(T/\eta)$ . Further the contribution to the linewidth from the methylene protons has been neglected and the van der Waal's radius of the probe has been taken to be 2.8 Å in this study. As is clear the theory applies only to a free radical rapidly tumbling in solution or when  $\omega_0 \tau_c^2 \ll 1$ .

The linewidth and  $\tau_c$  values as outlined above were simulated and calculated for systems involving hydrophobic interactions, by Jolicœur and Friedman.<sup>7</sup> They have plotted width against  $(T/\eta)$  at room temperatures and obtained plots which followed the Kivelson behaviour i.e.  $W_H = k_1(T/\eta) + k_2(\eta/T)$ . Deviations from this behaviour were taken to be indicative of hydrophobic interactions contributing to the linewidth altering (mostly broadening) mechanism.

In their study Jolicœur and Friedman have used glycerol as a standard compared to which one can estimate the deviation.  $\tau_c$  values that were obtained were corrected for viscosity or medium effect and using such plots, they have clearly demonstrated the gradual changes that occur when long chain compounds having both polar as well as non-polar groups interact with water. For example, in the series  $n\text{-hexyl NH}_3^+ \text{Br}^-$  to  $n\text{-octyl NH}_3^+ \text{Br}^-$ , there is a smooth transition which takes into account micelle formation in  $n\text{-octyl ammonium bromide}$  solutions. The explanation for certain solutes like

$\text{NaBPh}_4$  is also understood in terms of ion-dipole interactions in solution and the results confirm this aspect although it is hardly hydrophobic in character. The most interesting hydrophobic solute for which an explanation has not been advanced conclusively is the n-tetrabutyl ammonium bromide salt. It has been known to form aggregates in solution but  $\tau_c$  studies of Jolicœur and Friedman reveal that  $\tau_c$  is insensitive to clustering. This led them to speculate on a spin-rotational contribution effect which somehow broadens the lines at concentrations where glycerol shows a minimum in  $W_H$  vs  $T/\eta$  plots. It is reasonable not to expect the g-tensor elements to vary much and hence they believe that the changes that occur are due to changes in  $\tau_j$ . Estimation of  $\tau_j$  based on a Debye sphere model tells us that  $\tau_c$  and  $\tau_j$  are inversely related. This in turn led to the failure of the one-state model used by them and they speculate in terms of a two state model wherein two different states are obtainable and the average of the two states is what is experimentally detected.

Their results are based on the Kivelson-type plots and it is essential to understand the importance of a  $T/\eta$  or an  $\eta/T$  variation of the width parameter. We could plot width against  $\eta/T$  as well and still, obtain the optimum. These studies were carried out at room temperatures and the variant here is the viscosity of the solution. Such a plot thus takes into account changes that occur due to changes in

viscosity of the medium. A better guide to the structural changes affecting the rotation of the probe would also be to apply a medium viscosity correction to the correlation time, as has been used by Jolicoeur and Friedman. Plots of  $\tau_c/\eta$  against concentration of solute would reflect changes that enter solely through structural factors involved in the solute-solvent interaction.

In our treatment of solutes like urea, GuHCl and tetra-n-amyl ammonium bromide (TAAB), which are interesting because of their denaturing and hydrophobic properties, we have followed the Jolicoeur and Friedman format to a large extent. In addition to this we have also attempted to estimate the  $a_0(\text{SR})$  contribution. Since  $a_0(\text{SR})$  is the only term which varies as  $T/\eta$ , a plot of  $W_H$  versus  $T/\eta$  with changing temperature, if linear, would reflect the magnitude of  $a_0(\text{SR})$  in its slope. This estimation is to a very low order in accuracy but yet we feel it is quite a relevant and interesting yardstick to the changes that overtake  $\tau_J$  and thus also the linewidths.

## EXPERIMENTAL

The spin probe used in this study 2,2,6,6-tetramethyl-4-piperidone-N-oxide (TEMPO), was synthesized by the procedure described by Rozantzev et al.<sup>8</sup> The scheme is as follows: A mixture of acetone and calcium chloride (anhydrous) is

stirred well while ammonia gas is passed through the mixture and condensed with the use of a liquid nitrogen trap, at intervals of 15 minutes for 5-6 hours. The resulting dark and strong smelling liquid mass is left overnight and then processed to obtain the amine, triacetoneamine, which when oxidized with hydrogen peroxide in the presence of a catalyst like sodium tungstate gives the desired compound. The product was recrystallized at least twice from a mixture of ether and n-hexane. The analysis of this compound, TEMPO, was found to be satisfactory.

The water used was deionized distilled water obtained by passing doubly distilled water through a Barnstead mixed-bed ion-exchange resin column. All other chemicals were Analar Grade or better through recrystallizations.

In a typical experiment, a fresh solution of TEMPO in water was prepared and using this, solutes of interest are dissolved. A small portion of the desired solution is then flushed with  $N_2$  gas exhaustively to free any dissolved oxygen. The deoxygenated solution is quickly transferred to a pyrex sample tube of inner diameter of 1 mm and sealed. The spectrum was recorded using a Varian V-4502 spectrometer (12 in. magnet) operating at a frequency of 9.5 GHz. Ambient temperature was around  $27^\circ C$ , and where temperature variation studies were made a Varian E4 (4 in. magnet) spectrometer with a V-4540 thermostat unit was used. The

modulation amplitude used was at least four times lower than the setting at which lineshapes are affected. Probe-probe association has been reported for TEMPO in solution, and to avoid this artifact to linewidths, the concentration of TEMPO was maintained below  $5 \times 10^{-4}$  M. The modulation frequency used while recording the spectra was 100 KHz, while the time required to scan the peak-to-peak width was about a minute.

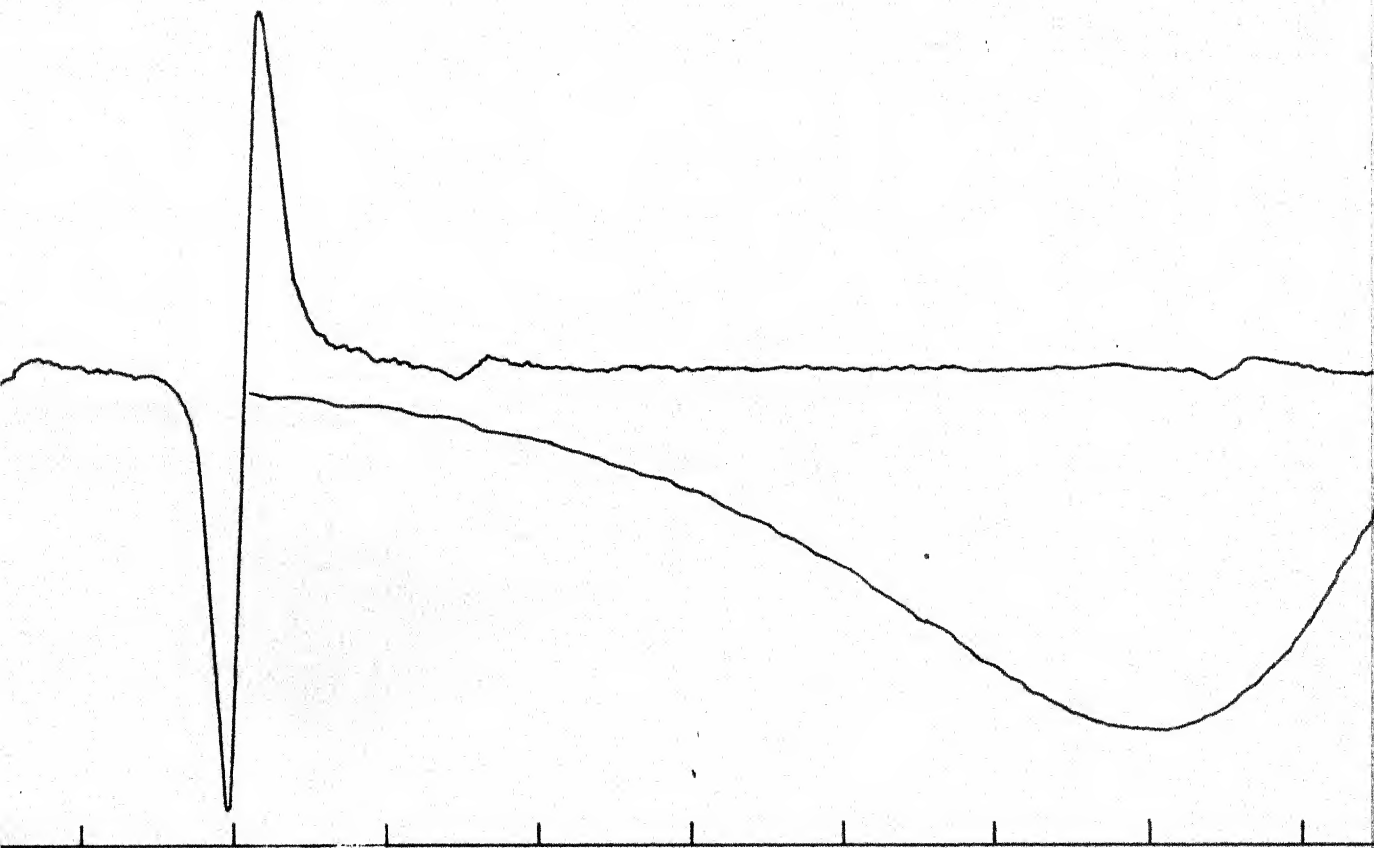
Reproducible spectra were obtained under these conditions and for a given typical sample the reproducibility of linewidths was within 10-15 mG. A typical spectra is shown in Fig. II.1.  $a_N$  was found to be 15.6 gauss.

In the analysis of spectra recorded as described above, a non-linear least squares method was adopted to obtain the overall envelope of the observed line after simulating the thirteen hydrogen hyperfine lines, lying buried in the envelope, assuming a Lorentzian lineshape for each one of these thirteen lines. The buried parameters were then obtained through an iterative process converging to the final value from a set of initial values. At least two sets were run for a single spectrum comprising a minimum of 20 experimental, observed data points. The convergence is unique provided reasonable initial values are assigned.

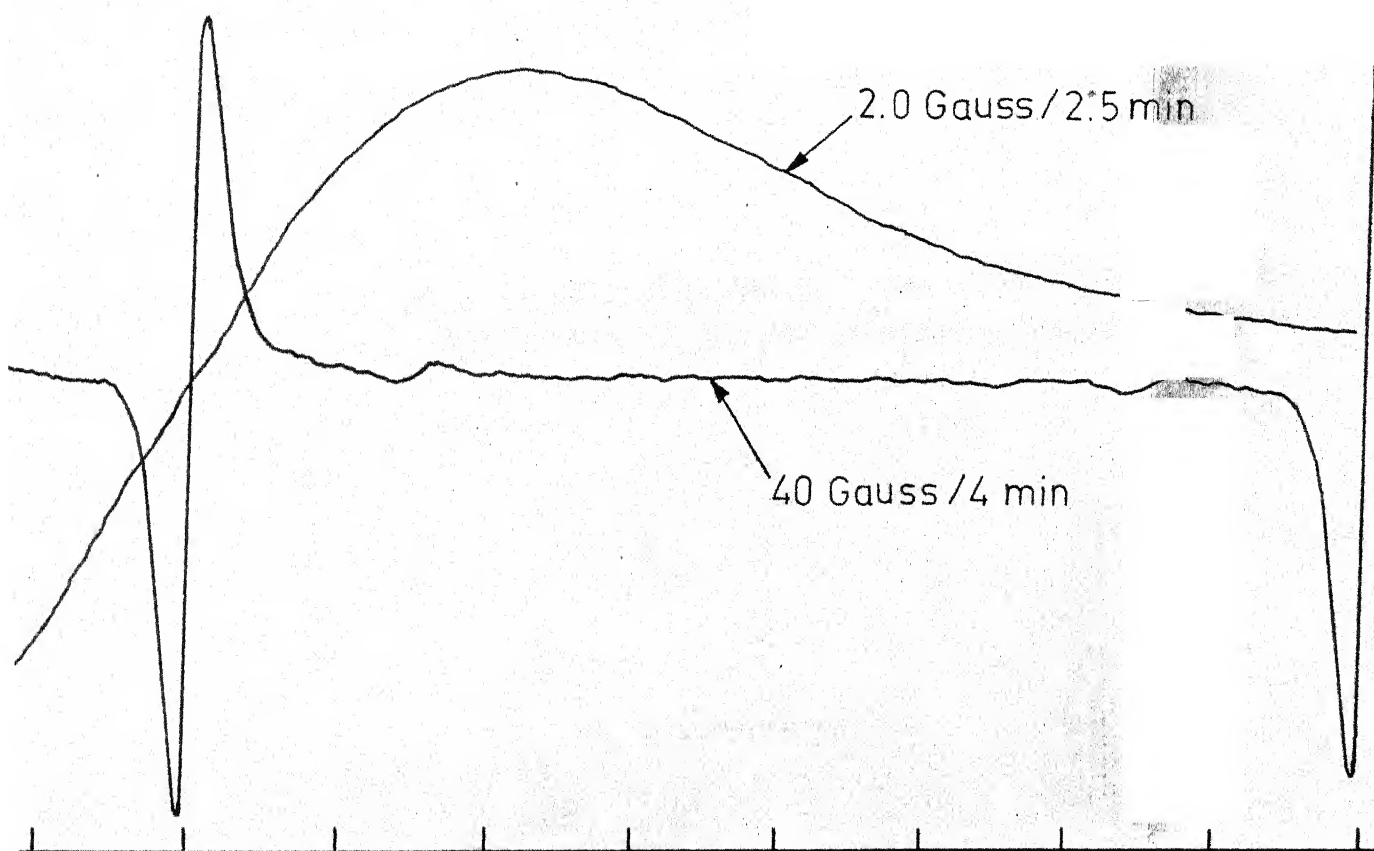
For the calculation of the correlation time of the tumbling probe knowledge of the  $b$  and  $\Delta g$  quantities is

Fig. II.1: ESR spectrum of the spin probe TEMPO showing the three lines due to the nitrogen nucleus and the  $m_N = 0$  manifold separately. The spectrum obtained at 40 gauss scan and a 4 min. scan rate was used to obtain  $a_N$  values while the spectrum at 2 gauss scan and 2 min. scan rate is the  $m_N = 0$  manifold and was used for the simulation to determine  $W_H$ , the width of the proton hyperfine line.





Magneti



0

netic field  $H_0$  , gauss  $\longrightarrow$

essential. Since the values of  $b$  and  $\Delta g$  have not been measured directly for the probe, TEMPO, the values obtained for the similar radical di-tert-butyl-nitroxide, by Griffith, et al.<sup>9</sup> have been used here.

REFERENCES

1. See e.g. Ayscough, P.B. (1967) "Electron Spin Resonance in Chemistry", Methuen, London.
2. Wilson, R. and Kivelson, D. (1966) J. Chem. Phys., 44, 154.
3. Atkins, P.W. and Kivelson, D. (1966) J. Chem. Phys., 44, 169.
4. Edelstein, N., Kwok, A. and Maki, A.H. (1964) J. Chem. Phys., 41, 179.
5. Carrington, A. and Longuet-Higgins, H.C. (1962), Mol. Phys., 5, 447
6. Stone, T.J., Buckman, T., Nordio, P.L., and McConnell, H.M. (1965) Proc. Natl. Acad. Sci. U.S., 54, 1010.
7. Jolicoeur, C. and Friedman, H.L. (1971) Ber. Bunsenges. Physik. Chem., 75, 248.
8. Rozantzev, E.G. and Nieman, M.B. (1964) Tetrahedron, 20, 1310.
9. Griffith, O.H., Cornell, D.W. and McConnell, H.W. (1965) J. Chem. Phys., 43, 2909.

### CHAPTER III

#### SPIN PROBE STUDIES ON THE EFFECT OF UREA- CLASS DENATURANTS ON WATER STRUCTURE

Compounds belonging to the urea-guanidinium class function as effective agents in the unfolding of globular proteins in solution and are termed denaturants. The role of these in the denaturation of proteins in solution has not been understood completely. There are two mechanisms by which this process can take place. One is the direct interaction of the denaturant with the macromolecule which brings about conformational changes leading to denaturation. The second mechanism involves a solvent structural change induced by the agent and this perturbation would then manifest itself in altering the solvent-macromolecule interactions and enable the macromolecule to unfold, causing denaturation. One could also envisage a process in which the above two mechanisms operate simultaneously. In the present chapter we shall be concerned with the validity of the second

has been called the hydrophobic interaction.<sup>1</sup> It is important to realize that this large-entropy term involved in hydrophobic interactions arises due to the unique hydrogen-bonded polymeric structure of liquid water. Therefore, changes in the structure of water might be expected to have important and direct bearing on the hydrophobic interaction. Any solute that alters water structure would indirectly affect the hydrophobic interaction itself and if such a situation exists, then the solute would also affect the conformation of a protein in aqueous solution since the hydrophobic interaction would be expected to be modified as a result of the alteration of the structure of water.

To understand the process by which such a destabilizing or denaturing takes place we have to study the solvent changes and construct a possible mechanistic pathway. Of all the reagents that are known to denature proteins in aqueous solution, urea has been studied most extensively. Urea in water has remarkable properties. For example, it enhances solubility of hydrocarbons,<sup>2</sup> inhibits micellar aggregation of surfactants<sup>3</sup> and affects the conformational properties of a wide range of water-soluble polymers.<sup>4</sup> The solubility of urea in water is greater than 20 m at 25°C. In addition, the urea-water interactions are similar to urea-urea interactions in the fused state and water-water interactions in pure water. A large amount of research has been carried out on urea-water systems, a fair reflection of the importance of urea as a denaturant as well as

the controversy that evolves around its role in protein denaturation. In addition to thermodynamic studies of urea in water as binary and in ternary systems,<sup>5,6</sup> spectroscopic studies are also abundant. NMR,<sup>7</sup> IR,<sup>8</sup> Raman scattering<sup>9</sup> and Ultrasonic attenuation studies,<sup>10,11</sup> supported by volumetric data<sup>12</sup> have all shown that urea does show a concentration-dependent effect on liquid water structure and measurement of properties of aqueous urea at one single concentration is not sufficient to predict urea behaviour.<sup>13</sup>

The general conclusion that is reported by most workers is that urea is a structure breaker although there have been instances where urea was reported to be a structure maker.<sup>14</sup> Others<sup>15</sup> have suggested that a monomer-dimer equilibrium exists in aqueous urea solutions but failed to explain the structuring properties. The most important conclusion that we can draw from these experimental studies is that none of these experimental techniques has been found to conclusively prove one mechanism or the other. This drawback arises out of the fact that the time of equilibrium in liquid water is of the order of  $10^{-11}$  sec and so far all the methods employed have characteristic times of measurement many orders of magnitude larger than this equilibrium time. Nevertheless the conclusions drawn are a useful pointer in the present study which takes a microscopic look at the urea-water system through the ESR technique with a time scale of measurement of the same order as that of the equilibrium time.

Equilibrium thermodynamic studies<sup>5</sup> on urea in water showed that the results could be interpreted in terms of little alteration in water structure upon adding urea at low concentrations, while urea does disrupt water structure at high molarities (7 M). Infrared spectral studies on aqueous urea (and urea derivatives) by Swenson<sup>8</sup> showed again little effect of these additives on water structure. Raman spectroscopy<sup>9</sup> does indicate that urea disrupts water-structure but less efficiently than bromide ion. Ultrasonic attenuation studies in aqueous urea by Hammes and Schimmel,<sup>10</sup> and by Arakawa<sup>11</sup> reveal that urea is a structure-breaking solute. By far the most convincing study has been by Finer, Tait and Franks<sup>7</sup> who have studied the nitrogen nuclear magnetic relaxation of urea (and O<sup>17</sup> linewidths) over a wide concentration range in water. This study reveals that urea disrupts water structure at all concentrations, urea-water hydrogen bonding is short-range and short-lived and also urea is not able to penetrate water clusters. They see the role of urea as a statistical structure breaker,<sup>16</sup> i.e. it shifts the cluster:monomer equilibrium of solvent water towards the monomer microphase. The need for <sup>an</sup> independent technique that is able to monitor the effect of urea in water structure is thus obvious.

Derivatives of urea have also been used as denaturants of proteins and biopolymers in aqueous solution. It has been known that thiourea and guanidinium salts are effective



denaturants,<sup>17</sup> while thiourea has limited solubility ( $<3 \text{ M}$  at  $25^{\circ}\text{C}$ ), guanidinium chloride is highly soluble and is a better denaturant than urea.<sup>18</sup> Among methylated ureas, N-methyl urea and N,N'-dimethyl urea are weak denaturants with the former somewhat better compared to the latter. Tetramethyl urea does not denature proteins and indeed has been seen to behave as a renaturant. The progressive substitution of methyl groups is apparently a factor that weakens the denaturing ability. Studies on their behaviour towards water structure are very few. Thermodynamic study<sup>5</sup> revealed thiourea to behave very similar to urea while guanidinium chloride was found to disrupt water structure. Infrared spectral measurements on aqueous solutions of several urea derivatives<sup>8</sup> showed no correlation between the spectral shifts and denaturing ability. There are no n.m.r. measurements available on these systems, but ultrasonic attenuation studies by Arakawa and coworkers<sup>11, 19</sup> have shown that N,N'-diethyl urea is a structure-maker, N,N'-dimethyl urea is weak structure-breaker, urea a good structure breaker, and guanidinium chloride a structure breaker better than urea.

As mentioned earlier, reported studies on the effects of solutes on water structure have employed methods that are too slow in their time scale of measurement compared to the 10 psec time-scale involved in the dynamics of water structure, or too fast. It would thus be very desirable if we were to choose a method wherein the time scale of reporting is comparable to that of the

molecular events occurring. The use of ESR spin probe method, as pioneered by Jolicoeur and Friedman,<sup>20</sup> has this advantage, and thus would be able to offer more or less a direct monitoring possibility that was not possible in other techniques.

### EXPERIMENTAL

The experiments involved measurement of the hyperfine linewidth, and the peak intensities of the  $m = 1, 0, -1$  lines in the ESR spectrum of  $5 \times 10^{-4}$  M TEMPO in aqueous solutions of urea, and of its analogues at several temperatures. The experimental details are given in Chapter II, as also the method of determining the hydrogen hyperfine linewidth, tumbling correlation time  $\tau_e, \tau_j$ , and the spin-rotation interaction coefficient  $a_0$  (SR).

Analytical reagent grade urea obtained from BDH Ltd. was used as such. Guanidine hydrochloride was recrystallized from water containing hydrochloric acid at  $\text{pH} = 4.6$  and dried in vacuum at  $60^\circ\text{C}$ . Thiourea was recrystallized from ethanol and dimethyl urea (sigma) from isopropanol. The water used was deionized distilled water obtained by using a Barnstead mixed-bed ion-exchange resin column.

Fresh solutions of the desired compounds were made and degassed with nitrogen to remove any dissolved oxygen. The

ESR spectra were then recorded using pyrex sample tubes.

## RESULTS AND DISCUSSION

The e.s.r. spectra of TEMPO in aqueous solutions of the various denaturants were recorded and the computer simulation of the observed  $m_N = 0$  manifold by non-linear least-squares fit yielded  $W_H$  values.  $\tau_\theta$  were calculated from the intensity ratios of the  $m_N = 0 : m_N = \pm 1$  lines. We discuss each of these separately.

### (1) Urea Solutions

Table III.1 lists the hydrogen hyperfine linewidth values,  $W_H$ , (computed using a nonlinear least square curve fitting program on the experimental e.s.r. spectra of TEMPO in urea solutions), tumbling correlation time  $\tau_\theta$  (calculated from the intensities of the  $m = 0$  and  $m = \pm 1$  lines of the e.s.r. spectra as per Equation II.35), and the statistical parameters of the fit. Figure III.1 shows the variation of the tumbling correlation time of TEMPO in urea solutions, and Figure III.2 is a plot of the reduced  $\tau_\theta$  value, i.e., the ratio  $\tau_\theta/\eta$  versus molarity of urea. The ratio  $\tau_\theta/\eta$  in effect corrects for the bulk viscosity of the medium, a factor that directly influences the value of  $\tau_\theta$ . The corrected ratio removes the effect of the bulk viscosity and is expected to reflect motional effects of the probe caused by changes that have occurred in the solvent structure.

Table III.1

Computed ESR parameters, error function, error limits and  
Tau values for TEMPO in aqueous urea

$a_H$ Fixed at 0.065 gauss			Room temperature $\approx 27^\circ\text{C}$		
Concen- tration	Hyperfine linewidth $w_H$ (gauss)	Normalizing parameter $B(3)$	Error function PHI	Standard error for $w_H$ SE	Correlation time $\tau_\theta^* \times 10^{12}$ sec
1 $\overline{M}$	0.270	0.1130	0.65	0.0130	10.65
2 $\overline{M}$	0.245	0.0826	0.17	0.0071	6.025
3 $\overline{M}$	0.200	0.1090	0.13	0.0038	18.38
4 $\overline{M}$	0.221	0.0617	0.43	0.0136	15.96
5 $\overline{M}$	0.245	0.0705	0.50	0.0142	18.00
6 $\overline{M}$	0.221	0.1370	2.20	0.0139	15.76
7 $\overline{M}$	0.206	0.0521	0.20	0.0104	14.53

\*Tau values were calculated using the line intensity ratios according to the method described by Stone, T.J., Buckman, T., Nordio, P.L., and McConnell, H.M. (1965) Proc. Natl. Acad. Sci. U.S., 54, 1010.

lumbling correlation time  $\tau_g$  in picoseconds

$T = 27^\circ\text{C}$

Molarity of urea

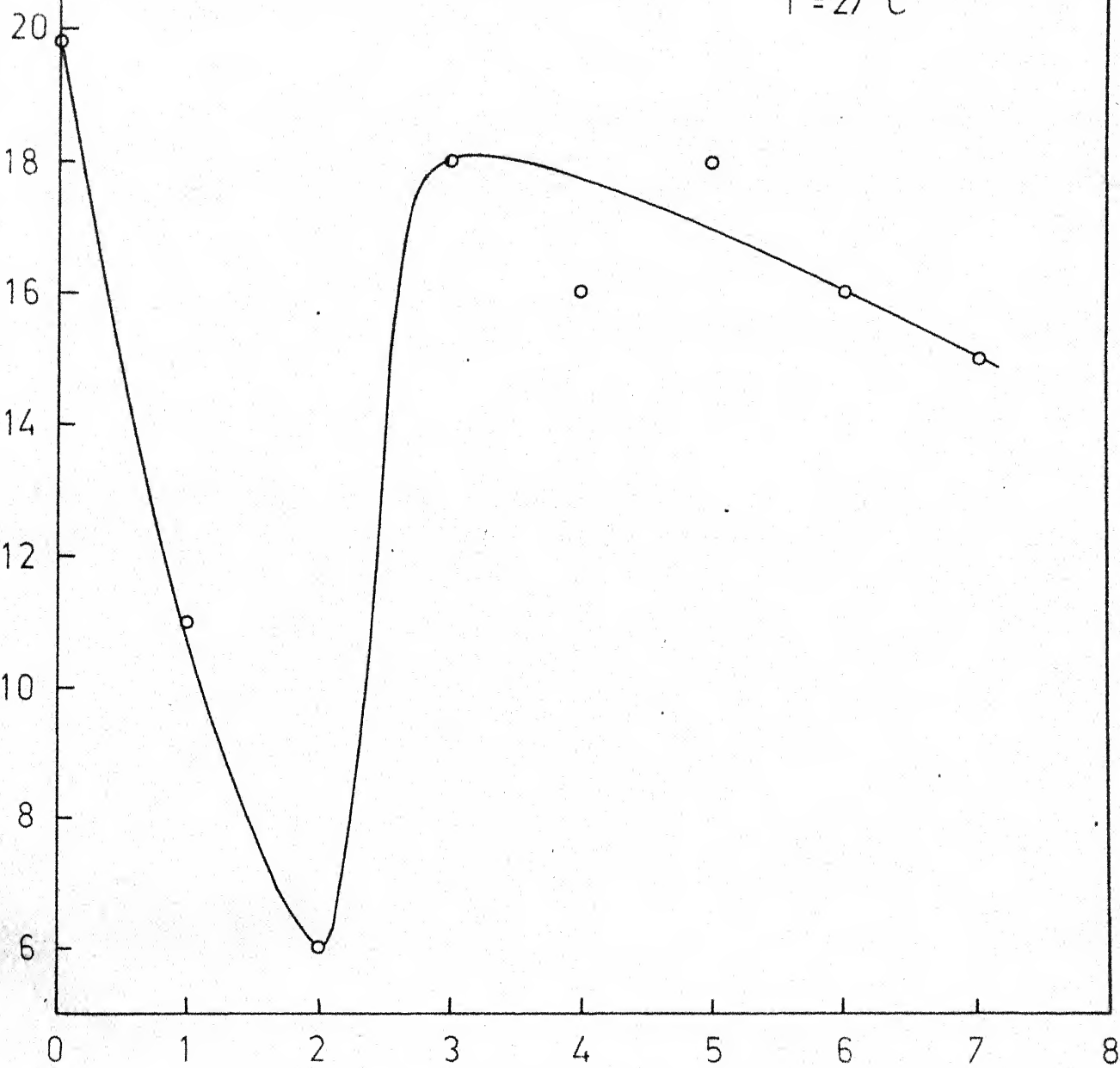


Fig. III.1: Tumbling correlation time  $\tau_c$  of the spin-probe TEMPO as a function of molarity of urea.

Fig. III.2: Tumbling correlation time corrected for viscosity,  $\tau_{\theta}/\eta$  as a function of molarity of urea.

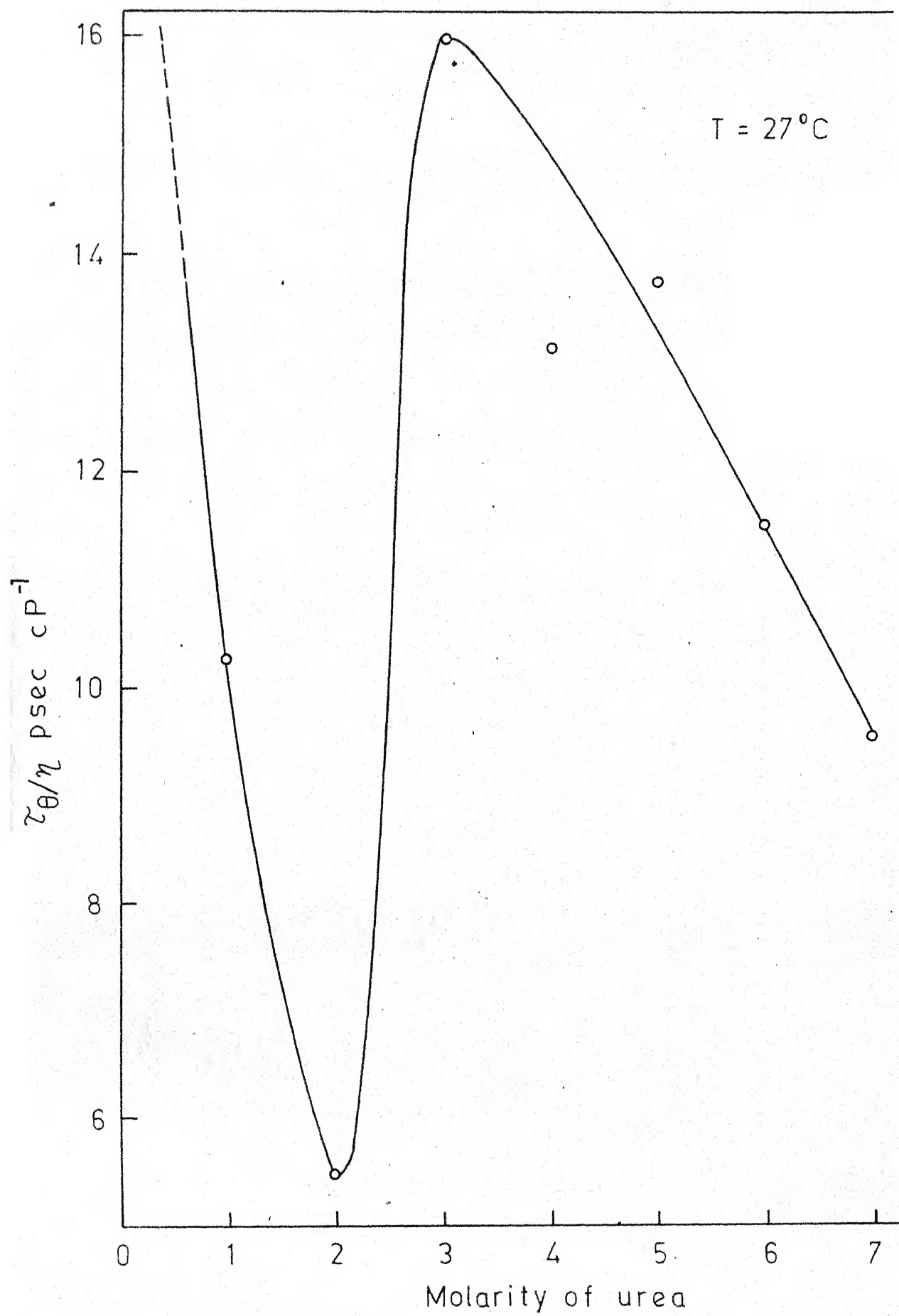




Figure III.1 displays the variation of the tumbling correlation time in increasing molarities of urea. It is striking that rather than vary in a linear fashion (as happens in solutions of aqueous glycerol),  $\tau_{\theta}$  decreases to a minimum value of 6 psec at 2 M urea, to increase again to 18 psec in 3 M, followed by a near constant value of 15-16 psec beyond 3 M urea. The usual reference used in such studies is aqueous glycerol where it is generally assumed that no structural alteration of liquid water occurs upon adding glycerol.<sup>20</sup> Between 0-50%  $\tau_{\theta}$  is found vary strictly linearly essentially reflecting bulk viscosity changes in the medium. It has also been suggested that motion of the probe may not be sensitive to solute-solute aggregation, or to small changes in the 'local' viscosity of the environment around the probe.<sup>20</sup> In light of this, it is remarkable that  $\tau_{\theta}$  varies in the fashion described in Figure III.1 in urea solutions. It is evident that rather drastic changes are occurring in the neighbourhood of the spin probe molecule that are reflected in its tumbling motion. Let us first look at the possibility of probe molecules interacting among themselves or with solute molecules. Jolicoeur and Friedman<sup>20</sup> have deduced that probe-probe association is negligible below  $5 \times 10^{-4}$  M, and accordingly we chose TEMPO concentrations below this value to avoid probe-probe aggregation in all our experiments. Regarding the interaction between the probe and solute or solvent molecules, the following points should be noted. In light of the size of TEMPO, a

van der Waals radius of 4 Å, it appears unlikely that it would be accommodated inside the cavities of clustered water molecules. However, it is to be noted that if the probe is assumed to rotate in solution following the Debye-Stokes hydrodynamic model, its hydrodynamic radius turns out to be about 2 Å. One is not completely justified then in ignoring the possibility of TEMPO molecules entering and occupying cavities in the water clusters that exist in liquid water. In such a situation, the spin probe may find itself in the cluster microphase or in the dense depolymerized microphase of liquid water with equal ease. The e.s.r. signal will be a composite one reflecting both environments and the calculated  $\tau_\theta$  a weighted average of both situations. The interactions between the probe and solvent water are expected to be, if any, of dipolar and hydrogen-bonding types. A probe occupying the cavity in a cluster will be expected to be well-bound by these forces. That probe-water interactions do occur is seen from the  $\tau_\theta$  value of TEMPO in water (20 psec), while  $\tau_\theta$  in methanol,  $\text{CCl}_4$  or  $\text{C}_{12}\text{H}_{26}$  are less than 10 psec,<sup>20</sup> the latter two solvents are more viscous than water. Interaction between the probe and urea molecules are expected to be of the same type as between it and water.

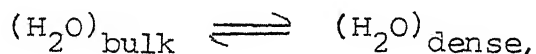
The data in Figure III.1 (and in Figure III.2) reveal broadly three regions in aqueous urea solutions, where the spin probe shows different trends of tumbling motion. Region I is from 0-2 M urea, where  $\tau_\theta$  for TEMPO drops from 20 psec to about

6 psec, despite an increase in the solvent bulk viscosity from 0.89 cP to 0.97 cP. In Region II that spans 2-3 M urea solutions,  $\tau_e$  shows a large increase from 6 psec to 18 psec, and this is followed by the Region III, beyond 3 M urea, where  $\tau_e$  drops gradually to 15 psec at 7 M. It thus appears that, as the concentration of urea in water is increased, the spin probe senses in effect three distinct kinds of micro-environments around it. Before we attempt to explain this, a brief review of the existing information from earlier work on aqueous urea systems may be in order.

The recent review by Sarma and Ahluwalia<sup>23</sup> has summarized various viewpoints about the effect of urea on water structure. The point of view that urea increases water structure,<sup>14</sup> originally raised in 1965 has since been proved incorrect. Thermodynamic evidence<sup>5</sup> and spectral studies on aqueous urea systems suggest that at high concentrations, urea disrupts water structure while the results at low or moderate concentrations are not unequivocal. Raman scattering,<sup>9</sup> Ultrasonic attenuation,<sup>10, 11</sup> and  $N^{14}$ ,  $O^{17}$  and  $H^1$  resonance measurements<sup>7</sup> on aqueous urea solutions all point out that urea disrupts water structure at all concentrations. There has been some attention given to the self-aggregation of urea molecules in water also; while Schellman,<sup>15</sup> Krescheck and Scheraga,<sup>22</sup> Stokes,<sup>23</sup> and Vold et al.<sup>24</sup> have suggested that urea exists as intermolecular self-aggregates, Finer et al. have disputed this on the basis of  $N^{14}$  relaxation studies and

inferred that urea aggregation is virtually nonexistent. However urea-water interactions do occur but of short-range and are short-lived in nature. In addition to these, is the important paper by Frank and Franks<sup>16</sup> on the urea-water system, which considers the effect of urea as statistically disrupting water clusters to produce a shift in the water polymer-monomer equilibrium towards greater disorganization. The possibility of urea entering water clusters has been discarded on geometry grounds, as also the possibility of any urea-urea or urea-water interactions in extenso. In a sense, this treatment regards water as a two-microphase system (the bulky cluster microphase and the dense monomeric microphase) and the addition of urea as to statistically alter the population of water more into the dense microphase.

We then have the following situation obtaining when increasing amounts of urea are dissolved in water. The main effect of urea appears to perturb the equilibrium towards the right



with the perturbation increasing as more urea is added into the system. One of the consequences of this urea-induced depolymerization of water would be to reduce the size of a given cluster of (bulk) water. In pure water, the viscosity experienced by a given TEMPO molecule would arise jointly from the several clusters present and the monomeric water species. The size of

water, the number of monomeric water and urea molecules in the "dense" microphase increase. While Vold <sup>24</sup>et al. have suggested self aggregation of urea beyond 2 M, such associations have been discounted by the near constancy of the tumbling rates of urea molecules.<sup>7</sup> On the other hand, interactions between urea and water molecules to produce short-lived and short-range mixed aggregates do occur at these concentrations of urea, as seen by the retardation in the tumbling of urea molecules themselves. We thus have a possibility of the environment around the probe in the "dense" microphase of water being altered due to: (a) urea-water associations, (b) urea-urea aggregations, which still may persist as short-lived at short-range, (c) competition between urea and water for the solvation of the probe molecules, (d) interactions between urea and the water molecules of hydration that surround the spin probe, which in effect retards the hydrodynamic motion of the probe, and (e) an increase in the local viscosity of the dense microphase arising due to the transient urea-water hydrogen bonding. Any or all combinations of all these factors may contribute to produce an increase in the resistance to the tumbling motion of the spin probe. These effects occur together and side by side with the urea-induced melting of the bulk water clusters and region I and II essentially reflect the predominance of the two processes. The minimum in  $\tau_\theta$  at 2 M urea and the maximum at 3 M urea are thus not unique but essentially points where the depolymerization of

clusters (and the consequent increase in fluidity) and the changing solvation/solvent patterns arising due to urea-water (and in principle urea-probe) interactions offset each other.

Beyond 3 M urea, we propose that the melting of water clusters is predominantly complete and we have little bulk microphase left. Long-range order in water has been destroyed and liquid water exists to a very high extent as unstructured or "dense" molecules, interacting with each other and with solute urea molecules on a short-range and short-time basis. In effect then, the spin probe molecule sees essentially the same micro-environment beyond 3 M urea solutions, and the  $\tau_{\theta}$  value changes little, from 17 psec to 15 psec in the region 3 M - 7 M urea. At high concentrations of urea, i.e. 6 M or beyond the clusters are completely non-existent and the solvent consists of dense water only. At medium to high concentrations of urea, the increase in the medium viscosity effect (from 0.89 cP to 1.35 cP at 7 M) is more than offset by the decrease in the local viscosity around the probe due to cluster melting, that  $\tau_{\theta}$  is consistently smaller in urea solutions than in pure H<sub>2</sub>O.

Figure III.3 shows the variation of the computed hydrogen hyperfine linewidths  $W_H$  of TEMPO in aqueous urea. The linewidth attains a minimum of 0.2 G at 3 M urea, rises again until 5 M urea followed by a gradual drop upto 7 M urea. The behaviour resembles that of  $\tau_{\theta}$  itself. In Figure III.4, we plot the dependence of  $W_H$  on the factor  $T/\eta$  in order to estimate its

Fig. III.3: Proton hyperfine linewidth of the  $m_I = 0$  manifold of TEMPO,  $W_H$ , as a function of molarity of urea.

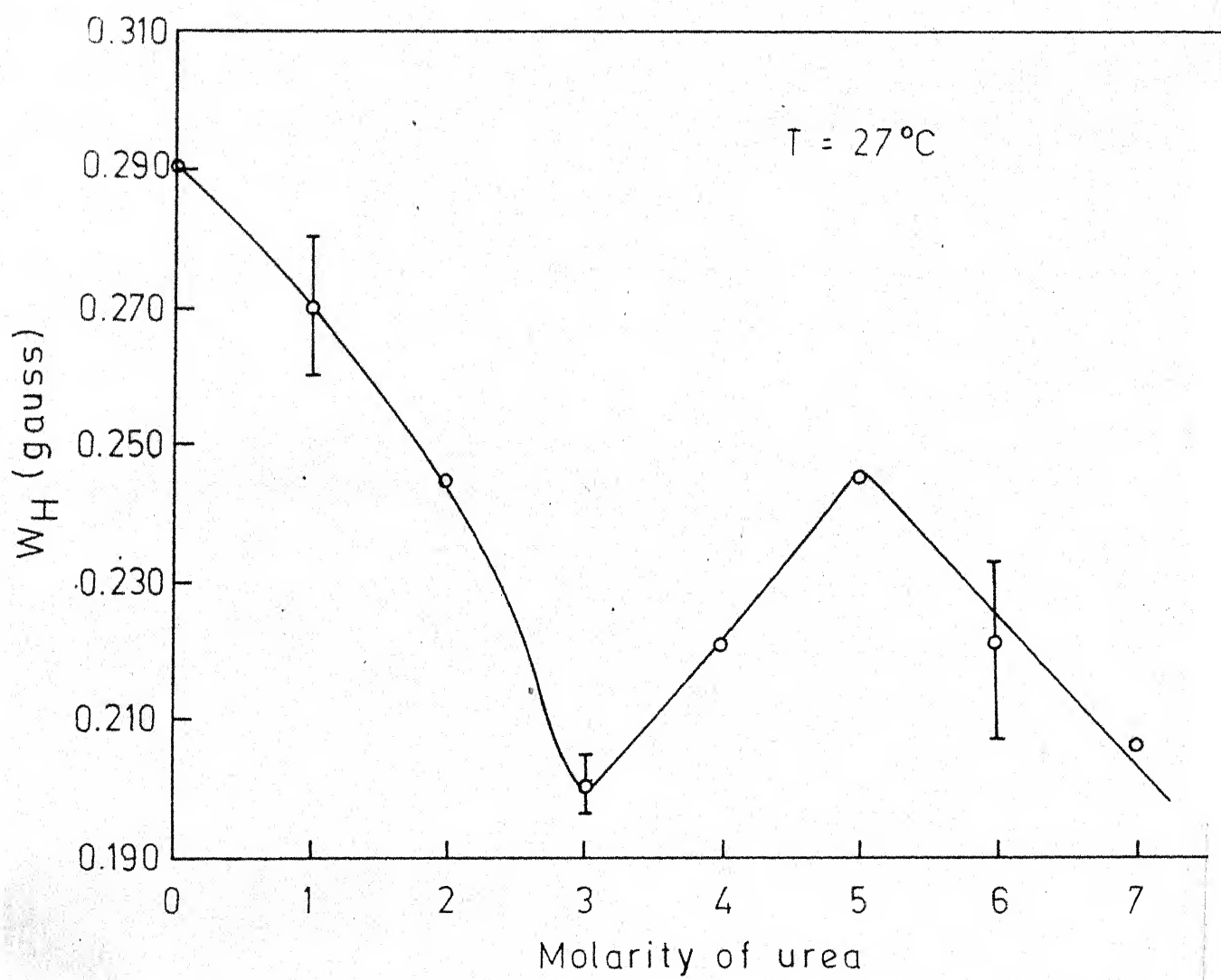
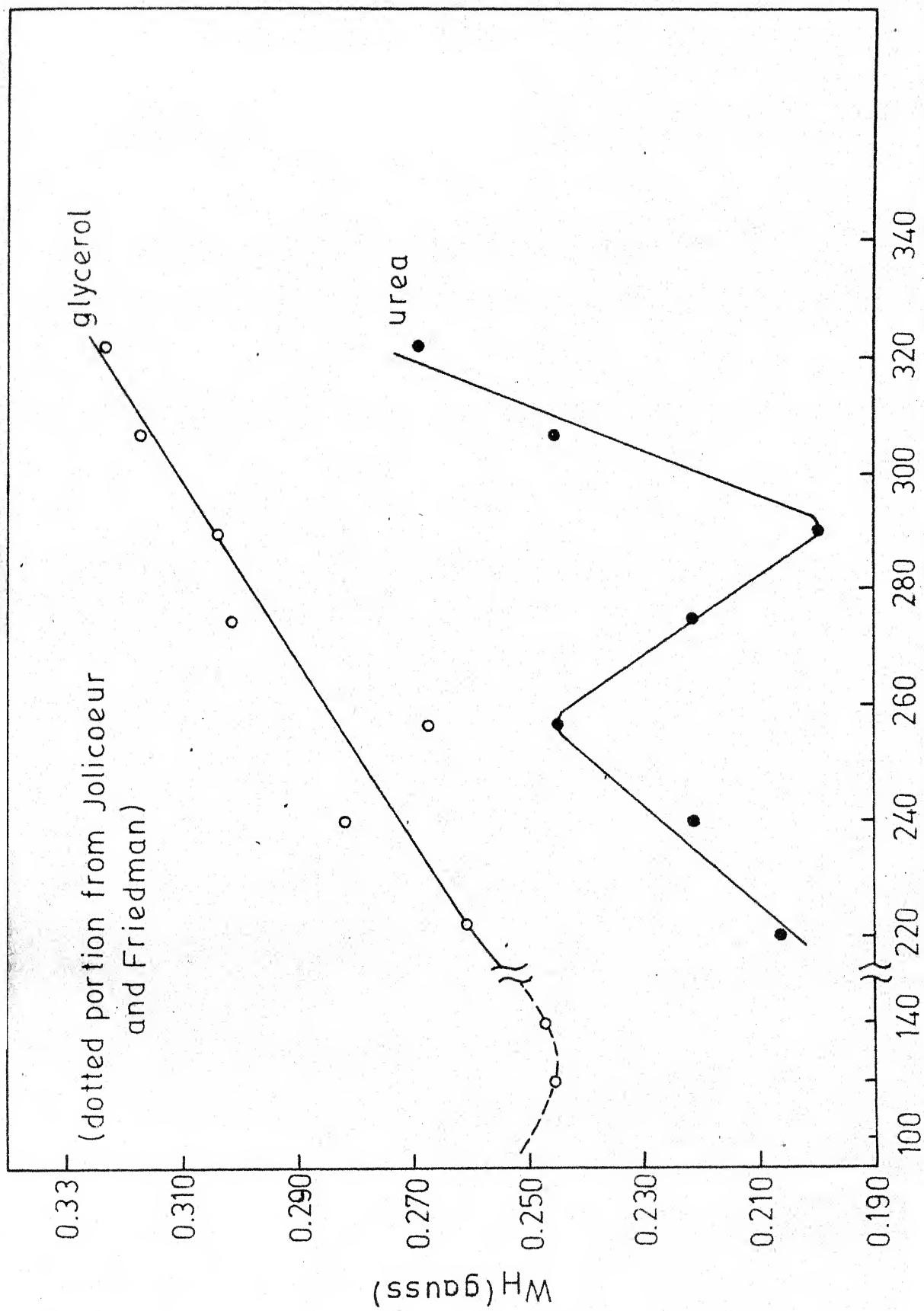




Fig. III.4: Proton hyperfine linewidth of the  $m_F = 0$  manifold of TEMPO,  $\Delta H$ , as a function of  $T/\eta$  at  $T = 298\text{K}$  for 1-7 M urea.



conformity to the Kivelson behaviour (cf. Equation I.3). In the same figure is plotted the behaviour of TEMPO in aqueous glycerol, an inert solute that allegedly does not disturb water structure. Under conditions where no structural effects arise, the plot should obey the relation

$$W_H = k_1 \left( \frac{kT}{\eta} \right) + k_2 \left( \frac{\eta}{kT} \right) + K \quad \dots (3)$$

While such a behaviour is indeed obtained obeying the above equation for glycerol, with a minimum in  $W_H$  at  $T/\eta = 1.3 \times 10^{-2}$  (K/cP), the curve for urea solutions is more complex. There are two optima obtained, reflecting that linewidth of TEMPO signals are governed by factors other than simple bulk viscosity effects. Interestingly, the linewidths in urea are smaller than in aqueous glycerol. This line narrowing ought to be consistent with the  $\tau_\theta$  results; we notice from Figure III.1 that it is indeed so. The  $\tau_\theta$  values for the probe in urea are consistently smaller than the value in glycerol solutions. The  $\tau_\theta$  values increase with increasing concentrations of glycerol, while with urea the values change in a rather unique fashion. The lack of any broadening of the line in urea solutions may be taken as an indication of the absence of any preferential interaction between the probe and solute urea.

We have also studied the temperature dependence of the linewidth  $W_H$  at four urea concentrations, i.e. 2, 3, 4 and 6 M.

The variation of the linewidth with temperature are shown in Figures III.5 to III.8 at various molarities of urea. The plots are essentially linear as expected. In Figure III.9 we have given the variation of  $W_H$  with  $T/\eta$  for 2 M and 6 M urea solutions. The plots are linear, indicating that spin-rotational contributions to linewidth do occur via the  $a_o(\text{SR})$  term. The slopes of this plot are  $4.8 \times 10^{-4}$  and  $5.1 \times 10^{-4}$  G cP K<sup>-1</sup> for 2 M and 6 M urea respectively, revealing a greater  $a_o(\text{SR})$  contribution at the higher molarity. The ratio of  $[a_o(\text{SR})/\text{overall width } W_H]$  turn out to be 0.45 and 0.42 for 6 M and 2 M urea solutions respectively. In order to check whether a Debye-type motion model is applicable to the probe in the urea solutions, the parameter  $\tau_J$  was calculated from the  $a_o(\text{SR})$  value in 2 M urea at 298 K.

Assuming a van der Waals radius of 2.7 Å for TEMPO, as suggested by Jolicoeur and Friedman,<sup>20</sup> leads to a calculated value for  $\tau_o$  that is in agreement with the observed  $\tau_o$  in 2 M urea and in 6 M only if the viscosity were corrected by a factor of 2.7 and 6.0 respectively. The Debye model is applicable without major rectification only at 2 M urea since the correlation between  $\tau_o$  and  $\tau_J$  at 6 M urea is not in agreement. As a further check, we computed the values of  $\tau_J$  on the basis of the radius and the viscosities mentioned above and obtained  $\tau_J = 5.5 \times 10^{-14}$  and  $9.0 \times 10^{-14}$  sec for 2 M and 6 M urea solutions. These values are considerably different for 6 M from the

Table III.2

Computed ESR parameters, error function and error limits  
for the spectrum of TEMPO in 2M urea

$a_H$  Fixed at 0.065 gauss

Temperature $T_C$	Hyperfine linewidth $W_H$ (Gauss)	Normalizing parameter B(3)	Error function PHI	Standard error for Width SE
25	0.342	0.143	1.600	0.0100
50	0.425	0.156	0.960	0.0095
60	0.450	0.154	0.480	0.0073
70	0.502	0.156	0.400	0.0078
80	0.519	0.149	0.760	0.0120
90	0.547	0.149	0.094	0.0046

Table III.3

Computed ESR parameters, error function, error limits of  
the spectrum of TEMPO in 3 M urea

$a_H$  Fixed at 0.065 gauss

Temperature $^{\circ}\text{C}$	Hyperfine linewidth $W_H$ (gauss)	Normalizing parameter $B(3)$	Error function $\Phi$	Standard error for width SE
25	0.322	0.0890	0.240	0.0097
50	0.377	0.0898	0.077	0.0068
60	0.393	0.0883	0.042	0.0057
70	0.407	0.0932	0.210	0.0127
80	0.471	0.0934	0.070	0.0096
90	0.488	0.1240	0.032	0.0053

Table III.4

Computed ESR parameters, error function, and error limits  
of the spectrum of TEMPO in 4 M urea

$a_H$  Fixed at 0.065 gauss

Temperature $^{\circ}\text{C}$	Hyperfine linewidth $W_H$ (gauss)	Normalizing parameter $B(3)$	Error function $\text{PHI}$	Standard error for width SE
25	0.290	0.0767	0.600	0.0150
40	0.333	0.1000	0.210	0.0085
50	0.325	0.0932	0.190	0.0083
60	0.409	0.0990	0.183	0.0110
70	0.434	0.0960	0.160	0.0122
80	0.453	0.0927	0.033	0.0061
90	0.484	0.1120	0.094	0.0098

Table III.5

Computed ESR parameters, error function, error limits  
of the spectrum of TEMPO in 6 M urea

$a_H$  Fixed at 0.065 gauss

Temperature $^{\circ}\text{C}$	Hyperfine linewidth $w_H$ (gauss)	Normalizing parameters $B(3)$	Error function $\text{PHI}$	Standard error for width SE
25	0.276	0.0852	1.200	0.0180
40	0.313	0.0876	0.250	Not obtained
50	0.337	0.0860	0.410	0.0139
60	0.368	0.0863	0.150	0.0096
70	0.387	0.0843	0.040	0.0055
80	0.508	0.0960	0.039	0.0082
90	0.487	0.1080	0.220	Not obtained



Fig. III.5: Proton hyperfine linewidth of the  $m_N = 0$  manifold of TEMPO,  $W_H$ , as a function of temperature,  $T$  for 2 M urea.

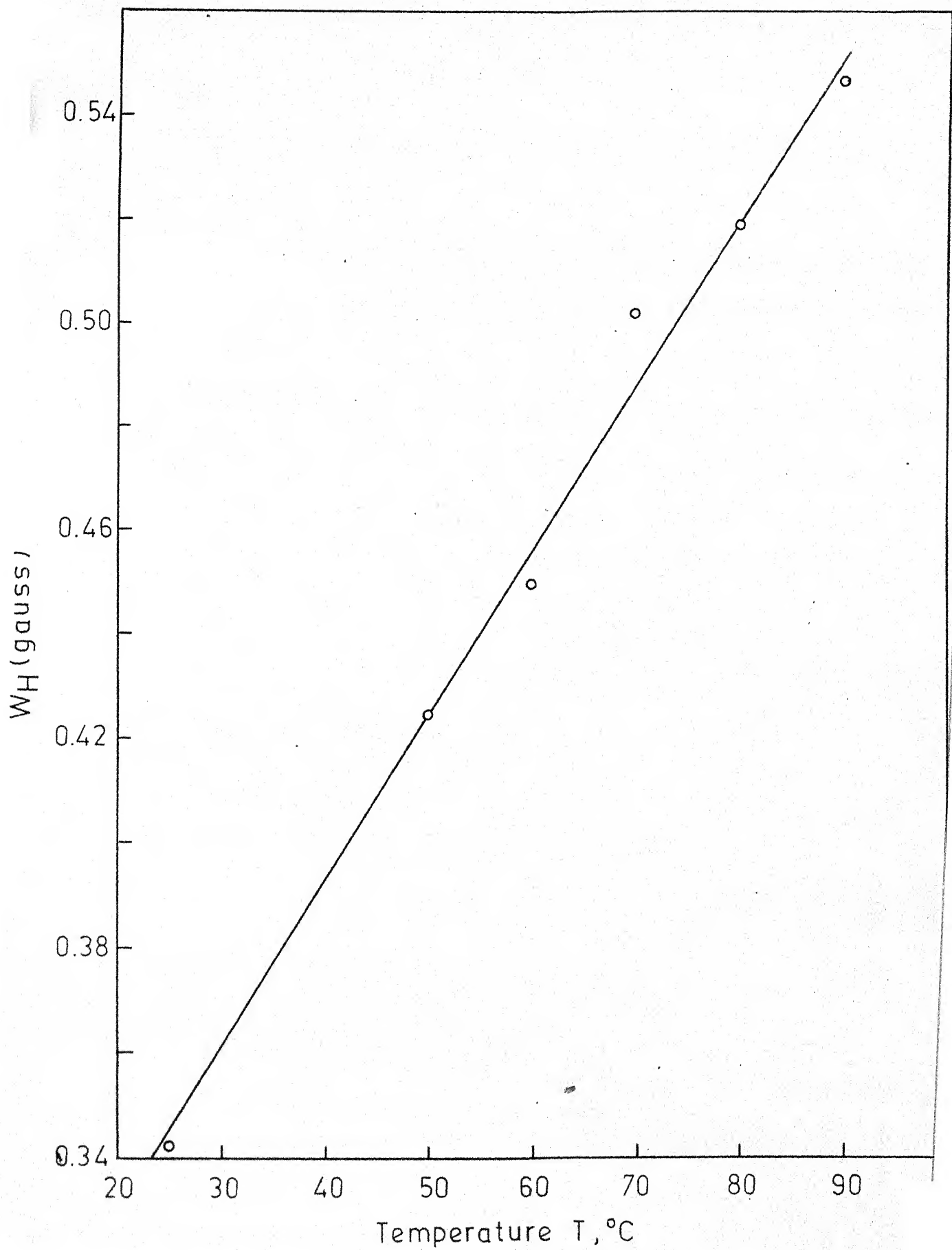


Fig. III.6: Proton hyperfine linewidth of the  $m_i = 0$  manifold of TEMPO,  $\nu_{\text{H}}$ , as a function of temperature,  $T$  for 3 M urea.

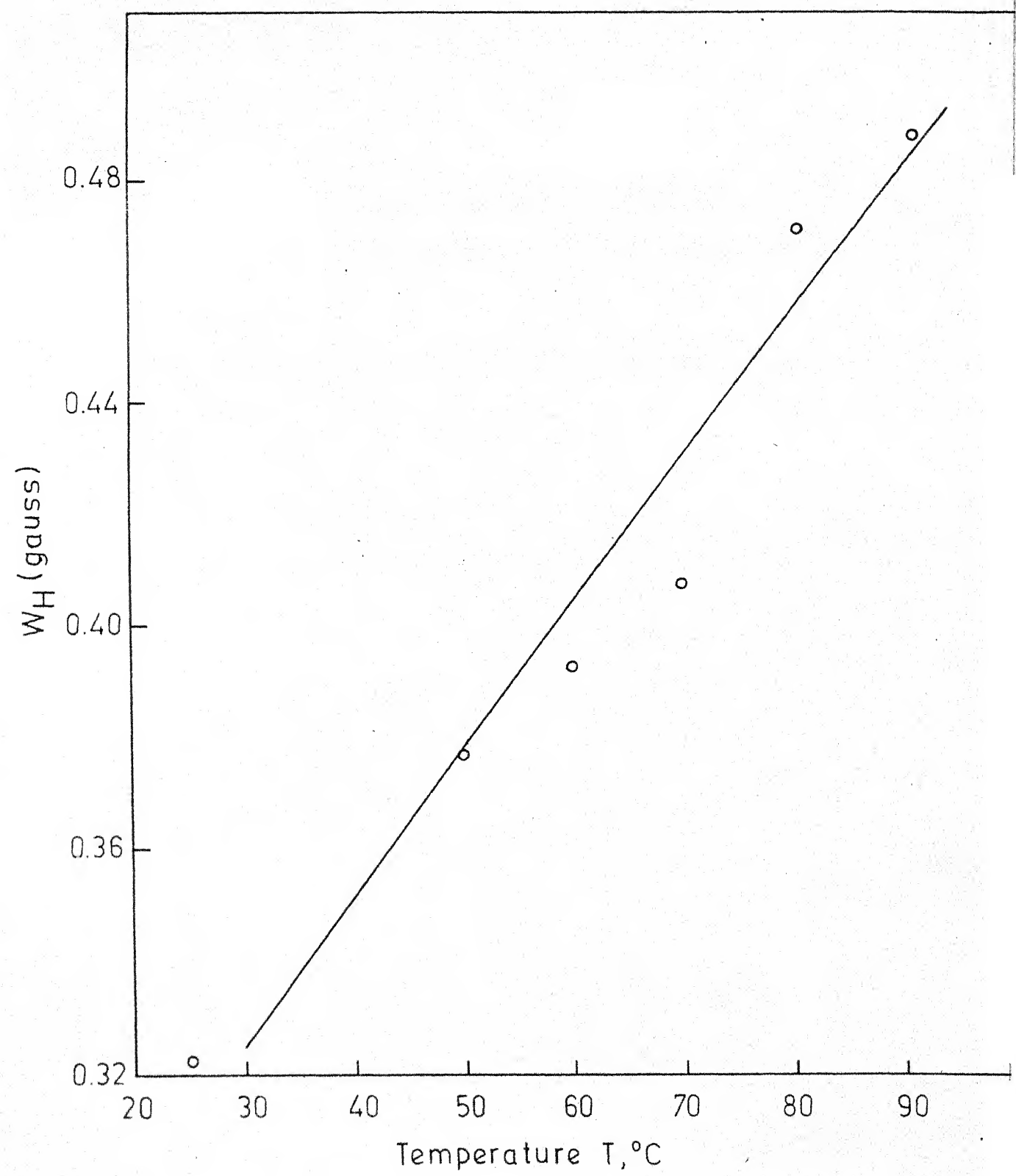


Fig. III.7: Proton hyperfine linewidth of the  $m_I = 0$  manifold of TEMPO,  $W_H$ , as a function of temperature,  $T$  for 4 M urea.

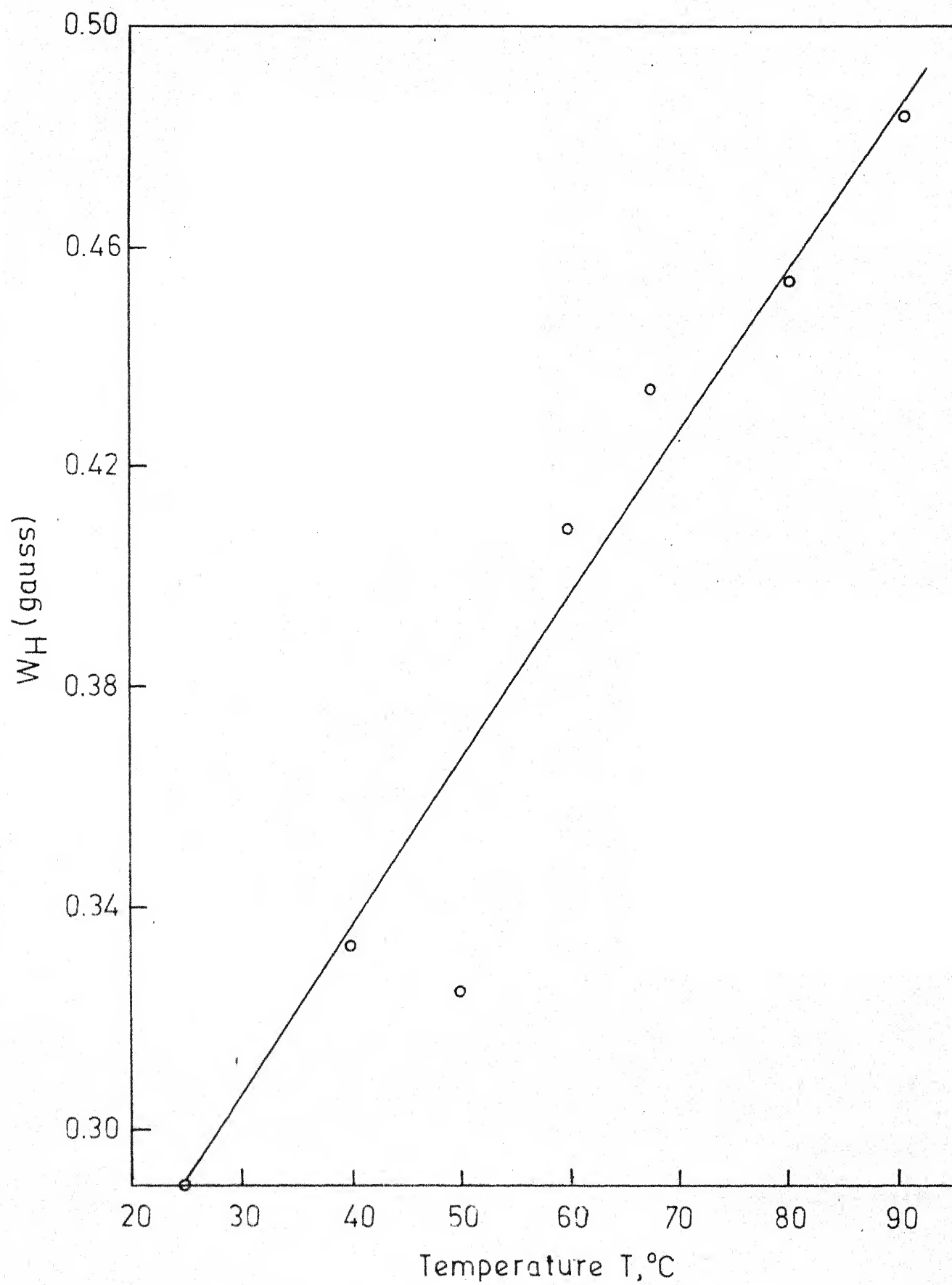


Fig. III.8: Proton hyperfine linewidth of the  $m_I = 0$  manifold of TEMPO,  $W_H$ , as a function of temperature,  $T$  for 6 M urea.

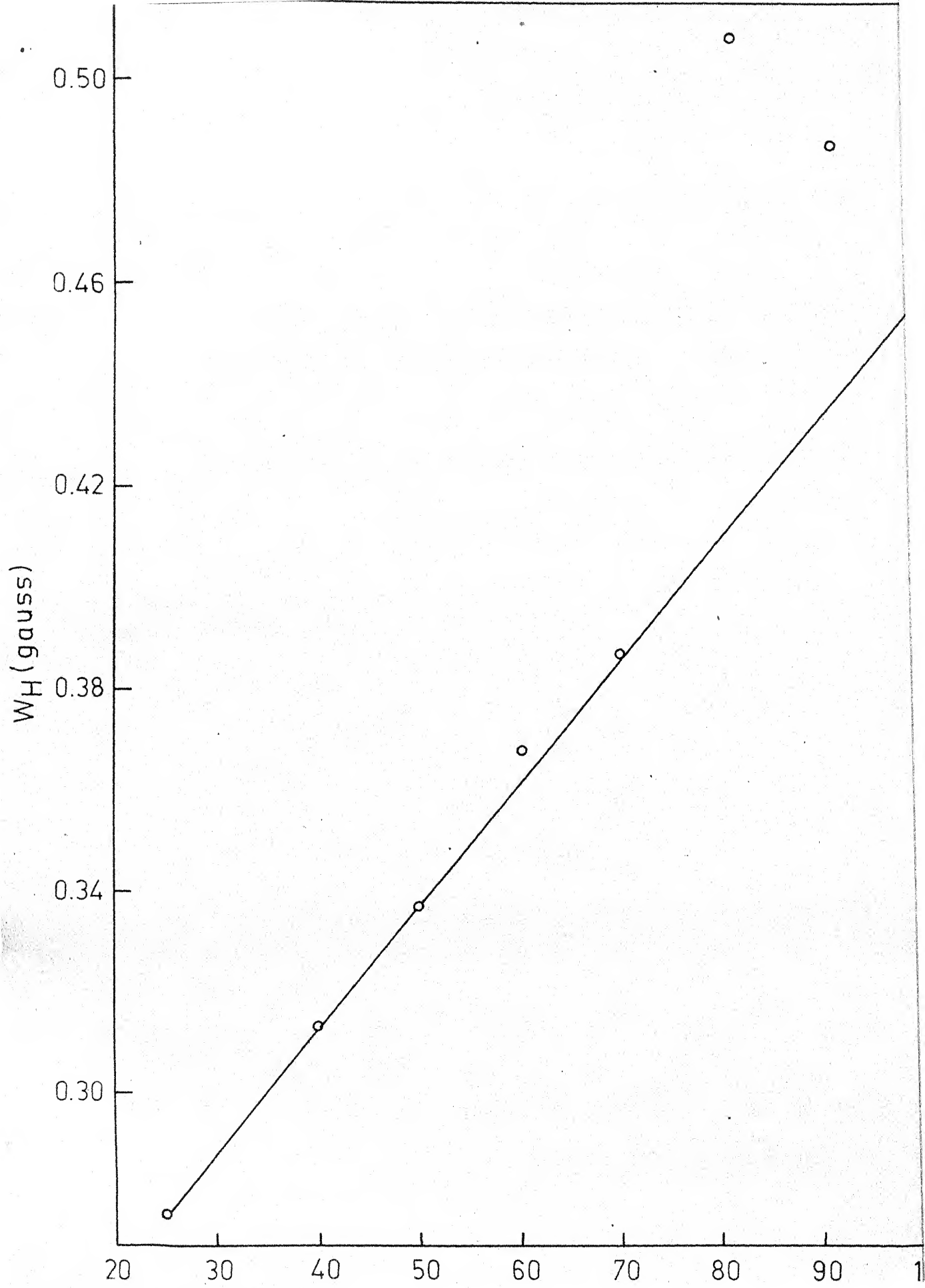
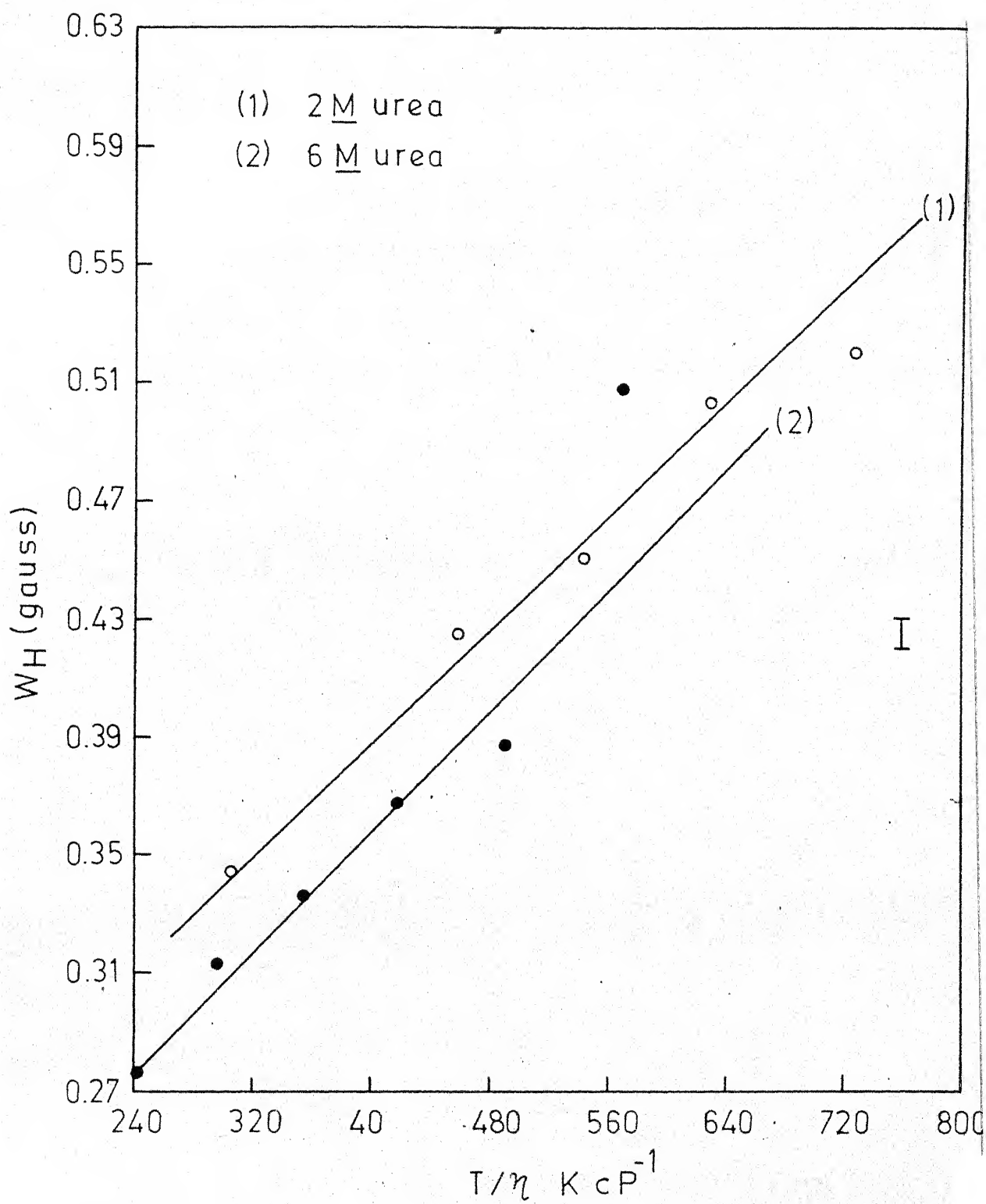




Fig. III.9: Proton hyperfine linewidth of the  $m_l = 0$  manifold of TEMPO,  $W_H$ , as a function of  $T/\eta$  at 2 M and 6 M urea.



calculated from the  $a_o(\text{SR})$  terms from the following relation

$$a_o(\text{SR}) = \left(\frac{2kT}{3I}\right) \left[ (g_{||} - 2.0023)^2 + 2(g_{\perp} - 2.0023)^2 \right] \tau_J$$

using appropriate values,  $\tau_J$  calculated this way turn out to be about  $10^{-14}$  sec in the above solutions. From these it seems to us that a simple Debye model for the Brownian motion of the probe may not be appropriate.

It is interesting to speculate on a two-state model in which the probe is far from a solute with a large  $\tau_{\theta}$  and very small  $\tau_J$ , and in another state where it is close to a solute with small  $\tau_{\theta}$  and large  $\tau_J$ . If the second state is less probable than the first,  $\tau_{\theta}$  may not be affected much on an average, while  $\tau_J$  may be significantly different from the first state and  $\tau_{\theta}$  and  $\tau_J$  may still follow the Debye pattern but the average values need not.

To summarize this portion, we believe the following processes occur in aqueous urea solutions, which are consistent with the changes seen in the tumbling correlation time and the linewidths of the spin probe dissolved in the medium.

1. At all concentrations, urea disrupts the cluster phase aggregation of liquid water. This disrupting effect is greatest at low concentrations of urea, indicative of a cooperative effect. The reduction in the size of the water clusters reduces the resistance to the motion (tumbling) of the dissolved spin-probe and

consequently at low concentrations of urea,  $\tau_{\theta}$  for TEMPO is decreased.

2. As the molarity of urea is increased further, a variety of factors such as urea-urea aggregation, urea-water association, alteration in the solvation profile of the probe molecule, and similar interactions in effect alter the immediate environment of the probe, causing an increase in its  $\tau_{\theta}$  value.

3. At 3 M urea, the bulk water microphase is predominantly destroyed and the solvent is essentially a non-structured collection of urea and water molecules in a "dense" microphase. The  $\tau_{\theta}$  of the spin probe accordingly levels off to an almost constant value that reflects the "bulk" viscosity of the medium.

These interpretations of the e.s.r.  $\tau_{\theta}$  results of the probe are consistent with the data on  $N^{14}$  relaxation time measurements of urea,  $O^{17}$  linewidths of  $H_2O^{17}$ , and the chemical shift measurements ( $H_2O$  and urea protons), in aqueous urea solutions,<sup>7</sup> and support the Frank-Franks<sup>16</sup> picture of liquid water and aqueous urea solutions. The advantage of having used the e.s.r. spin probe technique with a measurable  $\tau_{\theta}$  of picosecond range is clear. Since this is also the time scale involved for the water molecules to flicker between bulk and dense microphases, so that in effect tumbling correlation time measurements are able to report in situ events of comparable lifetimes, which

has not been possible with longer-time scale measurements such as ultrasonic attenuation.

## (2) Urea Derivatives

### (A) Thiourea

Thermodynamic studies by Subramanian et al.<sup>5</sup> have indicated that thiourea behaves similar to urea in its effect on water structure. It is also known that thiourea is as effective a denaturant as urea at comparable concentrations. Unfortunately however, the solubility of thiourea is limited to about 3 M in water at 25°C. Thus only limited comparison of urea and thiourea has been possible. In Table III.6 are collected the  $W_H$  values,  $\tau_\theta$  and the curve fitting parameters for the e.s.r. spectrum of TEMPO in aqueous thiourea solutions at 1, 2 and 3 M, concentrations and ambient temperature (27°C). The  $W_H$  value of 0.290 gauss at 0 M (pure water) decreases to 0.264 at 1 M and then shows a steady increase to 0.279 G at 2 M and 0.211 G at 3 M thiourea. The corresponding tumbling correlation times are 7 psec, 16 psec and 31 psec at 1 M, 2 M and 3 M thiourea, compared to 20 psec in water. Measurements could not be carried out beyond 3 M due to insolubility. However, one notices that the trends in both  $W_H$  and  $\tau_\theta$  with concentration in thiourea (Figure III.10) are comparable to the case of urea, showing thereby that replacement of the carbonyl oxygen by sulphur does not vastly alter the structural effects of urea derivatives on

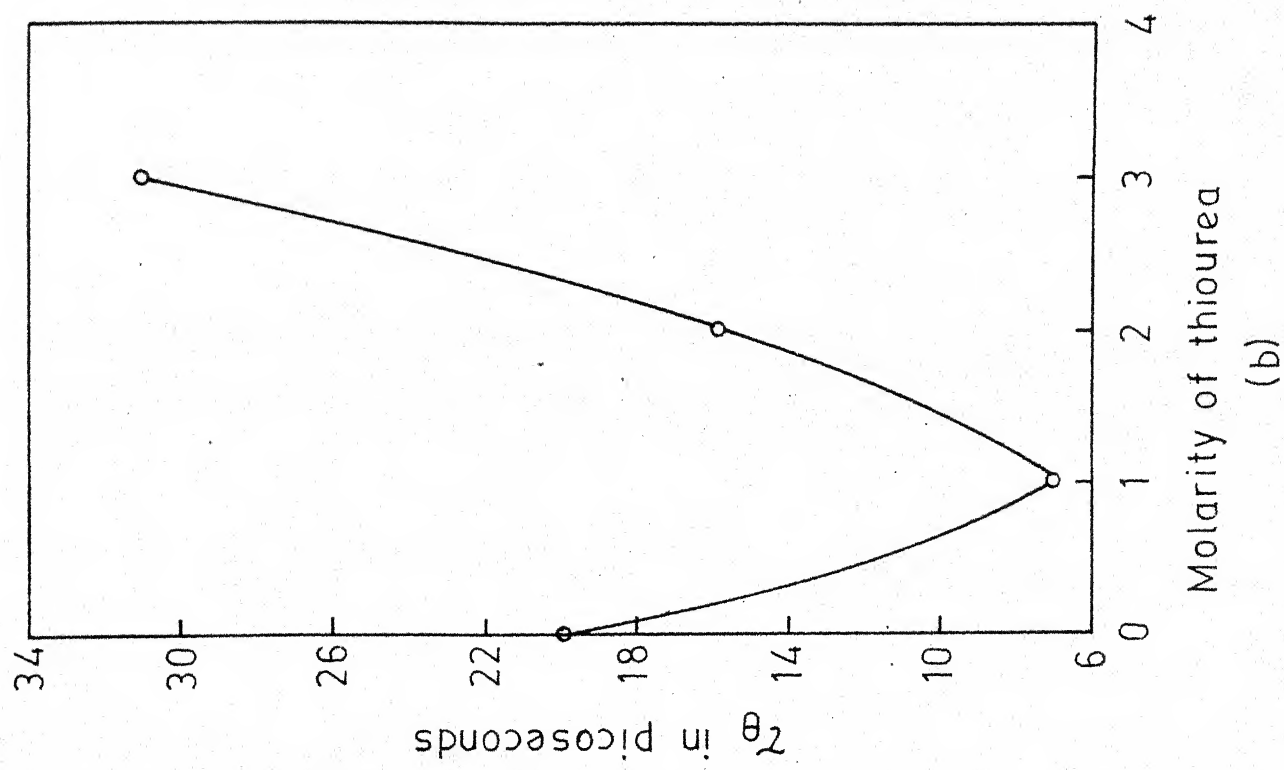
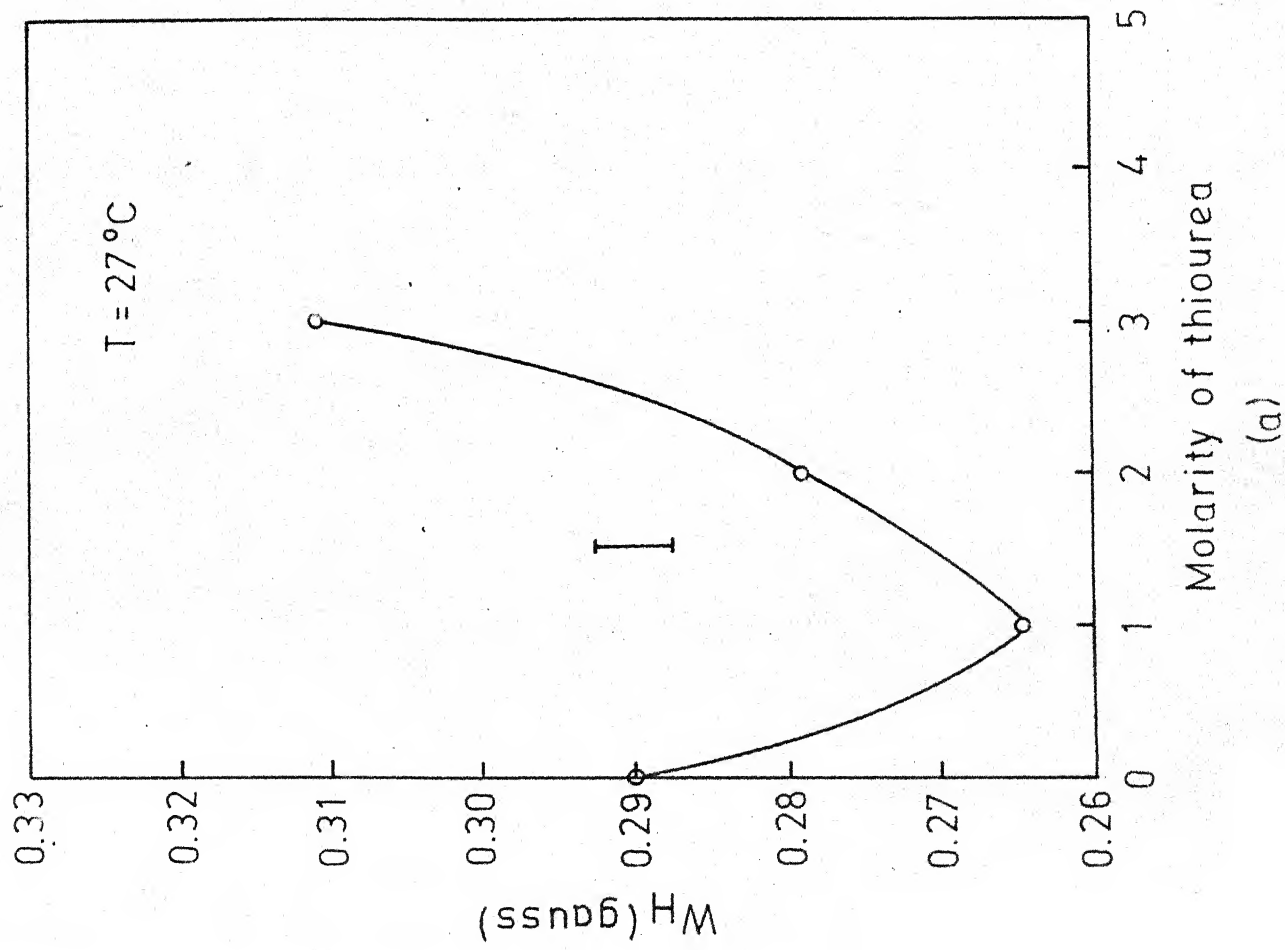
Table III.6

Computed ESR parameters, error function, error limits and  
Tau values for TEMPO in aqueous thiourea

$a_H$ Fixed at 0.065 gauss			Room Temperature $\Delta$ 27°C		
Concen- tration	Hyperfine linewidth $W_H$ (gauss)	Normalizing parameter $B(3)$	Error Function $\Phi H$	Standard error for $W_H$ $SE$	Correlation time $\tau_\theta \times 10^{12}$ sec
1 $\overline{M}$	0.264	0.0672	0.075	0.0063	6.93
2 $\overline{M}$	0.279	0.0752	0.130	0.0079	16.25
3 $\overline{M}$	0.311	0.1110	0.072	0.0047	31.25

Fig. III.10(a): Proton hyperfine linewidth of the  $m_s = 0$  manifold of TEMPO,  $W_H$ , as a function of molarity of thiourea.

(b): Tumbling correlation time  $\tau_c$  of the spin-probe TEMPO, as a function of molarity of thiourea.





water. It is to be noted that the tumbling correlation time of TEMPO in 3 M thiourea is larger than in water, indicating that the microviscosity in the medium is larger. Probe-solute interactions, or a mild structure making tendency, or even bulk viscosity increase could account for this. However, in the absence of data beyond 3 M, we are restricted to the interpretation that until this concentration, thiourea behaves essentially similar to urea; i.e., initial disruption of water clusters followed by a display of changed solvation profile of the probe or thiourea-water interaction.

(B) Dimethyl urea

N,N'-Dimethyl urea is known to be a weaker denaturant than urea. Its effect on water structure, as monitored by infrared<sup>8</sup> and ultrasonic attenuation methods,<sup>19</sup> is considered to be a mild structure-breaking one. The introduction of two methyl groups in urea leads to the decreased effectiveness (indeed tetramethyl urea and also N,N'-diethyl urea are structure makers<sup>19</sup>). Again the solubility of dimethyl urea in water is limited to 3 M at 25°C, and so experiments could be done only upto this concentration region.

Table III.7 lists the relevant e.s.r. spectral values of TEMPO in aqueous dimethyl urea solutions. The linewidth of the hyperfine lines are  $W_H = 0.241, 0.263, \text{ and } 0.235 \text{ G}$  at 1 M, 2 M

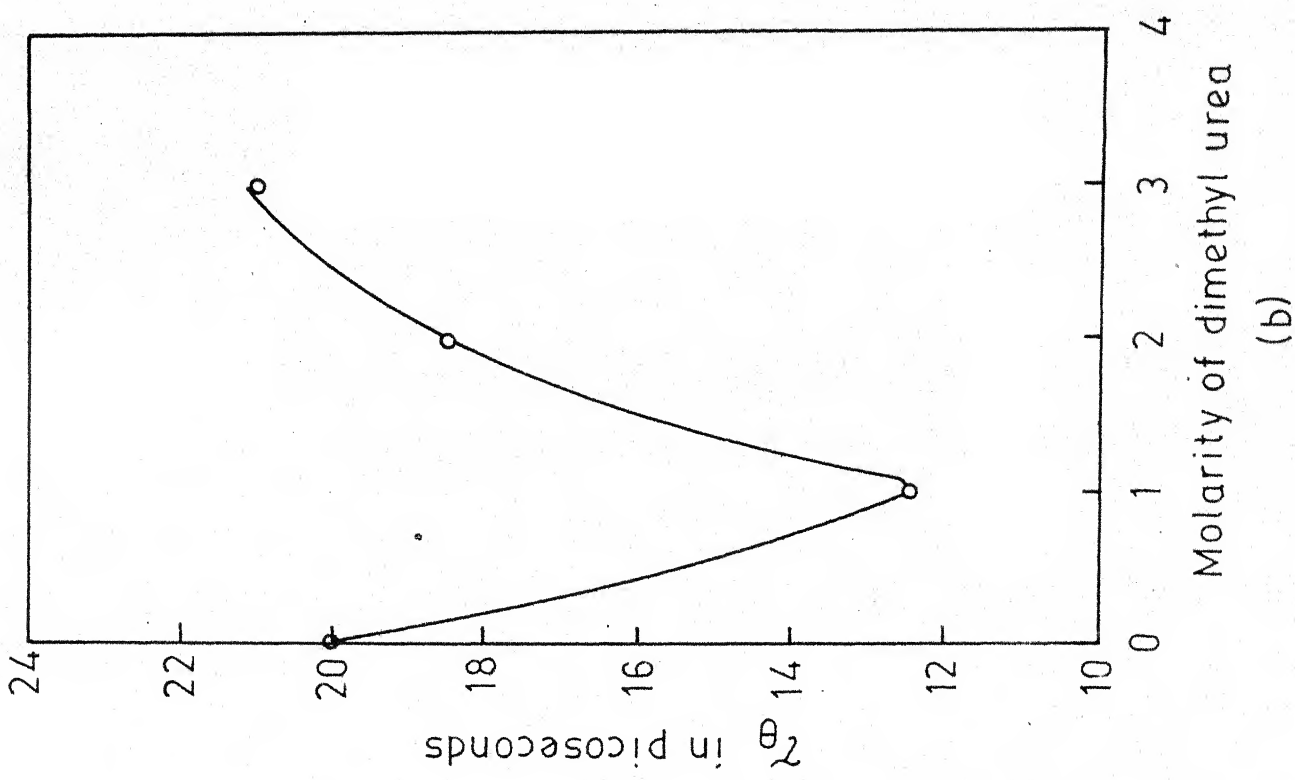
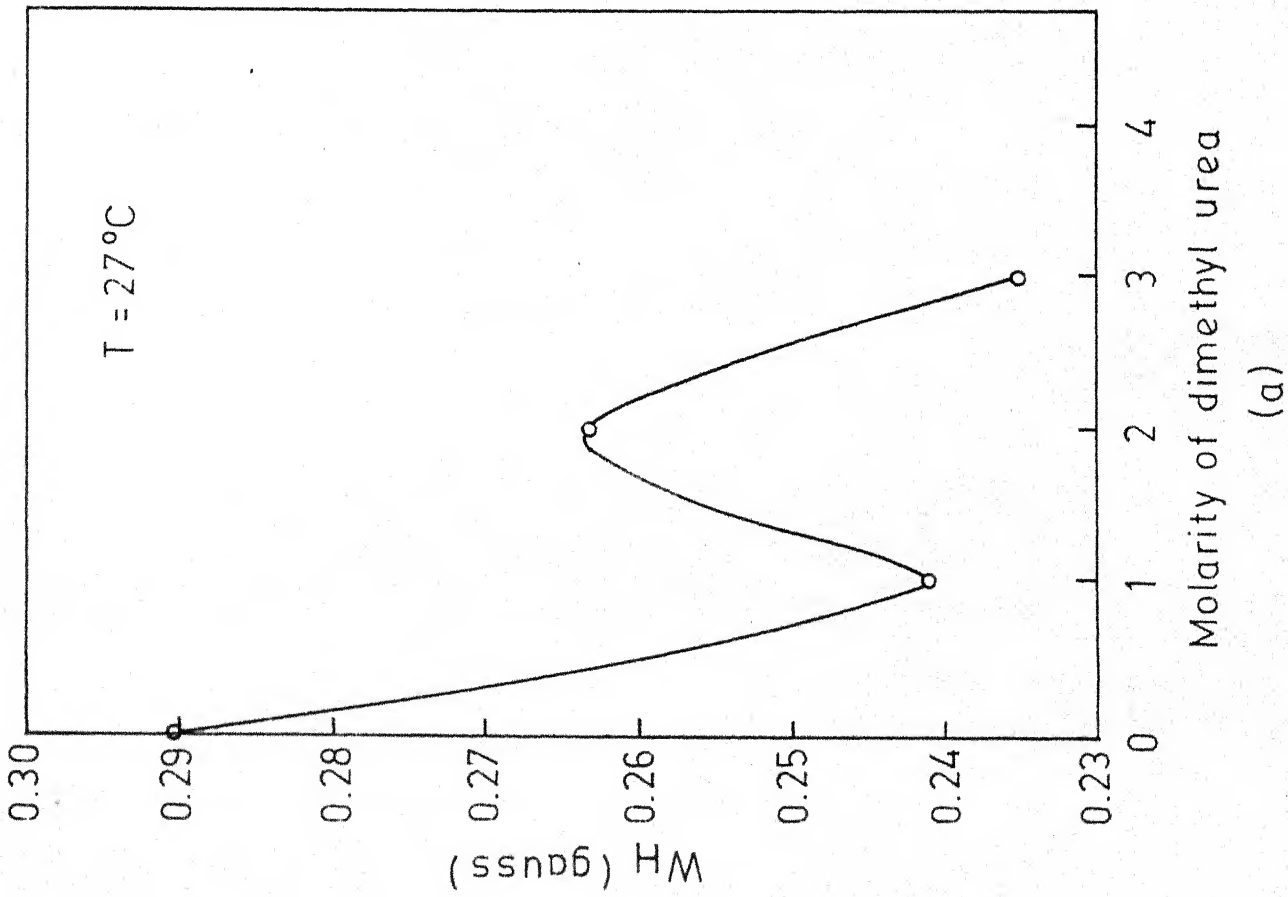
Table III.7

Computed ESR parameters, error function, error limits and  
Tau values for TEMPO in aqueous dimethyl urea

Concen- tration	$a_H$ Fixed at 0.065 gauss		Room Temperature $\pm 27^\circ\text{C}$	
	Hyperfine linewidth $W_H$ (gauss)	Normalizing parameter $B(3)$	Error function $\text{PHI}$ Standard error for $W_H$ SE	Correlation time $\tau_\theta \times 10^{12}$ sec
1 $\bar{M}$	0.241	0.0499	0.00690	12.5
2 $\bar{M}$	0.263	0.0640	0.00658	18.5
3 $\bar{M}$	0.235	0.0659	0.00990	21.5

Fig. III.11(a): Proton hyperfine linewidth of the  $m_I = 0$  manifold of TEMPO,  $w_H$ , as a function of molarity of dimethyl urea.

(b): Tumbling correlation time  $\tau_e$ , of the spin-probe TEMPO, as a function of molarity of dimethyl urea.



and 3 M dimethyl urea respectively. The tumbling correlation time  $\tau_{\theta}$  of TEMPO are 12, 18 and 21 psec at 1 M, 2 M and 3 M dimethyl urea solutions respectively. Figure III.11 illustrates the variation of  $W_H$  and  $\tau_{\theta}$  of the spin probe in these solutions. Once again, the similarity with urea is striking. The minimum in  $\tau_{\theta}$  occurs at 1 M followed by a steady increase upto 3 M; the limit of solubility. Dimethyl urea also breaks water-structure continuously but less efficiently than urea itself, a factor that can be attributed to the methyl group substitution.

The common features that emerge from the spin probe studies on the effect of the three ureas on water-structure are as follows. Even at low concentrations, the ureas disrupt the cluster microphase of liquid water. This is reflected in the large drop in  $\tau_{\theta}$ , initially; the subsequent increase can arise due to several factors that involve probe solvation changes and solute-solvent interactions, but the structure-breaking effect of the solute is still manifested. These results are in accord with the ultrasonic attenuation results and equilibrium thermodynamic study on these solutes.

### (3) Guanidinium Chloride

This isoelectronic analogue of urea is known to be a stronger denaturant than urea itself.<sup>18</sup> It has also been reported to be a more efficient structure-breaker.<sup>19</sup> In Table III.8,

we list the  $W_H$ ,  $\tau_\theta$  and the statistical parameters of e.s.r. spectra of the spin probe TEMPO in aqueous solutions of varying molarities of guanidinium chloride. Figures III.12 and III.14 plot the hydrogen hyperfine linewidth and the tumbling correlation times of TEMPO in these solutions respectively. It is very interesting to note that the linewidth plot is linear with guanidinium chloride molarity. This behaviour is different from what is seen in urea. In Figure III.13, we show the Kivelson plot (i.e.  $W_H$  versus  $T/\eta$ ) for guanidinium chloride. On comparing with glycerol solutions the curves look similar but the linewidths in guanidinium chloride are consistently smaller than in glycerol, and than in urea. Unfortunately we were not able to do temperature-dependent studies on  $W_H$  in guanidinium chloride, in order to estimate  $a_o(SR)$ , and  $\tau_\theta$ ,  $\tau_J$ . But if one turns to the variation of  $\tau_\theta$  of the probe in guanidinium chloride solutions, Figure III.14, the behavioural similarity with urea becomes apparent.  $\tau_\theta$  decreases from 20 psec in pure water gradually to a minimum of 8 psec at 4 M guanidinium chloride after which it increases slowly to 10 psec at 7 M, while with urea, the minimum value of 6 psec is achieved at 2 M, increasing to 17 psec at 3 M after which no significant changes occur. This difference between urea and guanidinium chloride might arise due to the fact that the latter is an electrolyte, with structural effects that arise from the cation and the anion. Accordingly the solvation profile in this molecule will be different

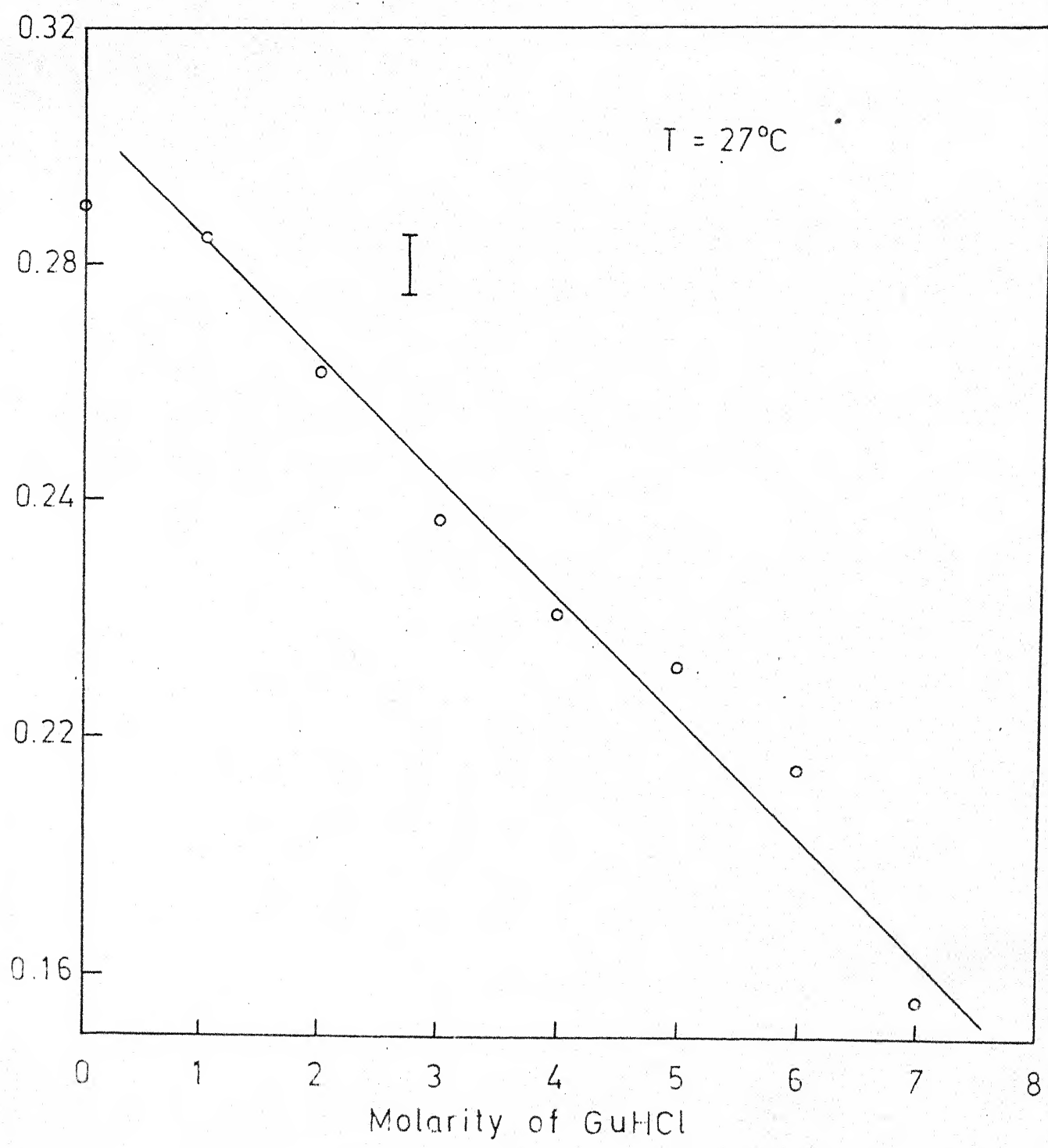
Table III.8

Computed parameters, error function, error limits and  
Tau values for TEMPO in aqueous guanidinium chloride

Concen- tration	$a_H$	Fixed at	0.065 gauss	Room Temperature $\approx 27^\circ\text{C}$		
				Hyperfine linewidth $w_H$ (gauss)	Normalizing parameter $B(3)$	Error function PHI Error limit for width $w_H$ SE $\tau_\theta \times 10^{12}$ sec
1 M		0.284	0.0671	0.92	0.0167	17.0
2 M		0.262	0.0640	0.86	0.0150	14.0
3 M		0.237	0.0538	1.80	0.0240	10.0
4 M		0.221	0.0464	0.31	0.0110	8.0
5 M		0.212	0.0357	0.74	0.0210	8.5
6 M		0.195	0.0402	0.88	0.0200	9.5
7 M		0.156	0.0369	0.78	0.0187	10.5

Fig. III.12: Proton hyperfine linewidth of the  $m_I = 0$  manifold of TEMPO,  $W_H$ , as a function of molarity of guanidinium chloride.





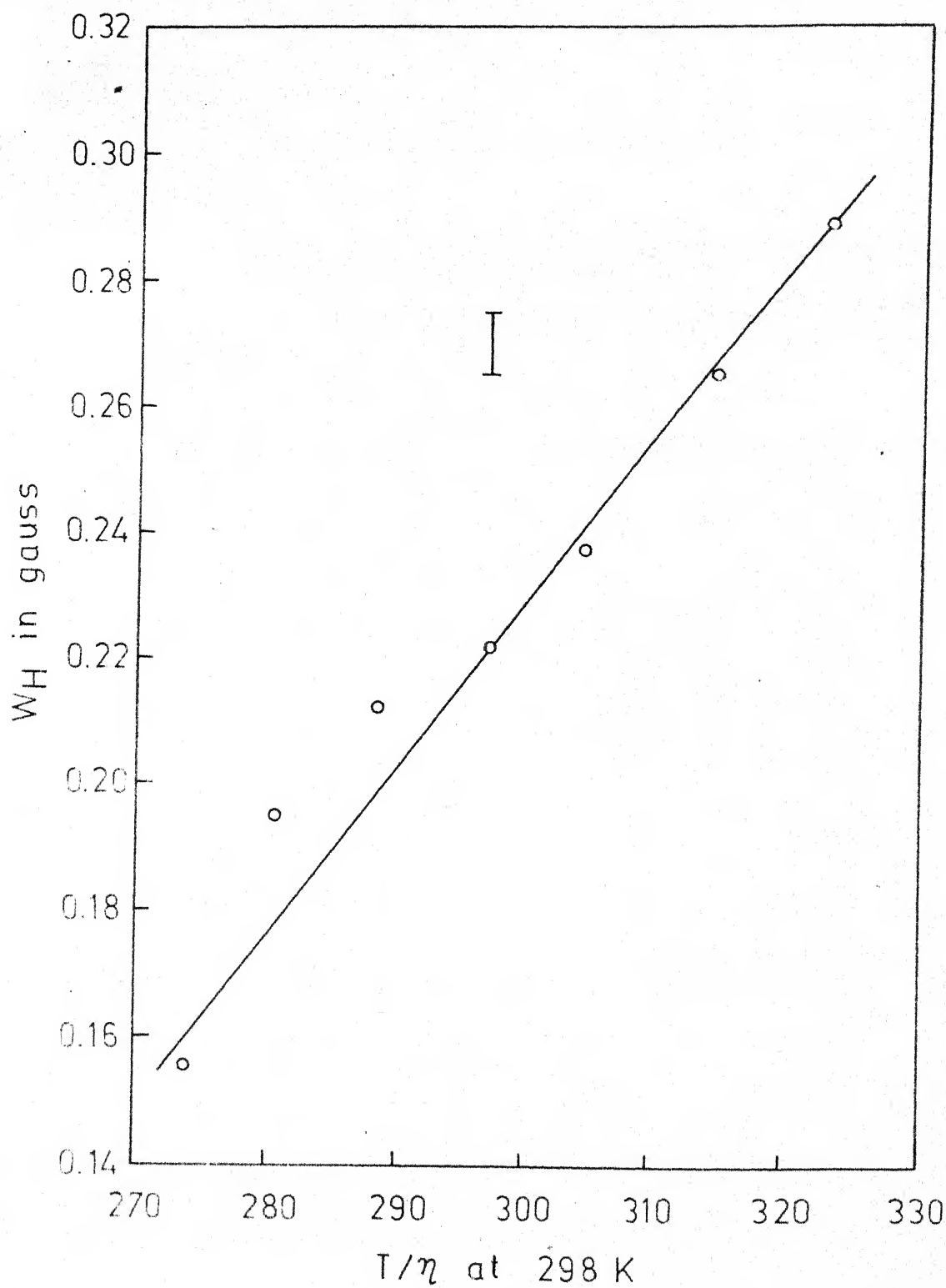
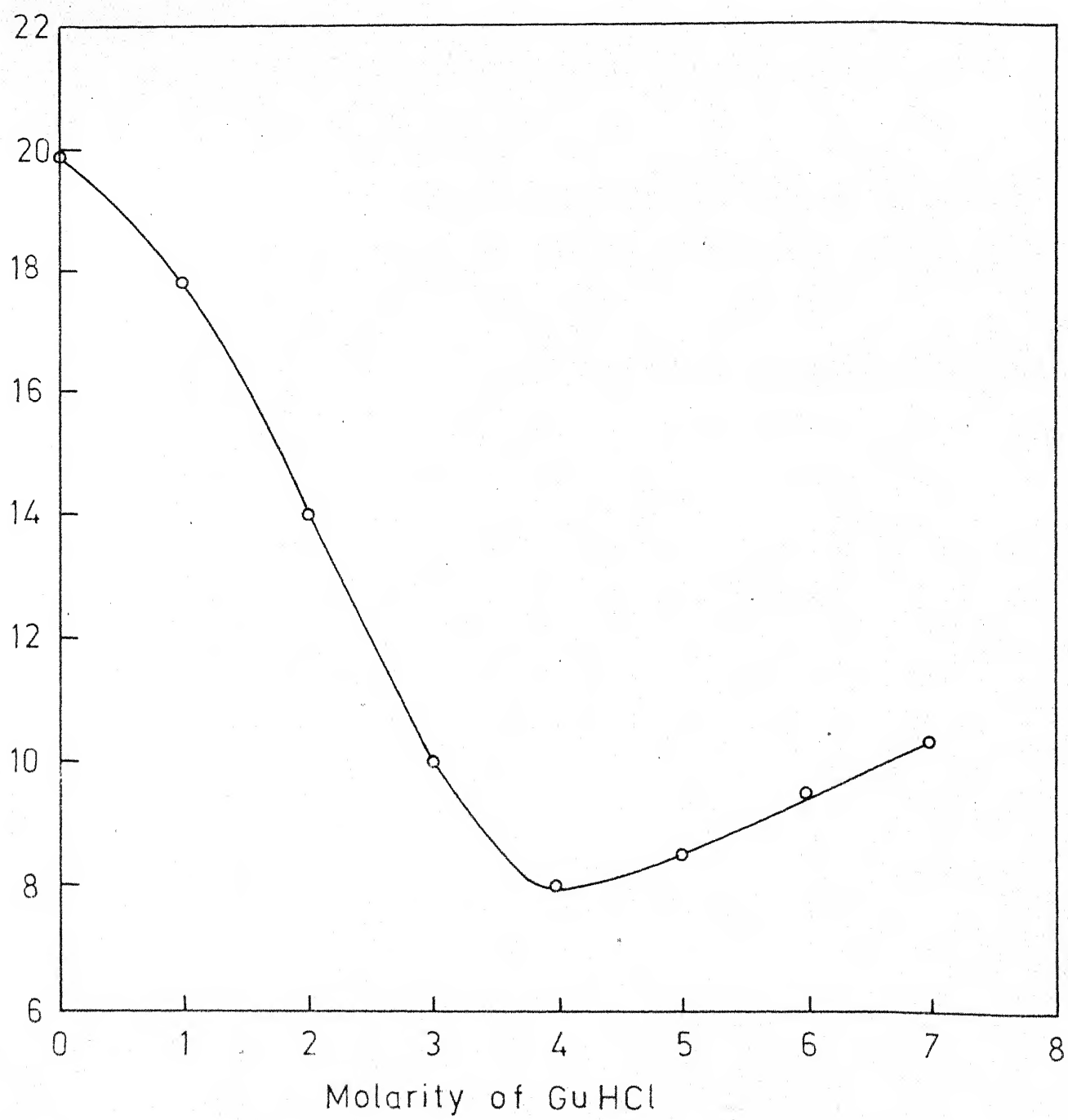


Fig. III.14: Tumbling correlation time,  $\tau_{\theta}$ , of the spin-probe TEMPO, as a function of molarity of guanidinium chloride.



from that of urea. Notwithstanding this, the  $\tau_{\theta}$  curve shows a rapid fall in the correlation time and even at high molarities, the  $\tau_{\theta}$  is about 10 psec, a value smaller than what is obtained with high urea. This may be a reflection of the reported tendency of guanidinium chloride to disrupt water-structure even better than urea. The initial drop in  $\tau_{\theta}$  (from 20 to 8 psec) between 0-4 M apparently indicates the effect of disruption of water clusters by the denaturant solute. Presumably the breakdown is complete at 4 M since beyond that  $\tau_{\theta}$  increases little, the small increase possibly reflecting viscosity increase in the medium. Our results, we believe, are consistent with the opinion that urea and guanidinium salts disrupt water structure at all concentrations efficiently, and this breakdown occurs more drastically at low concentrations, and that guanidinium chloride is a more efficient disrupter. In this light, it may be worthwhile to look at the effect of different guanidinium salts to assess the anion effect on water structure, solvation patterns on TEMPO, and water-denaturant interactions.

#### A NOTE ON THE LIMITATIONS OF THE METHOD

We have recently come to know (Jolicoeur, C., personal communication) that recent work on TEMPO in micelles solutions has led them to question the meaning of linewidth changes and apparent variations in  $\tau_{\theta}$ . In the micelle solutions, much of

the spectral changes occur because of changes in the spin parameters  $a_N$  and  $a_H$ .

In light of the above, there is a possibility that in mixed aqueous solutions apparent changes in  $\tau_e$  and  $W_H$  occur in part due to motional effects and in part due to changes that occur in the hyperfine constants  $a_H$  and  $a_N$ . It is thus important that we know to what extent such changes in  $a_N$  and  $a_H$  occur. Jolicoeur and Friedman<sup>20</sup> had used in their work on TEMPO in aqueous solutions a value of  $a_H = 0.06 \text{ G} \pm 10\%$ , since no reliable trend in the  $a_H$  could be detected. Also, for TEMPO in  $\text{CCl}_4$ , simulation of the e.s.r. spectrum and calculation of the  $a_H$  value using a computer program yielded for them  $a_H = 0.10 \text{ G}$ , in satisfactory agreement with values of  $a_H$  determined from NMR,  $a_H = 0.12 \text{ G}$ , and  $0.10 \text{ G}$ . It is thus important to estimate the values of and changes in  $a_H$  and  $a_N$  and to determine to what extent these affect the  $W_H$  and  $\tau_e$  values.

In our curve-fitting procedures, we adopted three different approaches. In the first, the value of  $a_H$  was fixed as  $0.065 \text{ G}$  in conformity with the aqueous solution value obtained by Jolicoeur and Friedman, and the  $W_H$  values calculated. In a second approach,  $a_H$  was fixed as  $0.10 \text{ G}$ , the value obtained in  $\text{CCl}_4$  solution and verified by NMR and  $W_H$  calculated. In the third, we let  $a_H$  be optimized, from a free-floating value, along with  $W_H$ . In Table III.9, we list the results obtained from all

the three approaches for urea solutions. It is apparent that the results obtained are inconsistent and not realistic when  $a_H$  is not fixed. For example, from Table III.9, we notice that when optimised from a free-float value,  $a_H$  varies from 0.044 to 0.081 G, and the patterns obtained in  $W_H$  are random. The changes in  $W_H$  as a function of molarity of urea using all three approaches are plotted in Figure III.15. On the other hand, when  $a_H$  is fixed at 0.065 G or at 0.10 G, the trends in  $W_H$  are similar as can be seen in the figure, excepting that with a higher  $a_H$  the linewidth falls. Incidentally, the range in the variation of  $a_H$  when floated and optimized is 0.04-0.08 G, and the mean value obtained from there is  $a_H = 0.06$  G. We have indeed simulated every spectrum of the probe in all solutions tried in this thesis using all the three approaches. In all these cases, letting  $a_H$  float did not yield us consistency. Perhaps a more direct case against letting  $a_H$  float and simulate the experimental spectrum comes from the data on aqueous glycerol solutions. In Table III.10, are given the linewidths of the hydrogen hyperfine interaction for the spin probe in glycerol solutions using  $a_H = 0.065$  G, 0.10 G and letting it float. Notice that  $W_H$  fluctuates without a definite trend when  $a_H$  is not fixed. We have as a comparison for this trend, the data of Jolicoeur and Friedman on aqueous glycerol. They have seen that the Kivelson behaviour is obeyed in this system, with a minimum of  $W_H$  occurring at  $T/\eta = 120 \text{ KcP}^{-1}$  at  $25^\circ\text{C}$ . Our data

Table III.9

Effect of changing  $a_H$  on linewidth  $w_H$  of TEMPO in aqueous urea

M Urea	$w_H$ in G, $a_H$ in G					
	$w_H$ with $a_H=0.065G$	Error in $w_H$	$w_H$ with $a_H=0.10G$	Error in $w_H$	$w_H$ with $a_H$ floating	Error in $w_H$
1 M	0.270	0.013	0.137	0.011	0.316	0.051
2 M	0.245	0.007	0.129	0.010	0.292	0.045
3 M	0.200	0.004	0.122	0.011	0.193	0.026
4 M	0.221	0.014	0.127	0.014	0.239	0.072
5 M	0.245	0.014	0.131	0.014	0.302	0.087
6 M	0.221	0.014	0.128	0.015	0.237	0.092
7 M	0.206	0.010	0.123	0.013	0.275	0.054

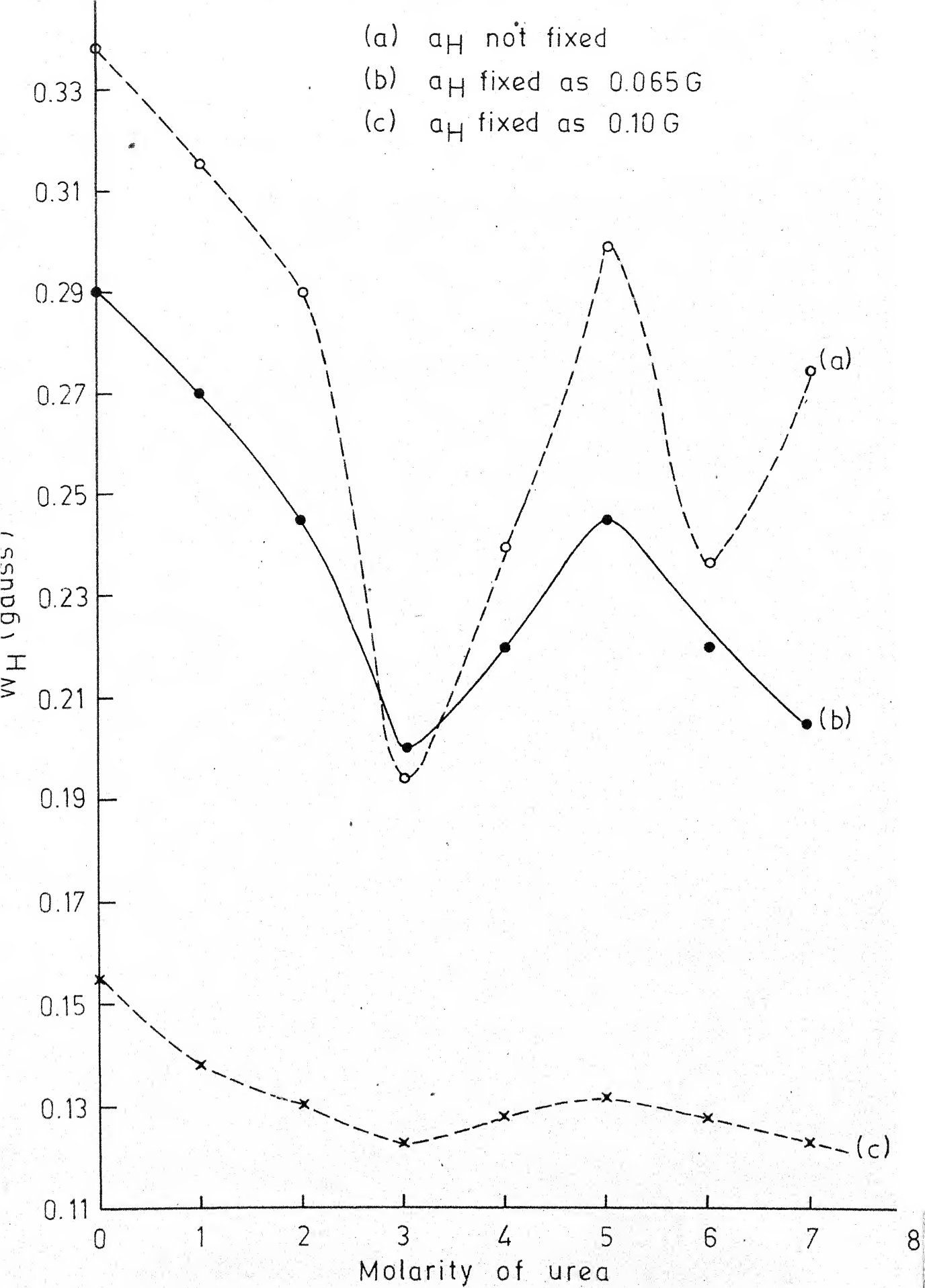


Table III.10

Effect of changing  $a_H$  on linewidth  $W_H$  of TEMPO in glycerol solutions $W_H$  in G,  $a_H$  in G

Concentration of glycerol	$W_H$ at $a_H=0.065G$		$W_H$ at $a_H=0.10G$		$W_H$ when $a_H$ floated		Optimal $a_H$	Error in $W_H$
	Error	$W_H$	Error	$W_H$	Error	$a_H$		
1 M	0.0082	0.323	0.0085	0.197	0.0095	0.289	0.0760	0.0410
2 M	0.0100	0.317	0.0128	0.191	0.0128	0.313	0.0663	0.0500
3 M	0.0065	0.304	0.0085	0.177	0.0085	0.291	0.0695	0.0308
4 M	0.0085	0.301	0.0095	0.172	0.0095	0.250	0.0800	0.0415
5 M	0.0089	0.267	0.0093	0.141	0.0093	0.231	0.0750	0.0400
6 M	0.0087	0.281	0.0096	0.152	0.0096	0.235	9.0786	0.0400
7 M	0.0110	0.261	0.0097	0.132	0.0097	0.239	0.0710	-

Fig. III.15: Proton hyperfine linewidth of the  $a_{\text{H}} = 0$  manifold of TEMPO,  $W_{\text{H}}$ , at different values of  $a_{\text{N}}$  as a function of molarity of urea.



on glycerol solutions agree with theirs in trend, only when  $a_H$  is fixed at 0.065 G. The trend in the values are similar when  $a_H$  is fixed at 0.10 G but the obtained  $W_H$  values are significantly lower than reported values. It is for these reasons, i.e., that the trend in  $a_H$  and  $W_H$  be in conformity with literature value, and that the trends not change upon allowing any value of  $a_H$  that we chose to fix  $a_H$  at 0.065 G and obtain linewidths. As long as one does not place undue importance on the actual values of  $W_H$  but notice the trends in these values only, one is on safe grounds; and as can be seen the trends are unaltered whether  $a_H = 0.065$  or 0.10 G. Precedence for the value of  $a_H = 0.06$  G  $\pm 10\%$  has come from earlier work on TEMPO in aqueous solutions and hence the use of this value in the present work.

It is also to be noted that we have computed values of the tumbling correlation time  $\tau_\theta$  from measurements of peakheights of the  $m_N = 0$ , and  $m_N = \pm 1$  lines, without any need for actual  $W_H$  values or  $a_H$ . Thus  $\tau_\theta$  values and associated arguments need not be qualified.

When we turn to variations in the nitrogen hyperfine splitting constant  $a_N$ , we notice from our spectra that  $a_N$  varies from a mean value of 15.5 G by 0.2 G, i.e. the spread is from 15.3 to 15.7 G. The error in  $a_N$  is thus about 1.5%. It seems to us difficult to assign such a variation to changes in the geometry and charge distribution of the probe molecule. However,

we include this correction factor in the belief that if variations in  $\tau_{\theta}$  and  $W_H$  are partly dependent on changes in  $a_N$  and  $a_H$ , such changes occur even if the change in  $a_N$  is by 1-2 per cent. The variations observed in  $\tau_{\theta}$  and  $W_H$  are much more dramatic than perhaps seen from the variation in  $a_N$  detected.

Atherton and Starch<sup>25</sup> have observed changes in  $a_N$  for the spin probe di-*t*-butyl N-oxide in aqueous solutions of the micellar surfactant sodium dodecyl sulphate. After a concentration of 4mM, the spin probe spectrum changes to one with  $a_N = 16.64$  G, superposed on the lower concentration spectrum with  $a_N = 17.0$  G. They have proposed that the post-micellar spectrum is due to the less polar environment of the micelles.

Caution is thus to be exercised in interpreting spectral changes. While variations in  $a_H$  or  $a_N$  may indeed lead to artifactual situations, we feel, as per Jolicoeur and Friedman, that a major part of the changes in the spectra of the probe in our experiments owes its origin to motional effects.

REFERENCES

1. Kauzmann, W.A. (1959) Adv. Protein Chem., 14, 1.
2. Wetlaufer, D.B., Malik, S.K., Stoller, L. and Coffin, R.L. (1964) J. Amer. Chem. Soc., 86, 508.
3. Schick, M.J. (1964) J. Phys. Chem., 68, 3585.
4. von Hippel, P.H. and Wong, K.Y. (1964) Science, 145, 577.
5. Subramanian, S., Balasubramanian, D. and Ahluwalia, J.C. (1969) J. Phys. Chem., 73, 266.
6. Chawla, B. (1974) Ph.D. Thesis, Department of Chemistry, Indian Institute of Technology, Kanpur, India
7. Finer, E.G., Franks, F. and Tait, M.J. (1972) J. Amer. Chem. Soc., 94, 4424.
8. Swenson, C.A. (1966) Arch. Biochem. Biophys., 117, 494.
9. Walrafen, G.E. (1971) J. Chem. Phys., 55, 768.
10. Hammes, G.G. and Schimmel, P.R. (1967) J. Amer. Chem. Soc., 89, 442.
11. Arakawa, K. and Takenaka, N. (1967) Bull. Chem. Soc. Japan, 40, 2739.
12. Hargraves, W.A. and Krescheck, G.C. (1969) J. Phys. Chem., 73, 3249.
13. MacDonalds, J.C., Serphillips, J. and Guerrera, J.J. (1973) J. Phys. Chem., 77, 370.
14. Abu-Hamdiyyah, M. (1965) J. Phys. Chem., 69, 2720.
15. Schellman, J.A. (1955) Compt. rend. trav. lab. Carlsberg, Ser. Chim., 29, 223.
16. Frank, H.S. and Franks, F. (1968) J. Chem. Phys., 48, 4746.
17. Gordon, J.A. and Warren, J.R. (1968) J. Biol. Chem., 243, 5663.
18. Tanford, C. (1968) Adv. Protein Chem., 23, 122; also (1970) 24, 1.

19. Arakawa, K., Takenaka, N. and Sasaki, K. (1970), Bull. Chem. Soc. Japan, 43, 636.
20. Jolicoeur, C. and Friedman, H.L. (1971) Ber. Bunsenges. Physik. Chem., 75, 248.
21. Sarma, T.S. and Ahluwalia, J.C. (1973) Chemical Society Reviews, Vol. 2, No. 2.
22. Krescheck, G.C. and Scheraga, H.A. (1965) J. Phys. Chem., 69, 104.
23. Stokes, R.H. (1967) Aust. J. Chem., 20, 2087.
24. Vold, R.L., Daniel, E.S. and Chan, S.O. (1970) J. Amer. Chem. Soc., 92, 6771.
25. Atherton, N.M. and Starch, S.J. (1972) Faraday Transactions, II, 2, 374.

## CHAPTER IV

### EFFECT OF TWO AMPHIPHILIC SOLUTES ON WATER STRUCTURE-SPIN PROBE STUDY

Amphiphiles such as fatty acid salts or tetra-alkyl-ammonium halides and similar compounds are characterized by the fact that they possess polar or ionic heads that interact with water very well and cause dissolution; the nonpolar 'tails' that they possess display hydrophobic character. As a result, they exhibit rather interesting properties in water. One characteristic property of amphiphilic salts of long chain fatty acids is the formation of inter-molecular aggregates known as micelles in which the nonpolar moieties of the molecules come together avoiding contact with water, and the polar heads all face out towards the solvent. The critical concentration beyond which such aggregation occurs is called the critical micelle concentration (cmc) and is usually  $10^{-3}$  to  $10^{-1}$  M in water.<sup>1</sup> Clearly



this would be determined by the nature and length of the non-polar chain in these compounds. For example, in the cationic detergents, n-octyl ammonium bromide has a cmc of  $2 \times 10^{-1} \text{ M}$ , while forttricetyl pyridinium bromide the value is  $10^{-3} \text{ M}$ ,<sup>1</sup> and for a salt such as tetra-n-propyl ammonium bromide, the cmc has been suggested to be  $1.4 \text{ m}$ .<sup>2</sup> Even below the cmc dimeric and multimeric association appears likely. Anionic detergents such as fatty acid salts also associate in water to form micelles. While Na oleate has a cmc value of  $10^{-3} \text{ M}$ , with Na butyrate such aggregation will be far less efficient and might be expected to occur, if at all, around  $10 \text{ M}$ .

Lot of attention has been given to the behaviour of tetra-alkyl ammonium salts in aqueous solution. In very dilute solutions approaching the infinite dilution limit, where solute association can be ignored, these exhibit unusual thermodynamic behaviour which are associated with structures induced in the water near the hydrophobic groups, called hydration of the second kind.<sup>3</sup> It is well to recall here that the interaction energy (induced-dipolar-dipolar type) between alkanes and water is favourable<sup>4</sup> and consequently favours structuring of water around an isolated hydrophobic group. If the entropy term does not offset this, free energy of the process will favour such hydration of the second kind. This is similar to the structuring of water in the clathrate hydrates of many nonpolar compounds that has been extensively studied.<sup>5</sup> Such a water-

structuring effect persists even in the solution state for dilute solutions of tetra-alkylammonium halides. At high concentrations, hydrophobic association between solute molecules will start occurring leading to solute aggregation, which for higher salts results in micelles. The water-structure-making tendency in a series of tetraalkyl ammonium salts has been investigated by heat capacity measurements,<sup>6</sup> apparent molal volume data,<sup>7</sup> spin probe measurements,<sup>8</sup> and so on. It is known that as one goes up in the series\*  $\text{Me}_4\text{N}^+$ ,  $\text{Et}_4\text{N}^+$ ,  $\text{Pr}_4\text{N}^+$ ,  $\text{Bu}_4\text{N}^+$  and  $\text{Am}_4\text{N}^+$ , the structure-making capacity increases almost linearly.<sup>6</sup> It has also been suggested that as the concentration of these cations in water is increased, micelle formation will start occurring. The cmc for  $\text{Et}_4\text{NBr}$  and  $\text{Pr}_4\text{NBr}$  have been suggested to be 4 m and 1.4 m respectively.<sup>2</sup> This possibility offers an alternate interpretation of the apparent molal volume data. If this were true, then a salt like  $\text{Am}_4\text{NBr}$  should form micelles at a much lower concentration. Furthermore, it may also be expected that the micellar aggregation should be more favourable (cmc smaller value) for a tetra-alkylated cation such as TAAB than for the corresponding monoalkylated analogue such as  $\text{AmNH}_3^+\text{Br}$ , since the hydrophobic moiety in the former is more than in the latter.

---

\*Abbreviations: Me = methyl, Et = ethyl, Pr = n-propyl, Bu = n-butyl, Am = n-amyl, TAAB = tetra-n-amyl ammonium bromide.

The case of the salt TAAB is of interest. Thermodynamic measurement<sup>6</sup> of the infinite dilution heat of solution, and the heat capacity, of this salt in water reveal that  $\text{Am}_4\text{N}^+$  ion is an excellent structure maker of water. Partial molal volume data<sup>9</sup> are consistent with the fact that TAAB does not form any polyhedral clathrate hydrate. While tetraisoamyl ammonium fluoride forms clathrate hydrates,<sup>10</sup> tetra normal amyl ammonium bromide does not.<sup>11</sup> The cation in TAAB, like  $\text{Et}_4\text{N}^+$ , is able to structure water but not stabilise it as clathrate. Wirth<sup>2</sup> has suggested micellar aggregation of TAAB, though this has been questioned by Lindman, Forsen and Forslind.<sup>12</sup> These authors have done  $\text{Br}^{79}$  quadrupole relaxation measurements in aqueous solutions of tetraalkyl ammonium bromides and have suggested that the  $\text{Br}^-$  ions are rapidly exchanging between two sites, one being water lattice and the other associated with a clathrate-like lattice around the cation. Jolicoeur and Friedman<sup>8</sup> have measured the linewidth of hydrogen hyperfine lines ( $W_H$ ) and the tumbling correlation time  $\tau_\theta$  of the spin probe TEMPO in aqueous solutions of tetraalkyl ammonium salts. The reduced correlation time, corrected for bulk viscosity  $\eta$ ,  $\tau_\theta/\eta$ , reduces linearly with concentration for  $\text{Et}_4\text{NBr}$  and  $\text{Bu}_4\text{NBr}$ , while for n-octyl ammonium bromide,  $\tau_\theta/\eta$  increases sharply past 0.2 M indicating micellar aggregation of this salt. In the case of  $\text{Bu}_4\text{NBr}$ , the Kivelson plot of the linewidth  $W_H$  against  $T/\eta$  showed that perhaps a two state model may be worth considering

wherein the probe is sometimes far away from the solute with large  $\tau_{\theta}$  and small  $\tau_J$ , and at other times close to the hydrophobic solute with a smaller  $\tau_{\theta}$  and large  $\tau_J$ . Such a two-state model becomes feasible particularly if the quaternary ammonium ion is able to order water around it stably. In this sense, TAAB offers itself as a good candidate for spin probe studies of the above kind.

When we turn to the amphiphiles with nonpolar anions, the simplest examples would be sodium salts of paraffin chain acids. Here again, experimental studies have been reported on their effect on water structure. In the series sodium formate, acetate, propionate and butyrate, Chawla<sup>6</sup> has found the water structure-making capacity of the anions to increase as one goes up the series. While formate is a structure-breaker, the butyrate is an excellent structure-inducer as seen by heat capacity measurements. Lindenbaum's heat of dilution study,<sup>13</sup> the near infrared spectral study of aqueous solutions of these salts,<sup>14</sup> and Snell and Greyson's<sup>15</sup> measurements on enthalpies of transfer all point to the same conclusion. However, the possibility of micellar aggregation in these systems is not well studied. While Na stearate, oleate and palmitate form excellent micelles at  $10^{-3}$  M, such a tendency should exist even in butyrate albeit concentrations as high as 1-3 M or so. Thus again the study of the concentration dependent effects on water structure by a salt such as sodium butyrate, using the spin-probe method,

would be interesting. The advantages of using the spin probe method have already been mentioned earlier. To this end, we describe the spin-probe spectral studies in aqueous solutions of TAAB and of sodium butyrate (abbreviated as NaBu) in this chapter. The results on TAAB solutions are compared with those of other homologous quaternary ammonium salts,<sup>8</sup> and also other experimental results on TAAB. The results on NaBu are quite similar to those seen by Jolicoeur and Friedman<sup>8</sup> for n-heptylammonium bromide, and are interpreted in a straight forward fashion. The results on TAAB however, are a little more complex and point to the possibility of a two-state residence model for the spin-probe in these solutions.

#### EXPERIMENTAL

Sodium butyrate was prepared by reacting a solution of analytical grade butyric acid (in slight excess) with pure NaOH. The excess acid was removed from solution with pure ether, and Na butyrate obtained by evaporation, and purified by recrystallization from methanol-water, and ether. The recrystallized salt was dried in a vacuum oven at 60-80°C for 8-10 hours and stored dry, and gave satisfactory analysis for elements. TAAB was obtained from Eastman Organic Chemical Distillation Product Industries, USA and recrystallized from acetone-ether mixture. The e.s.r. spectra of TEMPO dissolved in aqueous solutions of

NaBu, and of TAAB were obtained by the experimental procedures described in earlier chapters, and the parameters  $W_H$  and  $\tau_\theta$  obtained as mentioned earlier. In the case of TAAB, spin-probe e.s.r. measurements were also made as a function of temperature and the  $a_o$ (SR) contribution was estimated by the procedure described in Chapter II, and the correlation time  $\tau_J$  calculated from a Debye model of motion.

## RESULTS AND DISCUSSION

We shall take the case of sodium butyrate first, since its interpretation seems straight forward. Table IV.1 lists the tumbling correlation time  $\tau_\theta$ , the hydrogen hyperfine line-width  $W_H$ , and the statistical parameters for the e.s.r. spectrum of TEMPO in aqueous NaBu solutions. We have done the curve fitting using a value of 0.065 G for the proton hyperfine splitting constant. The argument for such a choice has been made in the end of Chapter III. (The trends seen in  $W_H$  with an assumed value of  $a_H = 0.10$  G are similar, except that the absolute values of  $W_H$  are consistently smaller). Figure IV.1 illustrates the variation in  $W_H$ , and in  $\tau_\theta$  of the probe in solutions of NaBu of increasing molarity. We were able to perform our measurements upto 3 M NaBu. Notice from Figure IV.1b that the tumbling correlation time  $\tau_\theta$  of the probe decreases slightly at 1 M NaBu beyond which it increases sharply to

Table IV.1

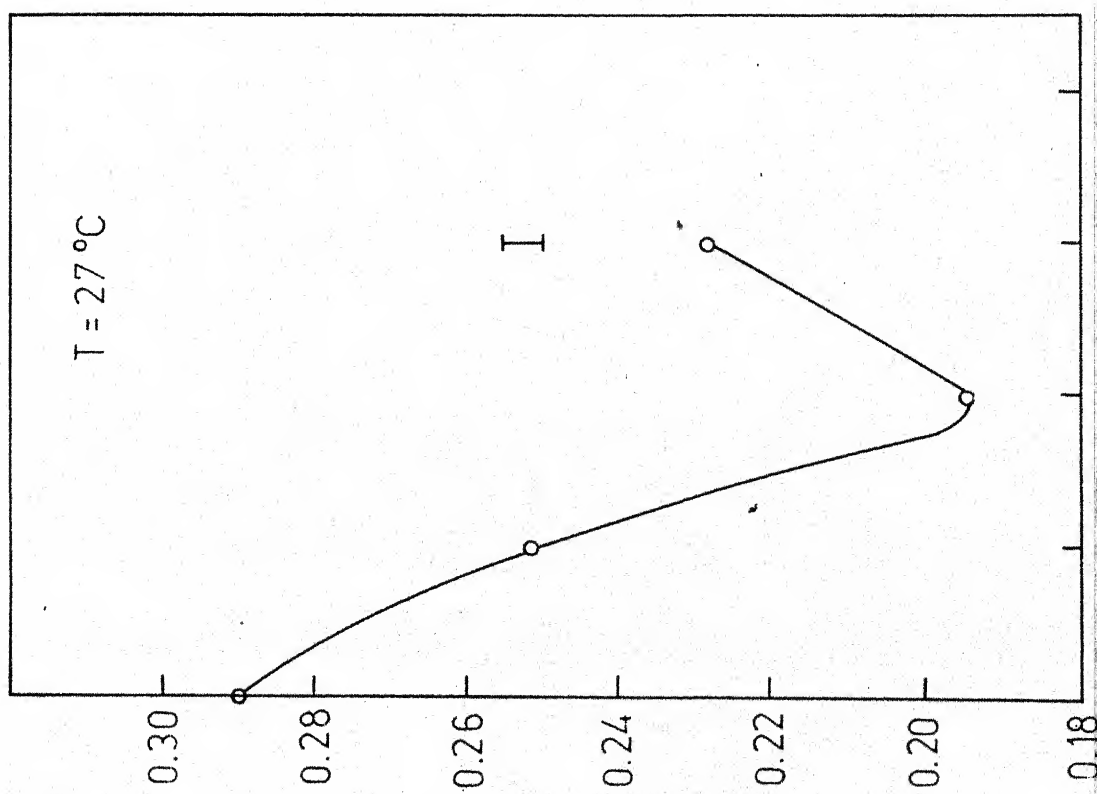
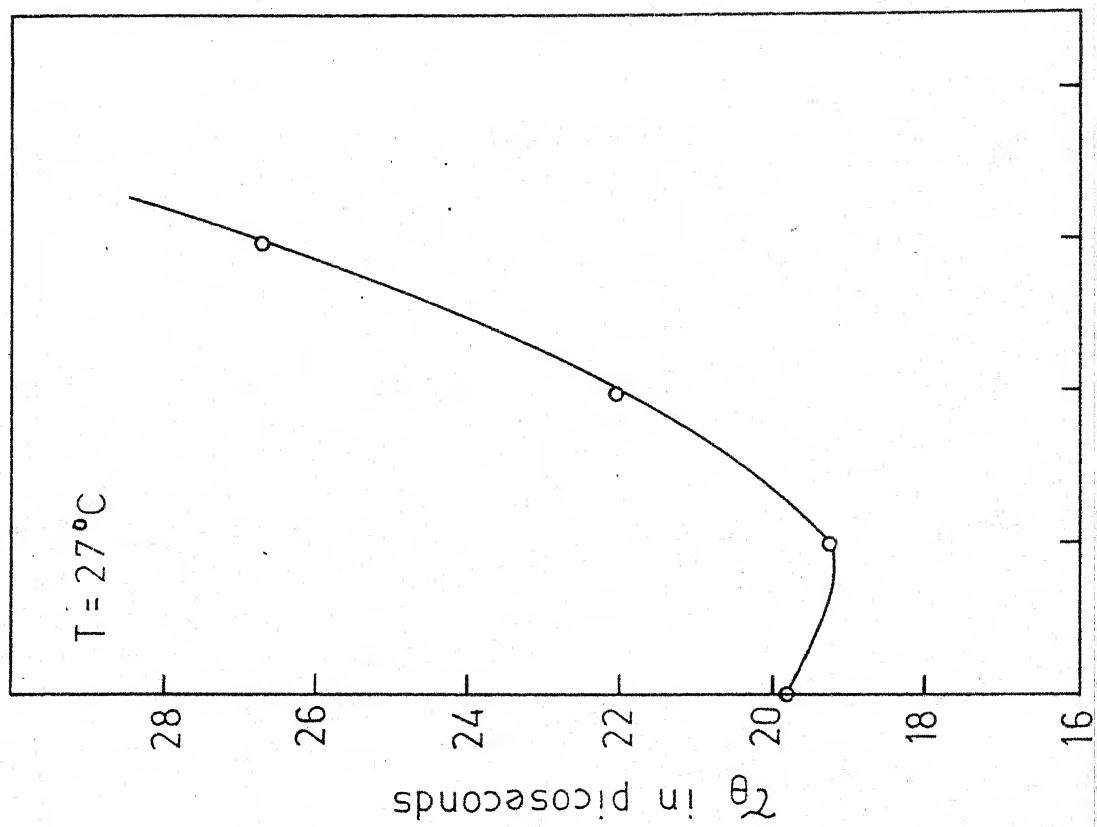
Computed ESR parameters, error function, error limits and  
Tau values for TEMPO in aqueous sodium butyrate

Concen- tration	$a_H$ Fixed at 0.065 gauss		Room Temperature $\approx 27^\circ\text{C}$		
	Hyperfine linewidth $w_H$ (gauss)	Normalizing parameter $E(3)$	Error function $\Phi H$	Standard error for width $w_H$ SE	Correlation time $\tau_\theta \times 10^{12} \text{ sec}$
1 $\underline{M}$	0.251	0.09285	1.089	0.0146	19.5
2 $\underline{M}$	0.195	0.07710	0.850	0.0130	22.0
3 $\underline{M}$	0.229	0.07570	0.460	0.0100	26.8

Fig. IV.1(a): Proton hyperfine linewidth of the  $m_I = 0$  manifold of TEMPO,  $W_{II}$ , as a function of molarity of sodium butyrate.

(b): Tumbling correlation time,  $\tau_c$ , of the spin-probe TEMPO as a function of molarity of sodium butyrate.



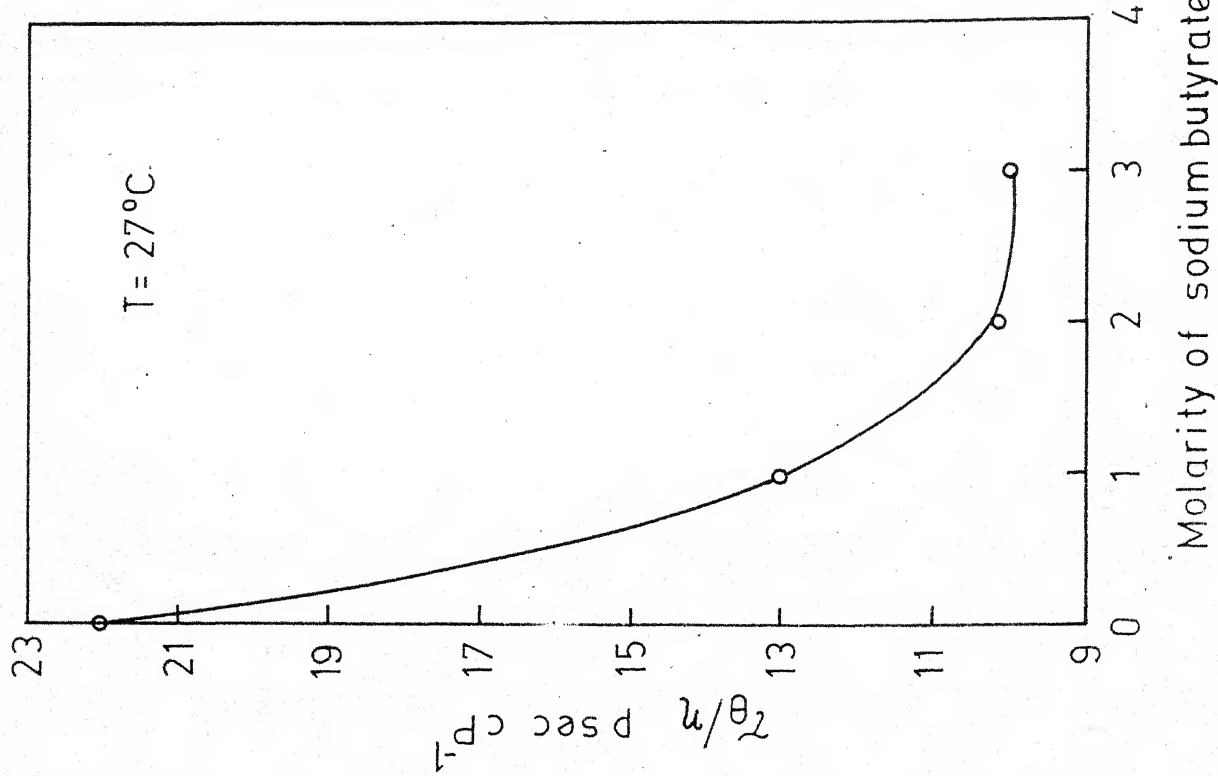
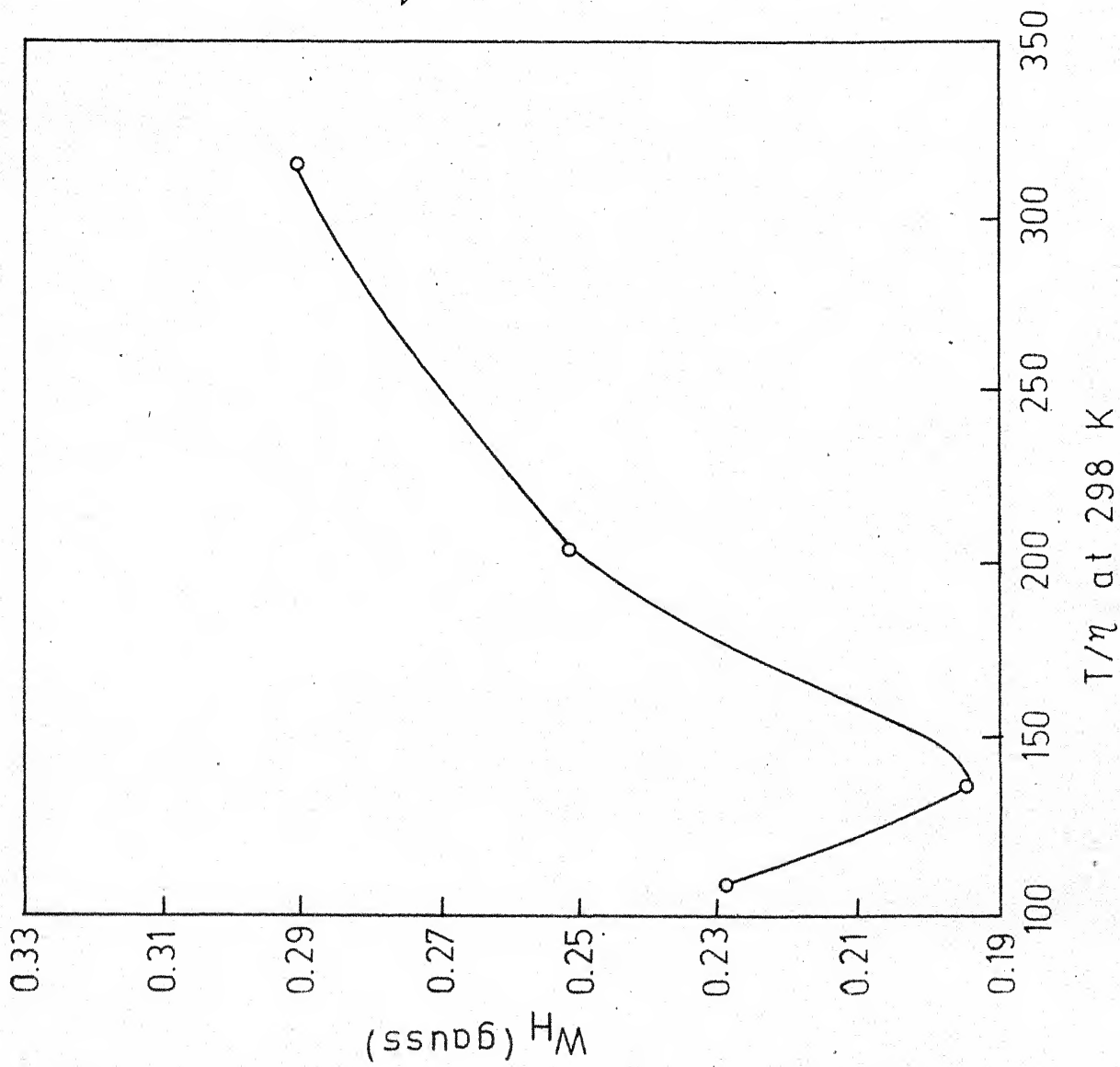


22 psec at 2 M and 27 psec at 3 M NaBu correction for bulk viscosity to yield  $\tau_e/\eta$  gives the following values: 22, 13, 10, 10 psec  $\text{cP}^{-1}$  at 0, 1, 2, and 3 M NaBu respectively, showing that the parameter decreases with molarity, attaining a constant value in high molarities. The linewidth behaviour depicted in Figure IV.1a is characterized by a minimum at 2 M NaBu and resembles in its general nature what has been observed<sup>8</sup> for cationic hydrophobic salts such as n-hexyl ammonium bromide and n-heptyl ammonium bromide. Indeed the similarity in the  $W_H$  and  $\tau_e/\eta$  behaviour of the probe in NaBu and in n-hexyl ammonium bromide and  $\text{Bu}_4\text{NBr}$  solutions is rather striking suggesting that the action on water structure by these two solutes is very similar. Incidentally this also shows the importance of interpreting  $\tau_e$  data in terms of solvent viscosity corrections. Turning to the Kivelson plot, i.e.  $W_H$  versus  $T/\eta$  for NaBu solution (Figure IV.2), again the similarity with n-hexyl ammonium bromide and  $\text{Bu}_4\text{NBr}$  is striking. Jolicoeur and Friedman<sup>8</sup> have computed  $W_H$  from  $\tau_e$  using the m-dependent broadening effects and have shown that in this case at high concentrations, an extra broadening occurs. Part of the increase in  $W_H$  in the solution has been thought of to arise from a possible two-state model for the probe motion. This leads us to believe that a similar situation exists in NaBu solutions.

Chawla<sup>6</sup> has shown that the butyrate anion is a structure-maker of liquid water; its  $\Delta C_p^\circ$  at 30°C in water is

Fig. IV.2(a): Proton hyperfine linewidth of the  $\alpha$ -D radi-  
fold of TEMPO,  $W_H$ , as a function  $T/\eta$  at  
 $T = 298K$  for 1-3 M sodium butyrate.

(b): Tumbling correlation time corrected for vis-  
cosity,  $\tau_c/\eta$ , as a function of molarity of  
sodium butyrate.



+32 cal mol<sup>-1</sup>K<sup>-1</sup>. Other have agreed with this conclusion using different methods.<sup>13-15</sup> One expects a similar structure-making tendency for n-hexyl ammonium bromide on the same principle. Before interpreting the data, we ought to worry about the possibility of NaBu aggregating in solution to form micelles. There is no experimental report either way about this. However, if one were to use the general relation given by Kleven<sup>16</sup> for sodium carboxylates, i.e.,

$$\log (\text{cmc}) = a_0 - a_1 n$$

where  $a_0 = 2.41$ ,  $a_1 = 0.341$  and  $n$  the number of carbon atoms in the nonpolar sidechain of the carboxylate, one obtains a value for cmc for NaBu of about 24 M! Thus micellar aggregation at 3 M can be ruled out on the same grounds; pre-micellar aggregation of NaBu into dimers or oligomers may also be considered unlikely at 3 M. Therefore under the conditions of experiment, NaBu is essentially dispersed as monomers. In any event, our results on  $\tau_\theta$  indicate that the radical is not sensitive to molecular aggregates of the hydrophobic solutes unless they have the size and stability of the micelles formed in higher homologues.

The similarity of the Kivelson plots for the probe in NaBu, and in Bu<sub>4</sub>NBr or n-hexyl ammonium bromide suggest that the structural situation obtained with NaBu and with the latter salts are similar. Since analysis<sup>8</sup> reveals extra broadening

in the latter solutions that is not accounted for by probe-probe interactions, conformational alteration of the probe, or from changes in  $a_H$  or  $a_N$ , a two-state model was considered as a possibility. In this, two situations are envisaged, one in which the probe is far from the solute with a large  $\tau_\theta$  and very small  $\tau_J$ , and the other where it is near the solute with a smaller  $\tau_\theta$  and large  $\tau_J$ . If the second situation is less probable than the first, the weighted  $\tau_\theta$  will change little from the value of the first site while the weighted average  $\tau_J$  could be very different. Such a situation is realistic particularly if the hydrophobic solute orders water around it as stable clathrate cages.

In light of the fact that butyrate is a structure-maker, and the spin-probe spectral features in NaBu are similar to those seen in solutions of the other structure-makers such as  $\text{Bu}_4\text{NBr}$  and n-hexyl ammonium bromide, we conclude that similar to these cases, the spin-probe may be experiencing a two-state residence situation. This is particularly of interest in high concentrations of NaBu. In general terms then our spin-probe results on NaBu solutions indicate that essentially similar effects are obtained whether the non-polar moiety exists in the cation or in the anion in amphiphiles, and also that effects of structural ordering may indeed be observable by the spin-probe Method. This agreement between our data and those of Jolicœur on similar systems is gratifying and point to the possibilities of this method.

We next turn our attention to the e.s.r. studies of the probe in aqueous solutions of TAAB. The solubility of TAAB in water is limited and we have not been able to go beyond 0.25 M in our measurements. Table IV.2 lists the e.s.r. spectral parameters in this solution. Figure IV.3 illustrates the variation of  $W_H$  and  $\tau_e$  with concentration of TAAB. The former (part a of the figure) shows a small minimum at 0.025 M TAAB with a value of 0.268 G after which it returns to the water value of 0.292 G at 0.05 M. There is a further reduction in the line-width to 0.238 G at 0.1 M after which it increases linearly upto a value of 0.270 G at the limit of solubility, 0.25 M at room temperature. Since the concentrations used were small, and the viscosity values not reported, we decided to use the  $W_H$  vs M curve itself for further treatment. In Figure IV.3b are plotted the  $\tau_e$  values for the probe in TAAB solutions. The behaviour is rather complex, going through two minima within this concentration range (0-0.25 M). The following points are worth noting as background material before interpretation is attempted.

Thermodynamic study<sup>17</sup> shows  $Am_4N^+$  ion to be a very efficient structure maker of water. The question of the compound associating to form micelles in high concentrations is open. Wirth<sup>2</sup> has suggested that  $Et_4NBr$  and  $Pr_4NBr$  might form micelles at 4 m and 1.4 m respectively. Thus  $Am_4NBr$  may form micelles at even lower concentrations. He has suggested that even at premicellar concentrations, dimeric and oligomeric association

Table IV.2

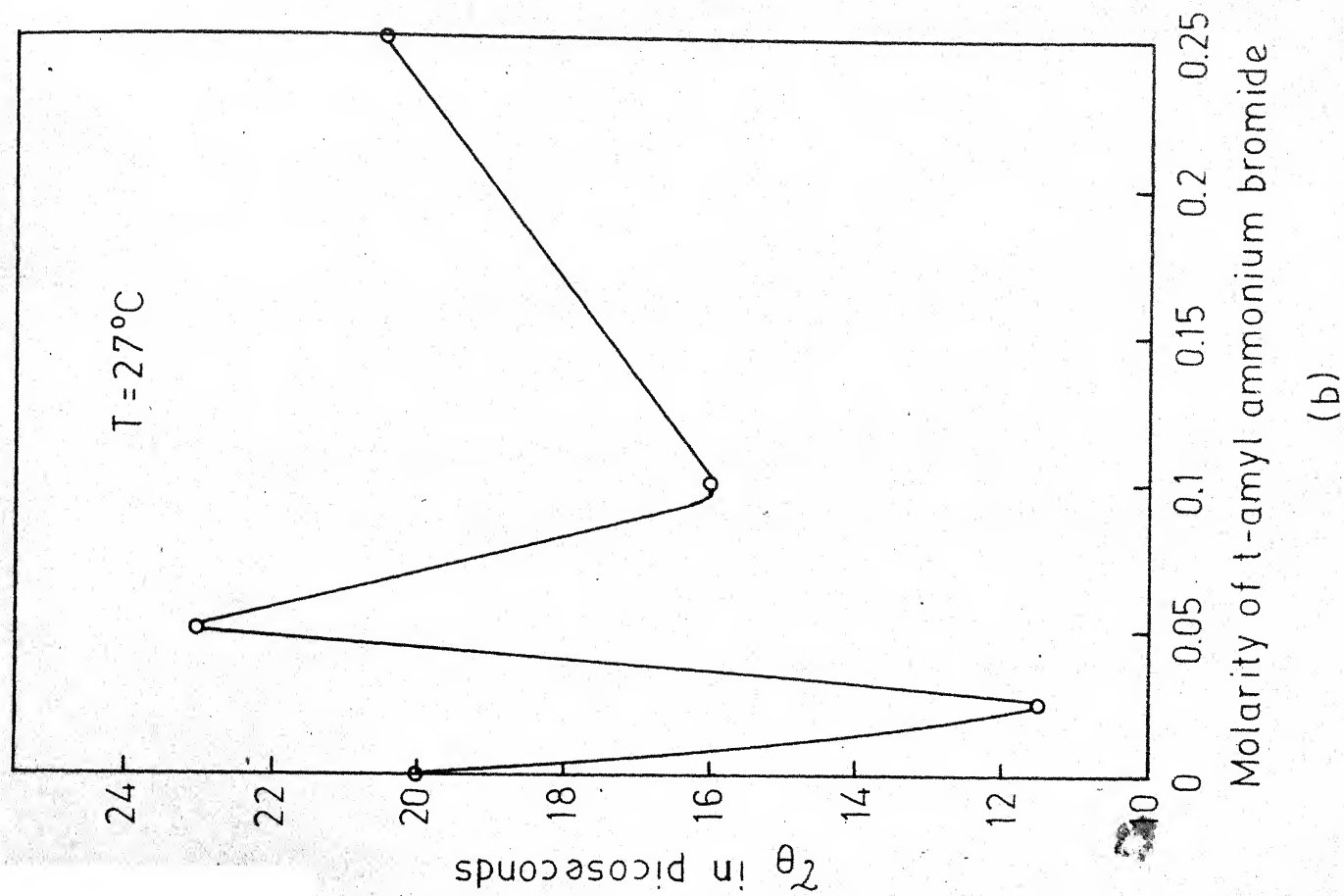
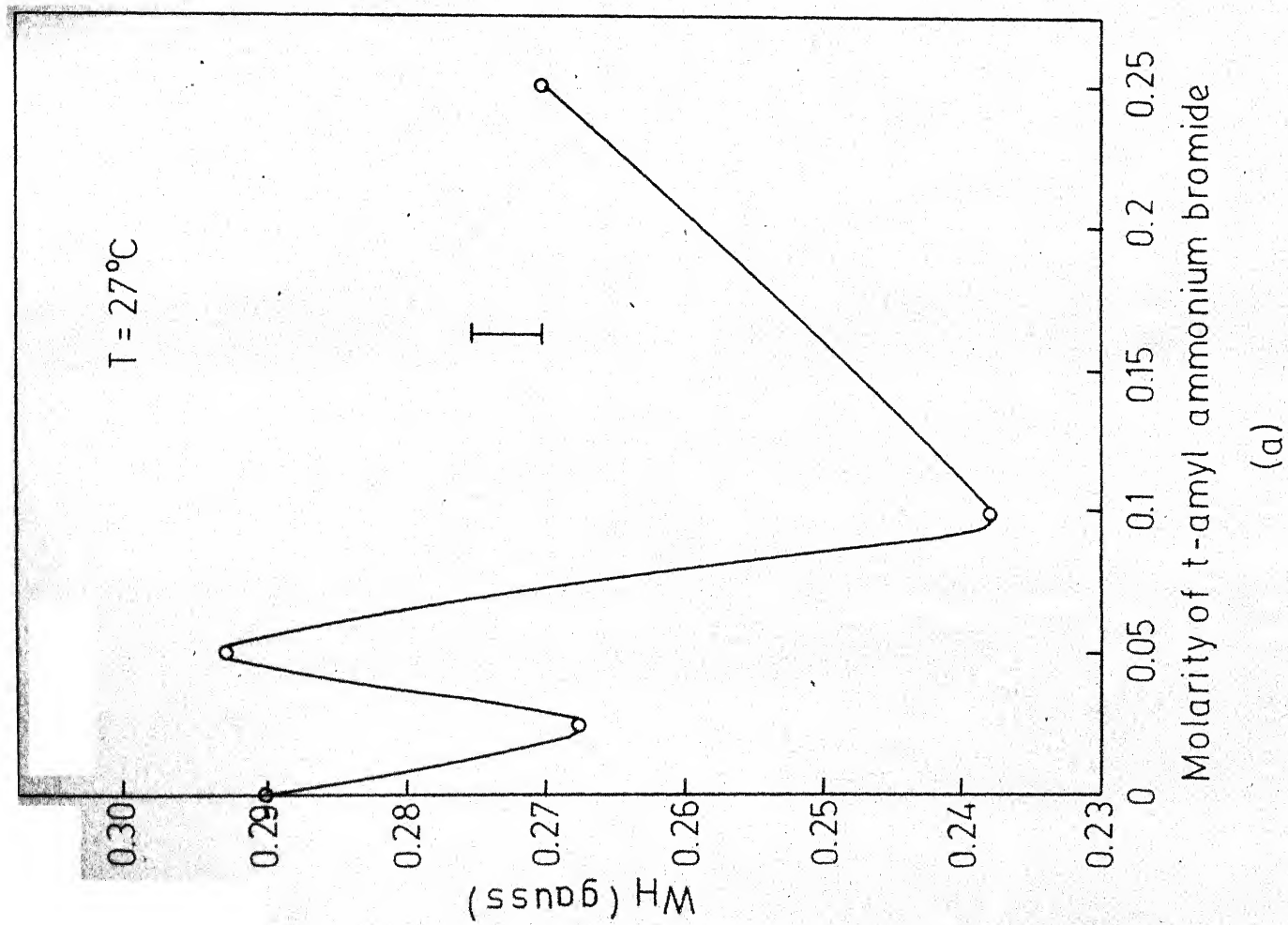
Computed ESR parameters, error function, error limits and  
Tau values for TEMPO in aqueous t-amyl ammonium bromide

Concen- tration	$a_H$ Fixed at 0.065 G			Room Temperature $\approx 27^\circ\text{C}$	
	Hyperfine linewidth $w_H$ (gauss)	Normalizing parameter $B(3)$	Error function $\Phi H$	Standard error for width $w_H$ SE	Correlation time $\tau_\theta \times 10^{12}$ sec
0.025 $\bar{M}$	0.268	0.0800	0.510	0.0139	11.5
0.05 $\bar{M}$	0.293	0.0620	0.100	0.0092	23.0
0.1 $\bar{M}$	0.238	0.0765	0.170	0.0075	15.7
0.25 $\bar{M}$	0.270	0.0583	0.076	0.0076	20.5



Fig. IV.3(a): Proton hyperfine linewidth of the  $m_H = 0$  manifold of TEMPO,  $W_H$ , as a function of molarity of TAAB.

(b): Tumbling correlation time,  $\tau_c$ , of the spin-probe TEMPO as a function of molarity of TAAB.



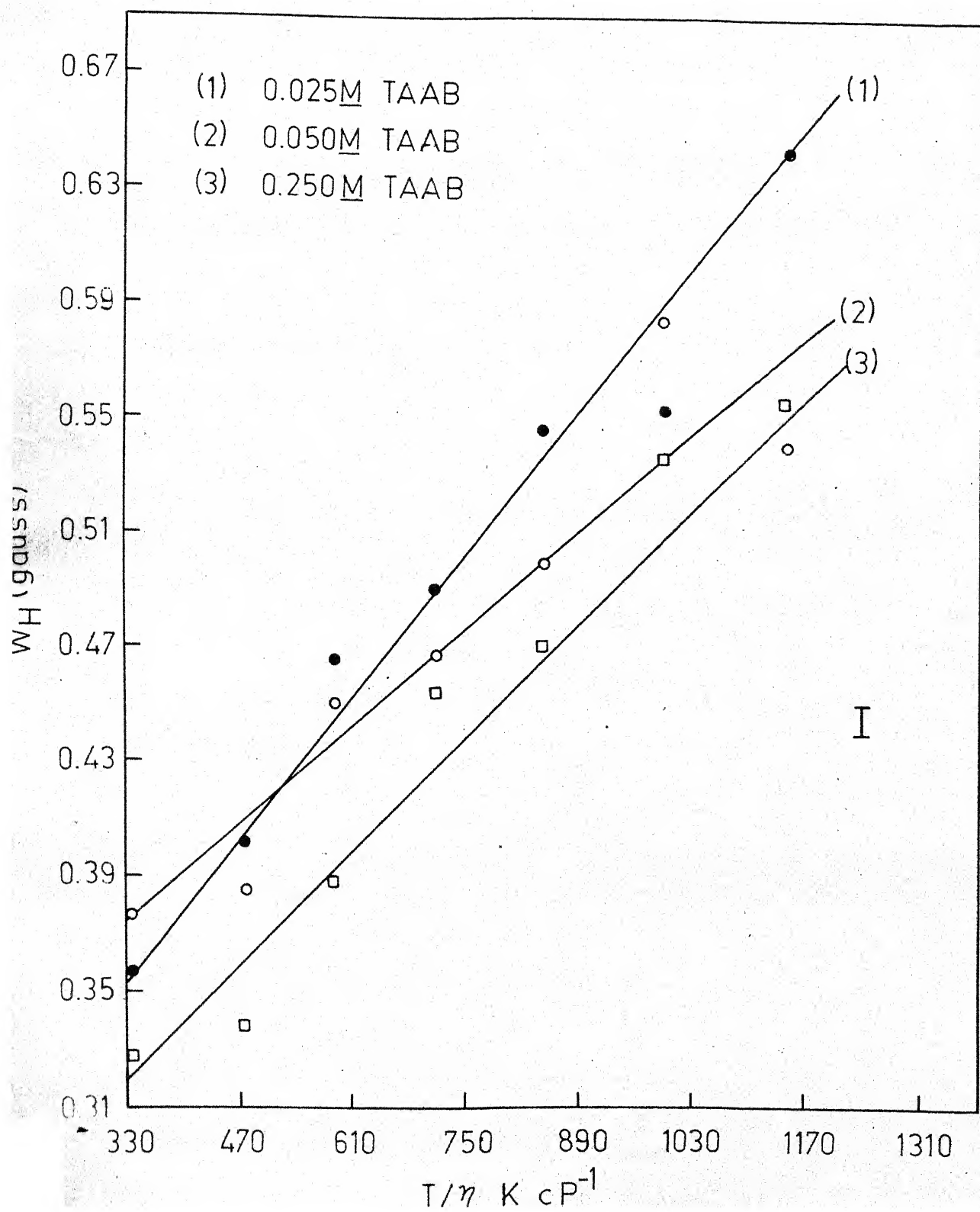
may occur that can explain the concentration dependence of apparent molar volume in these quaternary ammonium salts. Lindman and others<sup>12</sup> on the other hand have discounted this possibility but are in favour of a two site model. They have interpreted the  $^{79}\text{Br}$  quadrupole relaxation times in  $\text{R}_4\text{NBr}$  salts in terms of a rapid exchange situation where  $\text{Br}^-$  ions exchange between water lattice in the bulk and a second site of water molecules that are associated clathrate-like near the  $\text{R}_4\text{N}^+$  cations. Now while TAAB itself has not been observed to form stable low-melting clathrate hydrates,<sup>11</sup> the possibility of solvated structured water molecules surrounding the cation enhancing each other exists.<sup>9, 12</sup> A similar two-site residence model can be envisaged for the probe TEMPO itself in aqueous TEMPO solutions.

The data on TAAB solutions differ from those in  $\text{Bu}_4\text{NBr}$  or  $\text{NaBu}$  in that the linewidth plot shows an additional minimum around 0.025 M TAAB, and the  $\tau_\theta$  also decreases to a minimum value of 11.5 psec at this concentration. Besides this, the spectral features are similar to  $\text{Bu}_4\text{NBr}$ . This initial additional minimum is puzzling, and an exact interpretation of this feature is at best speculative at present. The feature appears real and not an artifact as shown by its reproducibility. One is left to consider the possibility of treating the anion-water interactions and the hydrophobic cation-water interactions

separately. Bromide ion is known to be a water structure-disrupter,<sup>18</sup> whereas  $\text{Am}_4\text{N}^+$  ion is a structure-promoter. If the two ions act independently, at least in low concentrations of TAAB, one gets two opposing situation. Another possibility is that of probe-probe interaction, but on the basis of arguments presented for NaBu, we disregard this. A third and distinct possibility is to invoke the two-site model for TEMPO itself with a dependence on the concentration of TAAB. With increasing concentration of TAAB, hydrophobic association of the salt to produce oligomeric aggregates in equilibrium with monomers, with differing hydrophobic hydration profiles for each. The linewidth and  $\tau_\theta$  of the probe would then be a weighted composite of probe finding itself in the two differing environments.

In order to assess the contribution to the linewidth by  $a_0(\text{SR})$  term, i.e. spin-rotation terms, we also investigated the temperature dependence of  $W_H$  at several concentrations of TAAB. The dependence is illustrated in Figure IV.4. The relative slopes come out to be 3.5, 2.358 and  $2.91 \times 10^{-4} \text{ G CP K}^{-1}$  at 0.025, 0.05 and 0.25 M respectively. Calculation of  $\tau_J$  from these values shows that  $\tau_J$  is smallest at 0.05 M and largest at 0.025 M. In light of the postulate of a two state model where in each state  $\tau_\theta$  and  $\tau_J$  are inversely related, this minimum of  $\tau_J$  at 0.05 M is consistent with the largest  $\tau_\theta$  value encountered at this concentration; likewise at 0.025 M we find the lowest  $\tau_\theta$  and highest  $\tau_J$  value.  $\tau_J$  calculated from the  $a_0(\text{SR})$  contribution

Fig. IV.4: Proton hyperfine linewidth of the  $m_i = 0$  manifold of TEMPO,  $W_H$ , as a function of  $T/\eta$  at 0.025 M, 0.05 M and 0.25 M TAA2.



before definite conclusions can be drawn about the anomaly of TAAB. The possibility of an artifact arising in the  $W_H$  and  $\tau_\theta$  plots also can not be ruled out. But in the framework of solutes like  $Bu_4NBr$ , n-hexyl ammonium bromide,  $NaBu$  and TAAB, the results at present point to similarity of behaviour of these solutes with respect to water structure-making.

REFERENCES

1. See for example Krescheck, G.C. (1975) in 'Water - a Comprehensive Treatise', Ed. Franks, F., Plenum Press, New York, Vol. 4, Chapter 2.
2. Wirth, H.E. (1967) J. Phys. Chem., 71, 2922.
3. Hertz, H.G. (1964) Ber. Bunsenges. Physik. Chem., 68, 907.
4. Kauzmann, W. (1959) Adv. Protein Chem. 14, 1.
5. Hagan, M. (1962) 'Clathrate Inclusion Compounds', Reinhold, New York.
6. Chawla, B. (1974) Ph.D. Thesis, Department of Chemistry, Indian Institute of Technology, Kanpur.
7. Kay, R.L., Vittuccio, T., Zawoyski, C. and Evans, D.F. (1966) J. Phys. Chem., 70, 2336.
8. Jolicoeur, C. and Friedman, H.L. (1971) Ber. Bunsenges. Physik. Chem., 75, 248.
9. Wen, W.Y. and Saito, S. (1964) J. Phys. Chem., 68, 2639.
10. Feil, D. and Jeffrey, G.A. (1961) J. Chem. Phys., 35, 1863.
11. Beurskens, G., Jeffrey, G.A. and McMullan, R.K. (1963) J. Chem. Phys., 39, 3311.
12. Lindman, B., Forsen, S. and Forslind, E. (1968) J. Phys. Chem., 72, 2805.
13. Lindenbaum, S. (1971) J. Chem. Thermod., 3, 625.
14. Worley, J.D. and Klotz, I.M. (1966) J. Chem. Phys., 45, 2868.
15. Snell, H. and Greyson, J. (1970) J. Phys. Chem., 74, 2148.



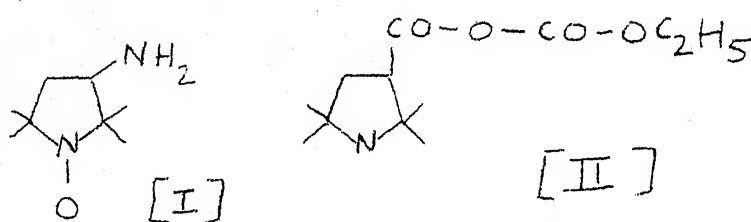
16. Klevens, H.B. (1948) J. Phys. Chem., 52, 130.
17. Mohanty, R.K. (1972) Ph.D. Thesis, Department of Chemistry, Indian Institute of Technology, Kanpur.
18. Verral, R.E. (1975) in 'Water - a Comprehensive Treatise', Ed. Franks, F., Plenum Press, New York, Vol. 3, Chapter 5.

## CHAPTER V

### AN ATTEMPT TO USE A SPIN PROBE TO MONITOR CONFORMATIONAL CHANGES IN A GLOBULAR PROTEIN

The technique of covalently attaching a spin probe to a protein by reacting it with a stable free radical molecule containing an appropriate functional group is termed spin labelling. This causes the protein molecule to exhibit electron spin resonance, and using this spin labelling technique a lot of useful information about the conformational dynamics of the protein has been obtained.<sup>1</sup> For example, the protein bovine serum albumin (abbreviated as BSA) has been spin-labelled by attaching to its side-chain functional group  $-NH_2$  (of lys residues) the free radical I, thereby making the protein esr active. A pH dependent esr spectral study of the spin labelled BSA molecule<sup>2</sup> shows that the intensity of the high field line undergoes a dramatic

change near pH 3, consistent with the changes observed in the optical rotation and intrinsic viscosity of BSA seen by Yang and Foster,<sup>3</sup> and attributed to an acid-induced conformational change in the protein molecule. Similarly, spin labelling of BSA by covalently attaching to its side-chain amino groups a mixed anhydride spin label (II) molecule has been done by Oakes and Cafe.<sup>4</sup> Measurements of the relative



intensities of the  $m_N=0$  esr line, and also the linewidth of the  $m_N=0$  central line of the labelled BSA as a function of pH showed that at pH  $< 4$ , the protein undergoes an isotropic expansion, and also that protein aggregation occurs at low pH in solutions of ionic strength  $> 0.1$ ; linewidth measurements indicate decreased protein mobility and/or spin-spin broadening due to the proximity of protein chains in the aggregate. At high pH, the esr measurements were found to be consistent with an expansion, or dissociation of the protein molecule into subunits.

It is clear that spin labelling of a protein is a useful technique in studying its structural dynamics. However,

once the label is covalently attached, it is bound and immobilized. Its tumbling motion is now actually that of the entire macromolecule itself and is thus slow (of the order of  $10^{-10}$  to  $10^{-9}$  sec), compared to the time taken for free I or II (picoseconds). It is also noted that the spectrum of the spin labelled protein is broad, formally resembling that of free radicals such as I or II placed in glasses.<sup>2</sup>

We attempted to approach this problem of monitoring the conformational transitions in a globular protein from a different point of view. Rather than covalently attach a radical, we let the radical TEMPO dissolve in an aqueous solution of BSA and look for changes in the esr spectrum of TEMPO as a function of the conformational status of BSA with changing pH. That is, to use a spin probe technique rather than a spin label technique. The rationale behind this is as follows:

BSA is known to be a globular protein with roughly 50% of its amino acid residues of nonpolar nature. It is partially helical in the native state in aqueous solution (pH 4-7) and folds with most of its nonpolar side chains inside the core and its polar side chain amino acid groups on the outside exposed to water. At pH  $< 4$  the protein undergoes a cooperative conformational unfolding, as also at high pH ( $\sim 10$ ).<sup>5</sup> Due to its hydrophobic content, a

globular protein (as BSA itself) binds small nonpolar molecules efficiently. The binding itself and associated conformational changes have been monitored.<sup>6</sup> For example globular proteins are known to bind small molecules like  $N_2O$ , halothane, butane, and the like.<sup>6</sup> We argued that accordingly a molecule such as TEMPO ought to bind to a globular protein like BSA noncovalently, and the esr spectrum of the probe noncovalently bound to the protein may offer us a monitoring device to detect conformational changes in the protein as a function of pH. Similar experiments with noncovalently bound fluorescent probes and NMR probes have been conducted.<sup>7</sup> Thus, our attempt to look at the esr spectrum of TEMPO that is noncovalently bound to BSA would be classified as a spin-probe method different from a spin-label method. In this chapter we report experiments conducted with this idea in mind.

## EXPERIMENTAL

Bovine Serum Albumin, Fraction V Powder, defatted and lyophilised, was purchased from sigma Chemicals, St. Louis, Missouri, USA, and used directly. Aqueous solutions of the protein were prepared (2%) at various pH, with no added salt, by carefully dissolving the protein in aqueous buffer solutions containing  $5 \times 10^{-4}$  M TEMPO, and taking

care not to shake the solution so as to avoid foaming and denaturation. The pH of the solutions were chosen by using appropriate buffer solutions. The measurements were done in the pH region 1-7. The technique of measuring the esr spectra and computing  $W_H$  and  $\tau_\theta$  have already been dealt with in Chapters II and III.

### RESULTS AND DISCUSSION

The esr spectral data of TEMPO in BSA solutions are listed in Table V.1. The calculated  $W_H$  values and  $\tau_\theta$  are plotted as a function of pH in Figure V.1. It is noted that the linewidth drops drastically between pH 1 to 4 and after that it rises a little until pH 7. It is not very clear whether this drop in  $W_H$  between pH 1-4 represents the acid unfolding of the protein. The increased width at low pH points to an increased microviscosity. It is known that at low pH BSA aggregates<sup>8</sup> in solution. Oakes and Cafe<sup>4</sup> have found that the intensity of the  $m_N=0$  esr line of spin-labelled BSA increases sharply in the pH 2-4 region to reach a plateau in the pH region 6-10 after which it again increases. The linewidth of this line ( $\Delta H_{pp}$ ) increases sharply as the pH is decreased below 4 - suggesting aggregation. It has not been possible for them to determine the hyperfine linewidth  $W_H$  since they were working with a spin-labelled

Table V.1

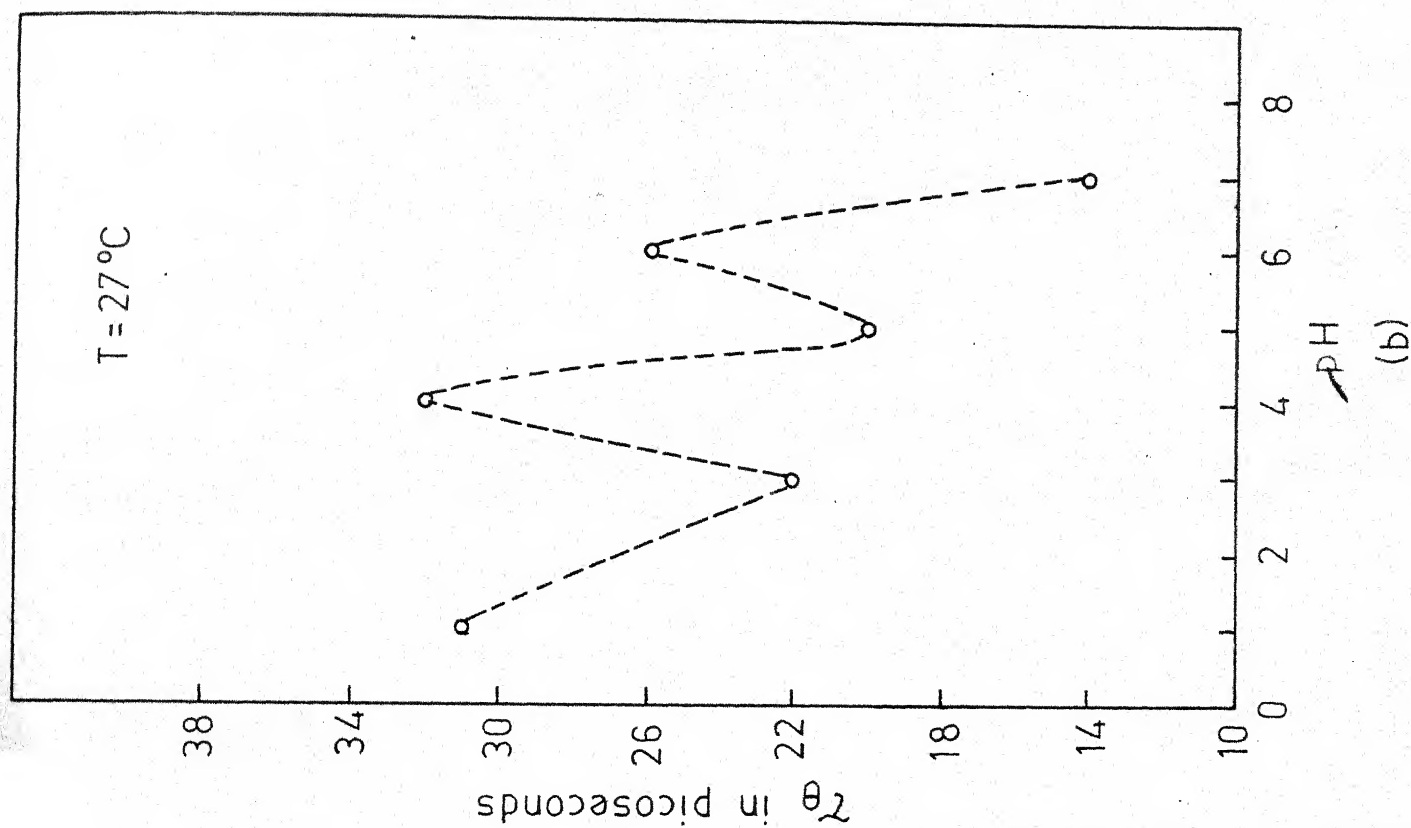
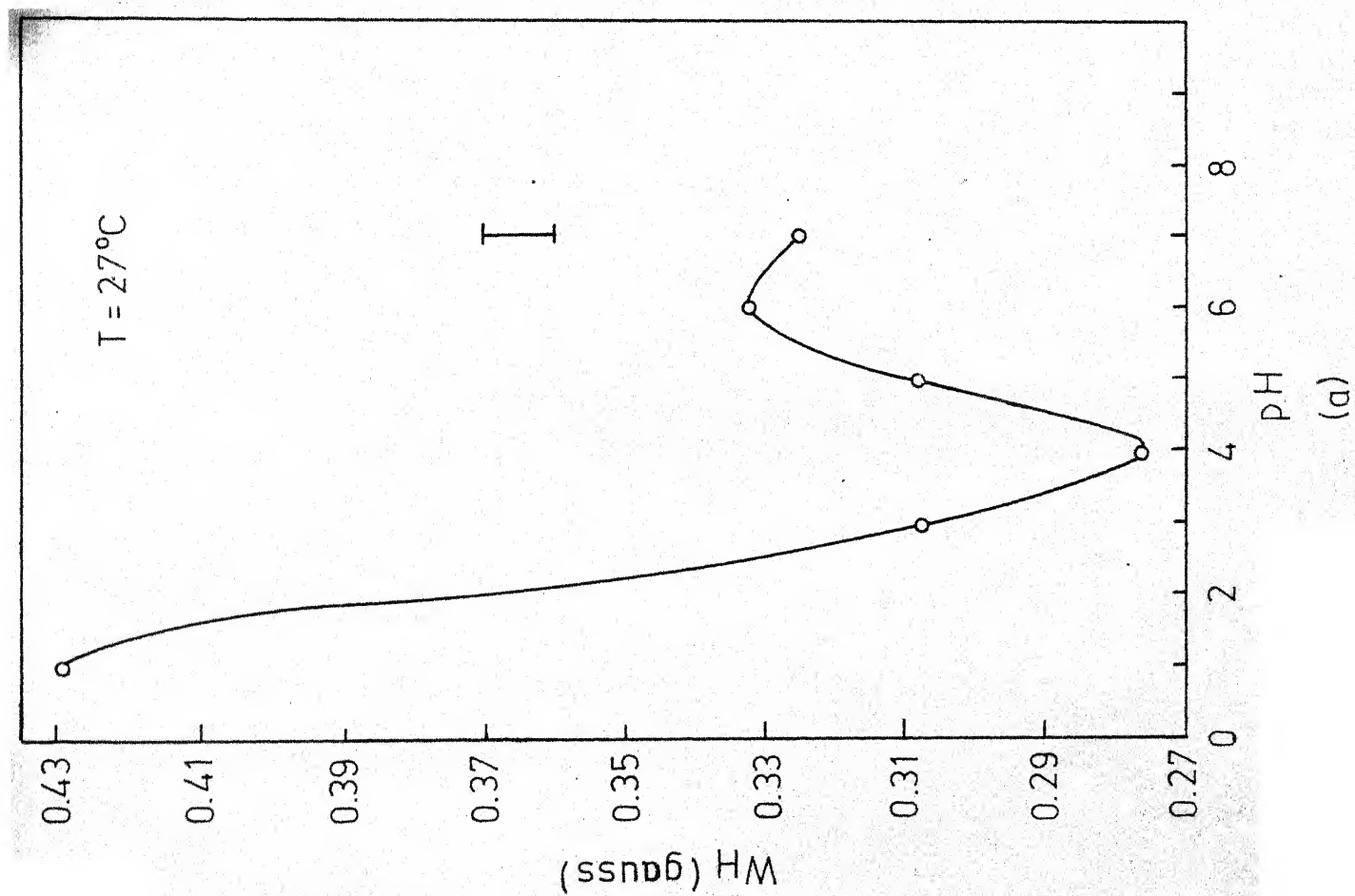
Computed ESR parameters, error function, error limits and  
Tau values for TEMPO in aqueous bovine serum albumin

a <sub>H</sub> Fixed at 0.065 gauss		Room Temperature $\approx 27^{\circ}\text{C}$			
pH	Hyperfine linewidth W <sub>H</sub> (gauss)	Normalizing parameter B(3)	Error function PHI	Standard error for W <sub>H</sub> SE	Correlation time $\tau_{\theta} \times 10^{12} \text{ sec}$
1	0.429	0.1110	0.091	0.0076	31.0
3	0.307	0.0838	0.940	0.0142	21.8
4	0.276	0.0837	1.000	0.0110	32.5
5	0.308	0.0977	0.420	0.0109	20.0
6	0.332	0.0938	0.530	9.0142	26.2
7	0.325	0.0983	0.210	0.0082	9.5
BSA in water	0.364	0.1200	0.980	0.0102	17.8

Fig. V.1(a): Proton hyperfine linewidth of the  $m_I = 0$  manifold of TEMPO,  $W_H$ , as a function of pH of medium for 2% BSA solutions.

(b): Tumbling correlation time,  $\tau_c$ , of the spin-probe TEMPO as a function of pH of medium for 2% BSA solutions.





protein. We have also monitored changes in  $\Delta H_{pp}$  and the intensity of the central line of the spin-probe TEMPO in aqueous solutions of BSA. The observed linewidth  $\Delta H_{pp}$  is altered very little in the entire range. However, the intensity of the line shows the following pattern:

pH	1.0	2.0	3.0	4.0	5.0	6.0	7.0
Intensity (relative)	3.0	3.4	3.7	3.8	4.0	4.3	4.7

The intensity sharply rises in the region pH 1-4 and again from 5-7. This is in contrast to the spin-labelled BSA case, where the intensity is constant in the pH region 6-10. Again, Stone *et al.*<sup>2</sup> have seen the intensity of the high field line of spin-labelled BSA to decrease in the pH region 2-4 after which it stays essentially constant. When we plot the high field line intensity of TEMPO in BSA solutions likewise, we notice that its behaviour is similar to the  $m_N=0$  line. Thus it appears to us that the use of TEMPO as a non-covalently used probe for monitoring changes in BSA is not successful. This is further illustrated by the plot of  $\tau_c$  as a function of pH (Figure V.1b) in BSA. The correlation time shows no discernible trend that reflects the changes in the conformation of the protein in solution.

A few lines are in order about the possible reasons for why the spin probe technique has not yielded satisfactory results. It is possible that the binding of TEMPO to BSA is weak so that effective binding has not occurred. It is also possible that the probe binds to the outer surface of the protein rather than in the hydrophobic interior. In such a case, the probe molecule will not "see" and report on the structural changes of the protein effectively. Perhaps a more hydrophobic stable free radical, e.g. di-*t*-butyl N-oxide ought to be tried. Also careful equilibrium binding study of the probe to the protein by equilibrium dialysis or gel filtration ought to be done to assess the extent and strength of binding. Thus, even though the present attempt has not been satisfactory, we believe this idea of using a non-covalently bound spin probe to monitor macromolecular structural changes is worth pursuing.

REFERENCES

1. McConnell, H.M. and McFarland, B.G. (1970) Quart. Revs. Biophys., 3, 91.
2. Stone, T.J., Buckman, T., Nordio, P.L. and McConnell, H.M. (1965) Proc. Natl. Acad. Sci. U.S., 54, 1010.
3. Yang, J.T. and Foster, J.F. (1954) J. Amer. Chem. Soc., 76, 1588.
4. Oakes, J. and Cafe, M.C. (1973) Eur. J. Biochem., 36, 559.
5. Foster, J.F. (1960) in "Plasma Proteins", Ed. Putnam, F.W., Academic Press, N.Y., Vol. I, 179.
6. Balasubramanian, D. and Wetlaufer, D.W. (1966) Proc. Natl. Acad. Sci. U.S., 55, 762.
7. Leach, S.J. (1969) "Physical Principles in Protein Chemistry", Academic Press, New York.
8. Putnam, F.W. (1948) Adv. Protein Chem., 4, 79.

VITAE

Ramachandran Chandrasekharan was born on February 18, 1950 at Alleppey, Kerala. He passed the Higher Secondary Exam. from St. Mary's Higher Secondary School, Secunderabad in 1965 and subsequently graduated from St. Xavier's College, Ahmedabad in 1968. He obtained his M.Sc. degree from IIT Madras in 1970 and joined the graduate programme of the Department of Chemistry, IIT Kanpur in July 1970. From November 1970 to August 1973 he was a J.R.F. of the CSIR. Since December 1973 he has been a Research Assistant at the Department of Chemistry, IIT-Kanpur.

**A 52174**

Date Slip **A 52174**

This book is to be returned on the date last stamped.

A blank ledger page with a vertical line down the center and horizontal lines forming a grid. The page is divided into two columns by a solid vertical line. There are 15 horizontal lines in total, creating 16 rows. The lines are evenly spaced and extend across the width of the page.

CD 6.72.9

CHM-187E-D-CHA-SP